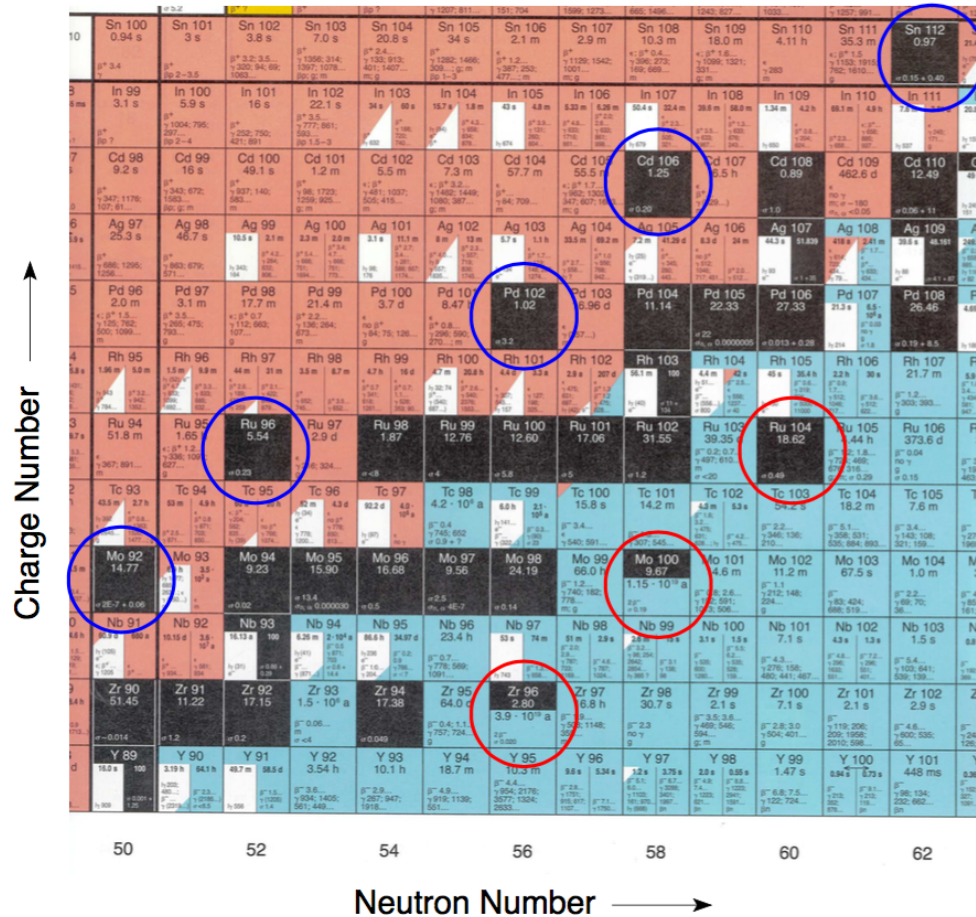


Astrofisica Nucleare e Subnucleare
Nuclear Astrophysics – I

Nucleosynthesis beyond iron



The stable nuclei beyond iron can be classified in three categories depending of their origin:

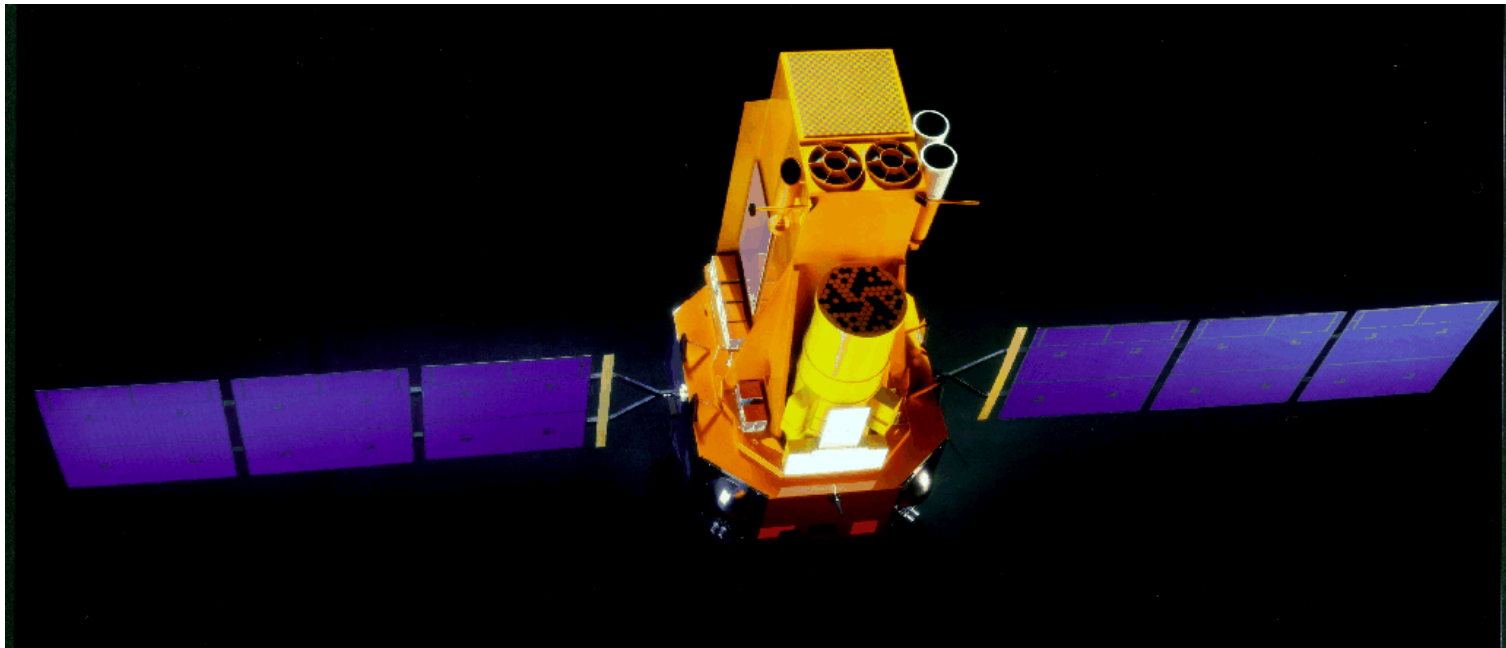
- s-process
- r-process
- p-process (γ -process)

Astrofisica Nucleare e Subnucleare

“MeV” Astrophysics

INTEGRAL

INTEGRAL, the **International Gamma-Ray Astrophysics Laboratory**
Fine spectroscopy ($E/dE=500$) and fine imaging (angular resolution of **12' FWHM**)
Energy range **15 keV to 10 MeV**
plus simultaneous **X-ray** (3-35 keV) and **optical** (550 nm) monitoring capability
Two main g-ray instruments: **SPI** (spectroscopy) and **IBIS** (imager)



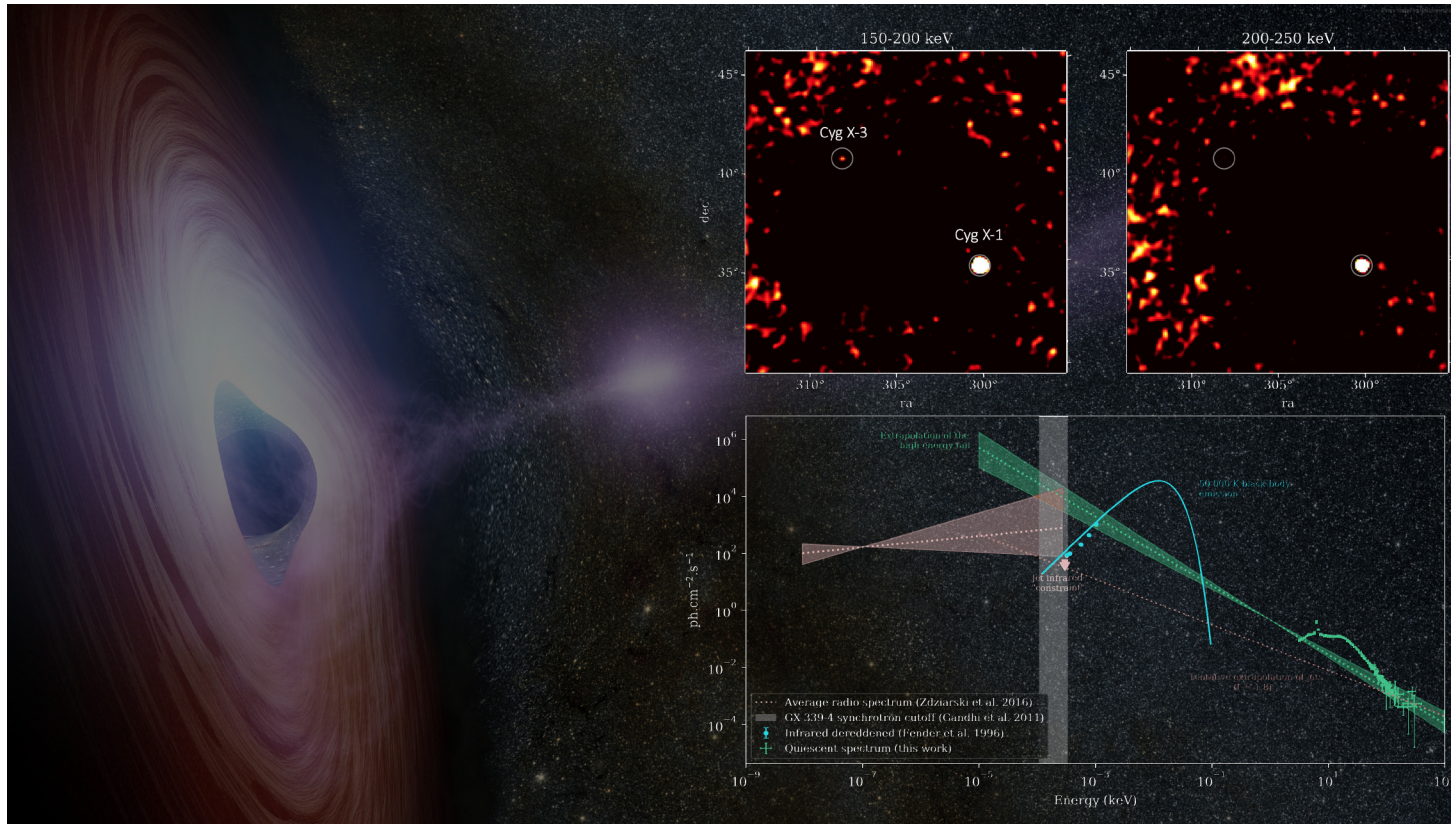
<http://integral.esa.int>

INTEGRAL



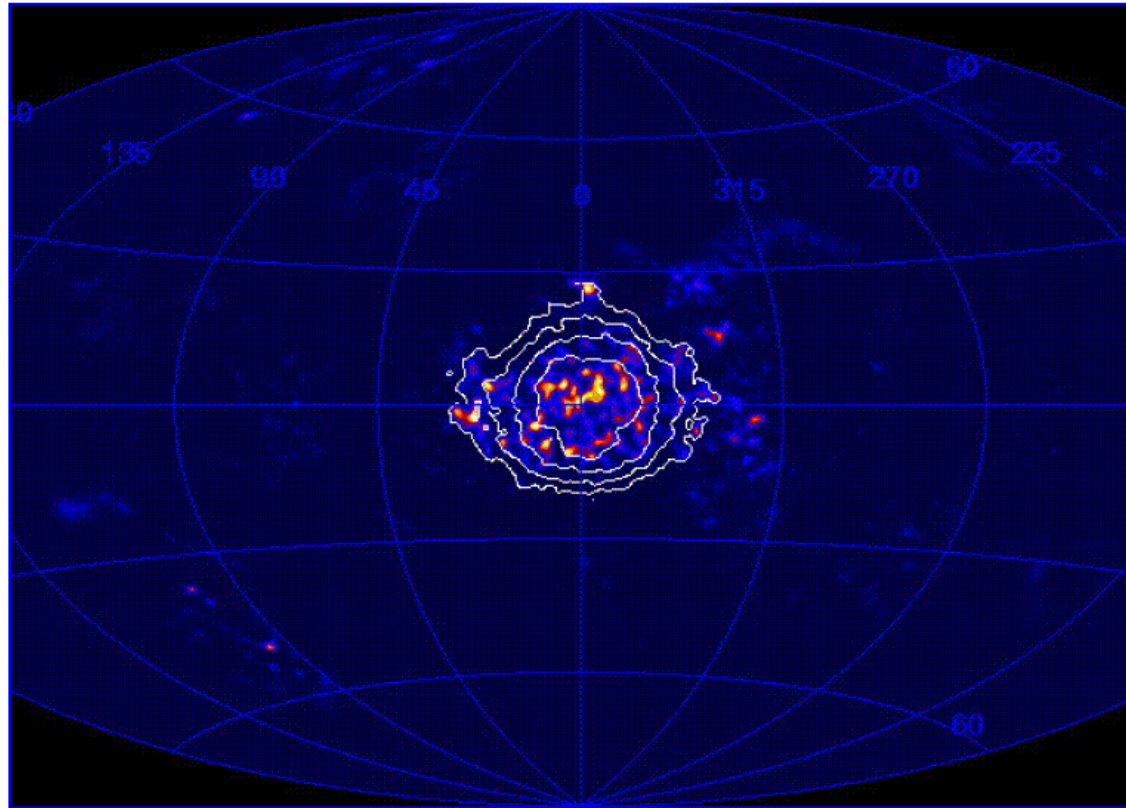
The central regions of our Galaxy, the Milky Way, as seen by INTEGRAL in gamma rays. With its superior ability to see faint details, INTEGRAL reveals the individual sources that comprised the foggy, soft gamma-ray background seen by previous observatories. The brightest 91 objects seen in this image were classified by INTEGRAL as individual sources, while the others appear too faint to be properly characterized at this stage.

INTEGRAL



Cygnus X-3 is one of the first discovered X-ray binaries and the only bright compact binary system known to host a Wolf-Rayet star as a companion. The intense stellar wind created by this companion is one of the reasons why Cygnus X-3 exhibits a very peculiar spectral behavior. Indeed, it shows a wider variety of states than the two canonical ones usually observed in other standard X-ray binaries. Despite the fact that the source is well known since many years, very little is known about its spectral behavior beyond 50 keV. This lack of knowledge is especially due to the source being very faint at these energies. Thanks to INTEGRAL, it is possible to explore more than 16 years of observations, and so to probe the sky region of Cygnus X-3 with the best sensitivity ever. As shown at the top of the figure, one can detect the source up to 200 keV. Moreover, one can create six X-ray spectra from 3 to 200 keV, one for each observed spectral state of the source.

INTEGRAL

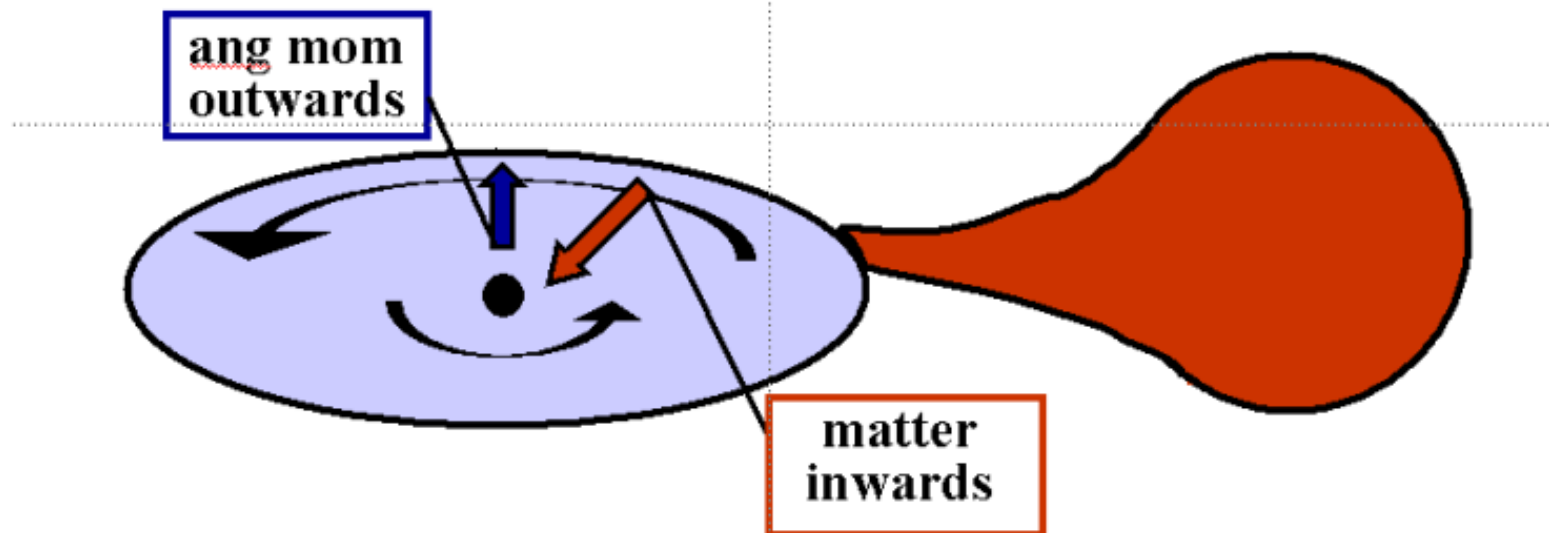


The SPI instrument onboard INTEGRAL has performed a search for 511 keV emission (resulting from positron-electron annihilation) all over the sky. The figure represents the results of this search: the all-sky map in galactic co-ordinates shows that 511 keV emission is - so far - only seen towards the center of our Galaxy. The SPI data are equally compatible with galactic bulge or halo distributions, the combination of a bulge and a disk component, or a combination of a number of point sources. Such distributions are expected if positrons originate either from low-mass X-ray binaries, novae, Type Ia supernovae, or possibly light dark matter.

Galactic Sources

Accretion disk formation

Matter circulates around the compact object:



https://mssl.ucl.ac.uk/www_astro/lecturenotes/hea/hea.html

Accretion Power

Accretion onto a compact object

- Principal mechanism for producing high-energy radiation
- Most efficient of energy production known in the Universe.

$$E_{acc} = G \frac{Mm}{R}$$

Gravitational potential energy released for body mass M and radius R when mass m accreted

Accretion Power

Origin of accreted matter

- Given M/R , luminosity produced depends on accretion rate, \dot{m} .

$$L_{acc} = \frac{dE_{acc}}{dt} = \frac{GM}{R} \frac{dm}{dt} = \frac{GM\dot{m}}{R}$$

- Where does accreted matter come from?
ISM? No - too small. Companion? Yes.

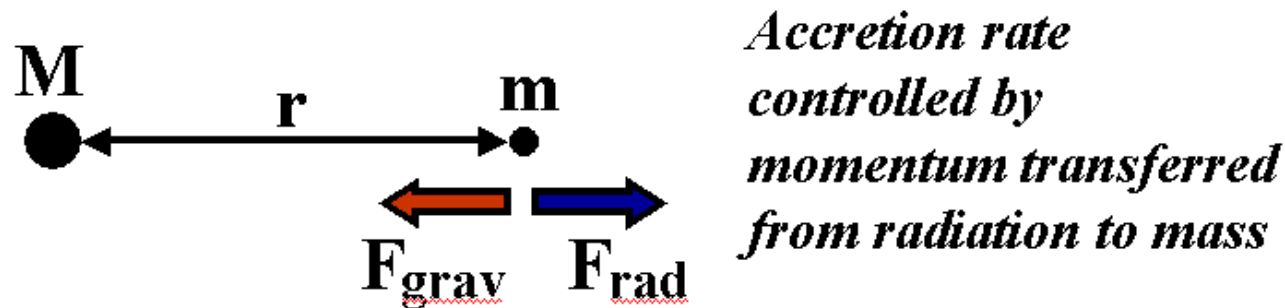
Accretion Power

The Eddington Luminosity

- There is a limit to which luminosity can be produced by a given object, known as the Eddington luminosity.
- Effectively this is when the inward gravitational force on matter is balanced by the outward transfer of momentum by radiation.

Accretion Power

Eddington Luminosity



$$F_{grav} = G \frac{Mm}{r^2} \text{ Newton}$$

Note that R is now negligible wrt r

Outgoing photons from M scatter material (electrons and protons) accreting.

Accretion Power

Scattering

L = accretion luminosity

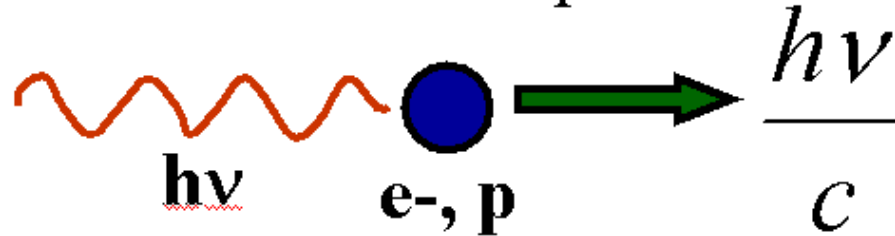
$$\begin{array}{l} \text{no. photons} \\ \text{crossing at } r \\ \text{per second} \end{array} = \frac{L}{4\pi r^2} \frac{1}{h\nu} \quad \text{photons m}^{-2} \text{ s}^{-1}$$

Scattering cross-section will be Thomson cross-section σ_e ; so no. scatterings per sec:

$$\frac{L\sigma_e}{4\pi r^2 h\nu}$$

Accretion Power

Momentum transferred from photon to
particle:



Momentum gained by particle per second
= force exerted by photons on particles

$$\frac{L\sigma_e}{4\pi r^2 h\nu} \frac{h\nu}{c} = \frac{L\sigma_e}{4\pi r^2 c} \text{Newton}$$

Accretion Power

Eddington Limit

radiation pressure = gravitational pull

At this point accretion stops, effectively imposing a 'limit' on the luminosity of a given body.

$$\frac{L\sigma_e}{4\pi r^2 c} = G \frac{Mm}{r^2}$$

So the Eddington luminosity is:

$$L = \frac{4\pi c G M m}{\sigma_e}$$

Accretion Power

Assumptions made

- **Accretion flow steady + spherically symmetric:** eg. in supernovae, L_{Edd} exceeded by many orders of magnitude.
- **Material fully ionized and mostly hydrogen:** heavies cause problems and may reduce ionized fraction - but OK for X-ray sources

Accretion Power

Accretion modes in binaries

ie. binary systems which contain a compact star, either white dwarf, neutron star or black hole.

(1) **Roche Lobe overflow**

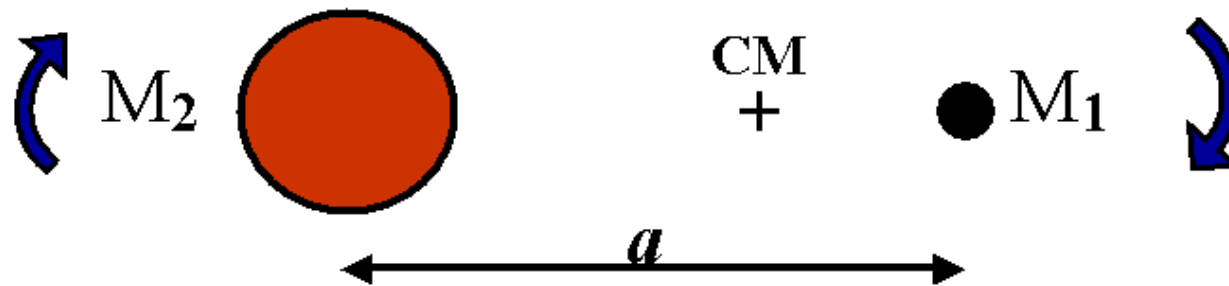
(2) **Stellar wind**

- correspond to different types of X-ray binaries

Accretion

Roche Lobe Overflow

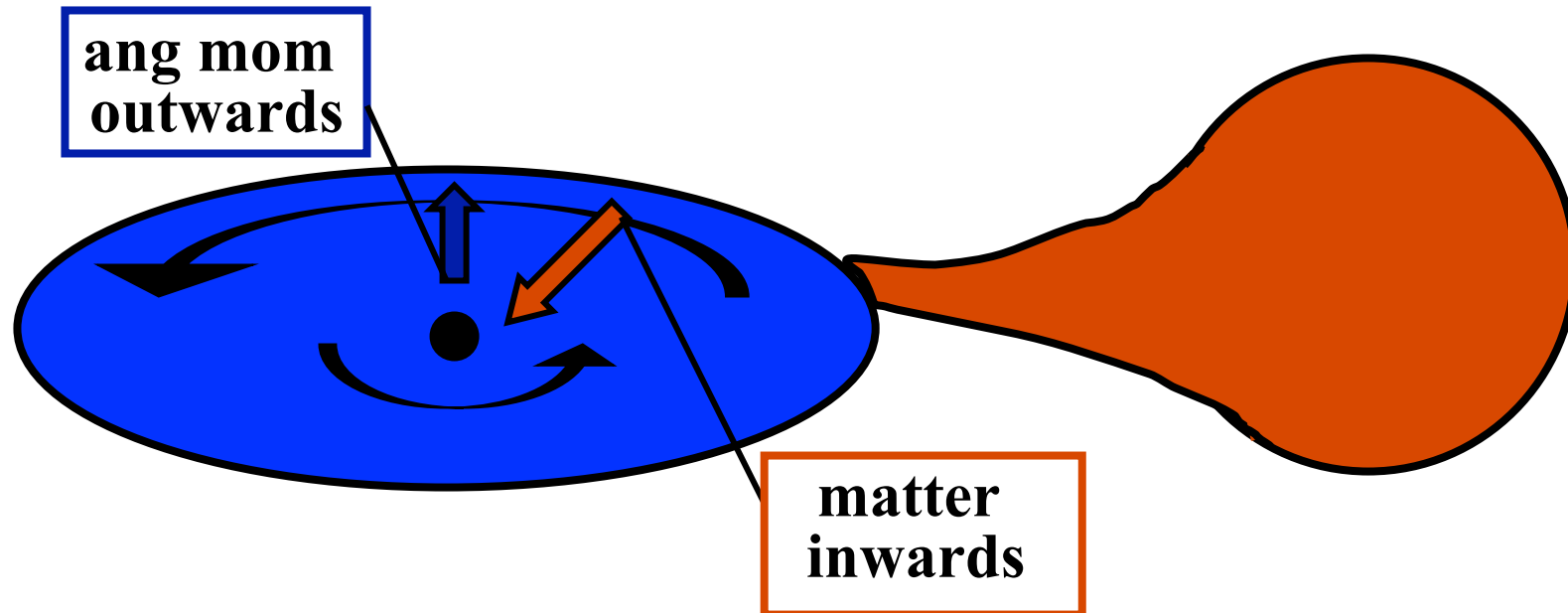
- Compact star M_1 and normal star M_2



- normal star expanded or binary separation decreased \Rightarrow normal star feeds compact

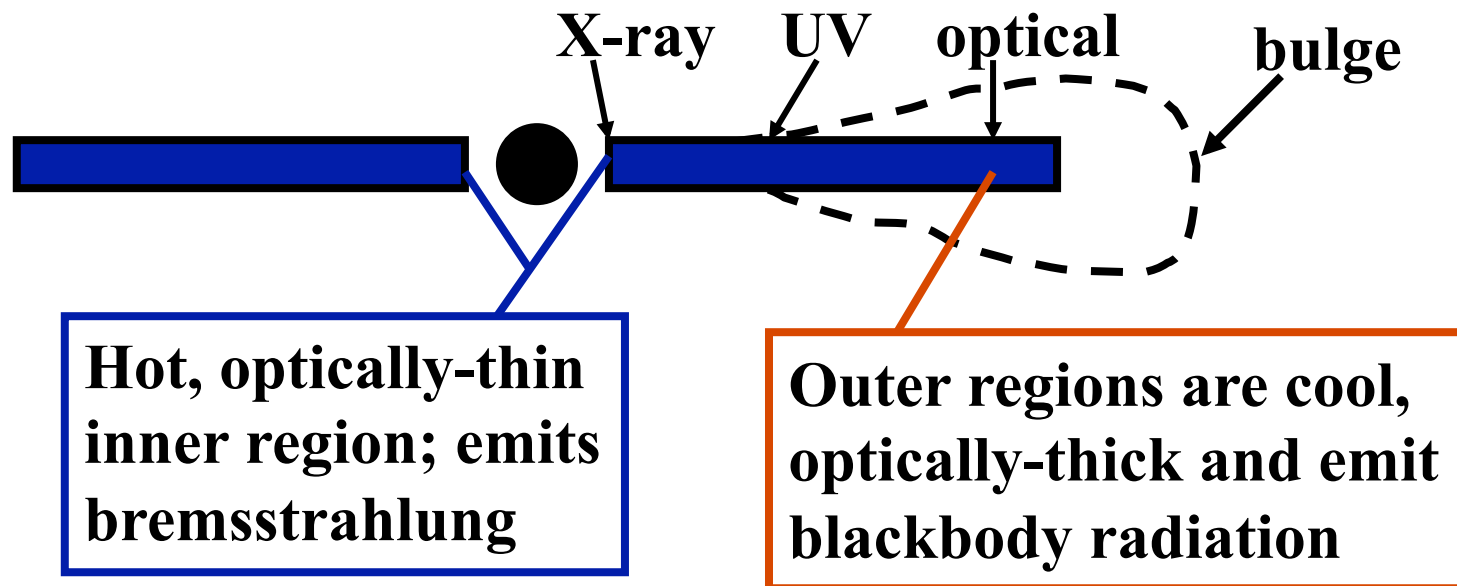
Accretion

Matter circulates around the compact object:



Disk structure

Half of the accretion luminosity is released very close to the star.



Stellar Wind Accretion

Stellar Wind Model

Early-type stars have intense and highly supersonic winds. Mass loss rates - 10^{-6} to 10^{-5} solar masses per year.

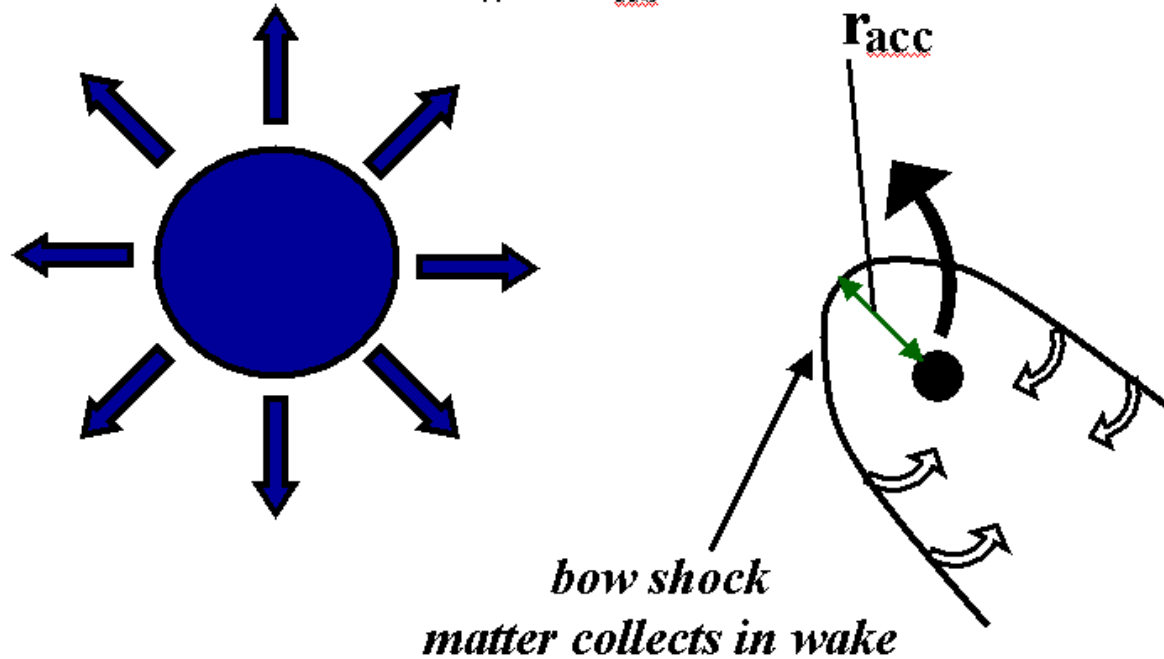
For compact star - early star binary, compact star accretes if

$$\frac{GMm}{r} > \frac{1}{2} m(\mathbf{v}_w^2 + \mathbf{v}_{ns}^2)$$

Stellar Wind Accretion

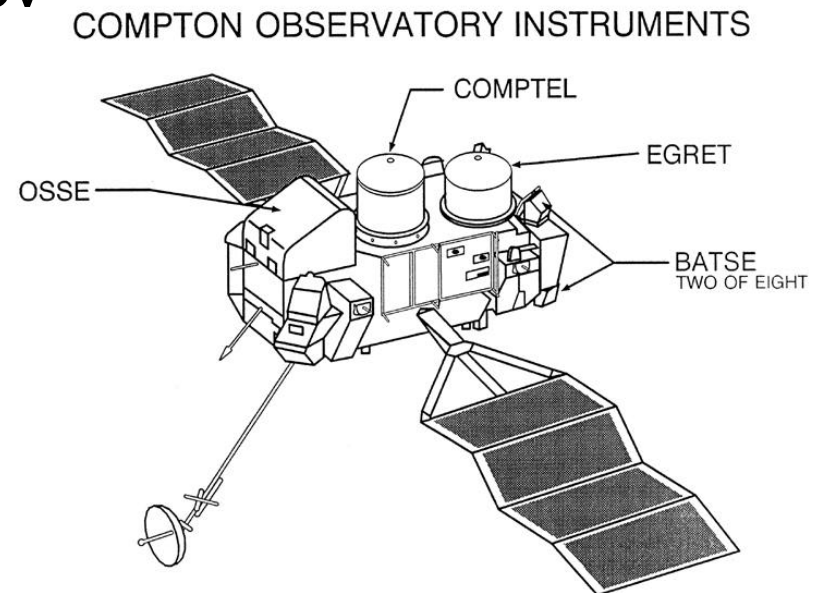
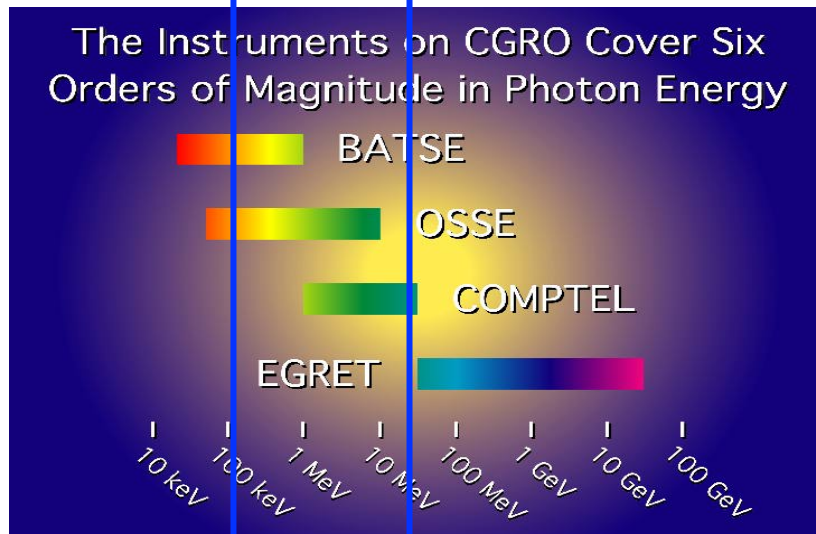
Thus :

$$r_{\text{acc}} = \frac{2GM}{v_w^2 + v_{\text{ns}}^2}$$



The Compton Gamma Ray Observatory

<http://coss.c.gsfc.nasa.gov>



The Compton Gamma Ray Observatory (CGRO) is a sophisticated satellite observatory dedicated to observing the high-energy Universe. It is the second in NASA's program of orbiting "Great Observatories", following the Hubble Space Telescope. While Hubble's instruments operate at visible and ultraviolet wavelengths, Compton carries a collection of four instruments which together can detect an unprecedented broad range of high-energy radiation called gamma rays. These instruments are the Burst And Transient Source Experiment (BATSE), the Oriented Scintillation Spectrometer Experiment (OSSE), the Imaging Compton Telescope (COMPTEL), and the Energetic Gamma Ray Experiment Telescope (EGRET).

The Compton Gamma Ray Observatory

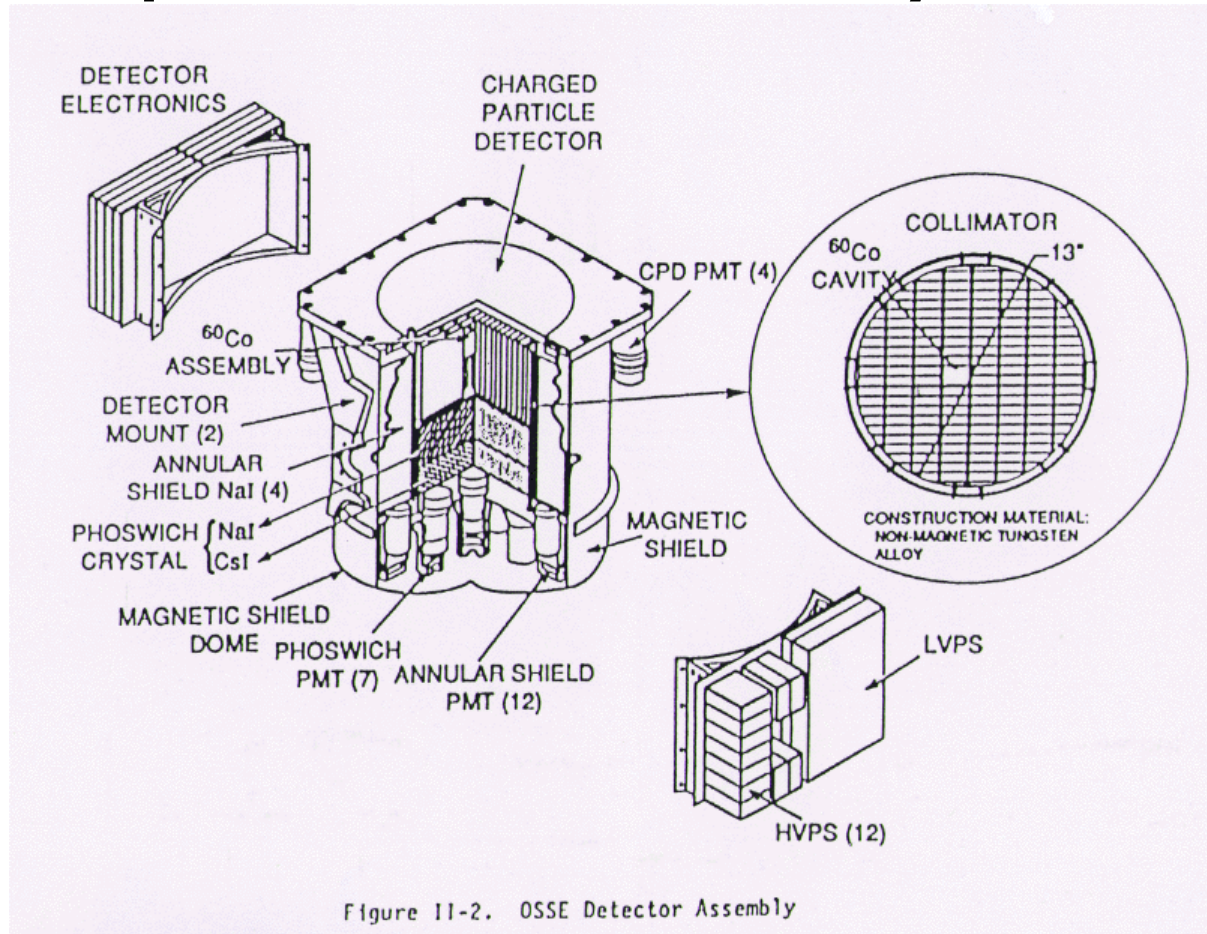
Table 1: SUMMARY OF COMPTON GRO DETECTOR CHARACTERISTICS

	OSSE	COMPTEL	EGRET	BATSE	
				LARGE AREA	SPECTROSCOPY
ENERGY RANGE (MeV)	0.05 to 10.0	0.8 to 30.0	20 to 3 x 10 ⁴	0.03 to 1.3	0.015 to 110
ENERGY RESOLUTION (FWHM)	12.5% at 0.2 MeV 6.0% at 1.0 MeV 4.0% at 5.0 MeV	8.0% at 1.27 MeV 6.5% at 2.75 MeV 6.3% at 4.43 MeV	~20% 100 to 2000 MeV	32% at 0.06 MeV 27% at 0.09 MeV 20% at 0.66 MeV	0.2% at 0.09 MeV 7.2% at 0.66 MeV 5.8% at 1.17 MeV
EFFECTIVE AREA (cm ²)	2013 at 0.2 MeV 1480 at 1.0 MeV 568 at 5.0 MeV	25.8 at 1.27 MeV 29.3 at 2.75 MeV 29.4 at 4.43 MeV	1200 at 100 MeV 1000 at 500 MeV 1400 at 3000 MeV	1000 ea. at 0.03 MeV 1800 ea. at 0.1 MeV 350 ea. at 0.66 MeV	109 ea. at 0.3 MeV 127 ea. at 0.2 MeV 52 ea. at 3 MeV
POSITION LOCALIZATION (STRONG SOURCE)	10 arc min square error box (special mode; 0.1 x Crab spectrum)	0.5 - 1.0 deg (90% confidence; 0.2 x Crab spectrum)	5 to 10 arc min (1 σ radius; 0.2 x Crab spectrum)	3" (strong bursts)	-----
FIELD OF VIEW	3.0° x 11.4°	~ 64°	~ 0.6 sr	4 sr	4 sr
MAXIMUM EFFECTIVE GEOMETRIC FACTOR (cm ² sr)	13	30	1050 (~ 500 MeV)	15000	5000
ESTIMATED SOURCE SENSITIVITY	LINE (3-8) x 10 ⁻³ cm ⁻² s ⁻¹ CONTINUUM (5 x 10 ⁴ sec. on source, all Galactic Plane) 3 x 10 ⁻⁷ cm ⁻² s ⁻¹ keV ⁻¹ (@1 MeV)	1.5 x 10 ⁻³ to 6 x 10 ⁻³ cm ⁻² s ⁻¹ 1.6 x 10 ⁻⁴ cm ⁻² s ⁻¹ (3 σ detection, 1-30 MeV)	7 x 10 ⁻⁶ cm ⁻² s ⁻¹ (> 100 MeV) 2 x 10 ⁻⁸ cm ⁻² s ⁻¹ (> 1000 MeV)	3 x 10 ⁻⁸ erg cm ⁻² (1 sec-burst)	0.4% equivalent width (5 sec integration)

CGRO performance

	BATSE	OSSE	COMPTEL	EGRET
Developer	NASA/Marshall	Naval Research Lab	Univ. N.H. & MPE	NASA/Goddard
Energy Range (MeV)	0.03 to 1.9	0.05 to 10.0	0.08 to 30.0	30.0 to 30000.0
Field of View	entire sky	3.0 x 11.4 degrees	64 degrees	0.6 steradians
Spectral Resolution (FWHM)	32 % at 0.06 MeV 27 % at 0.09 MeV 20 % at 0.66 MeV	12.5 % at 0.2 MeV 5. % at 1.0 MeV 4.0 % at 5.0 MeV	8.8 % at 1.27 MeV 6.5 % at 2.75 MeV 6.3 % at 4.43 MeV	20 %
Effective Area (cm²)	1000 ea. at 0.03 MeV 1800 ea. at 0.1 MeV 550 ea. at 0.55 MeV	2013 at 0.2 MeV 1400 at 1.0 MeV 55 at 5.0 MeV	25.0 at 1.27 MeV 29.3 at 2.75 MeV 29.4 at 4.43 MeV	1200 at 100 MeV 1600 at 500 MeV 1400 at 3000 MeV
Spatial Resolution (for strong sources)	3 degrees	10 x 10 arcminutes	0.5 - 1.0 degrees	5 - 10 arcminutes

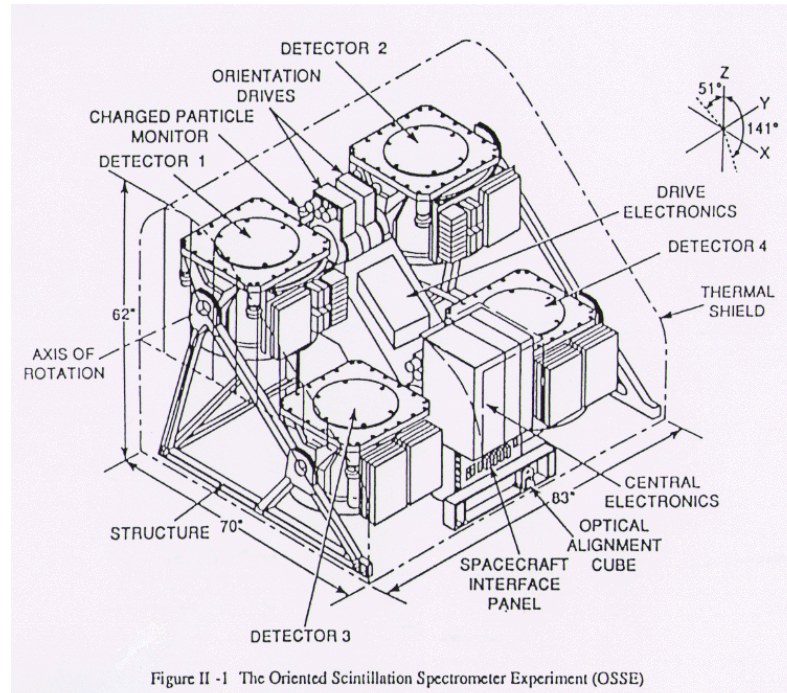
The Compton Gamma Ray Observatory



OSSE

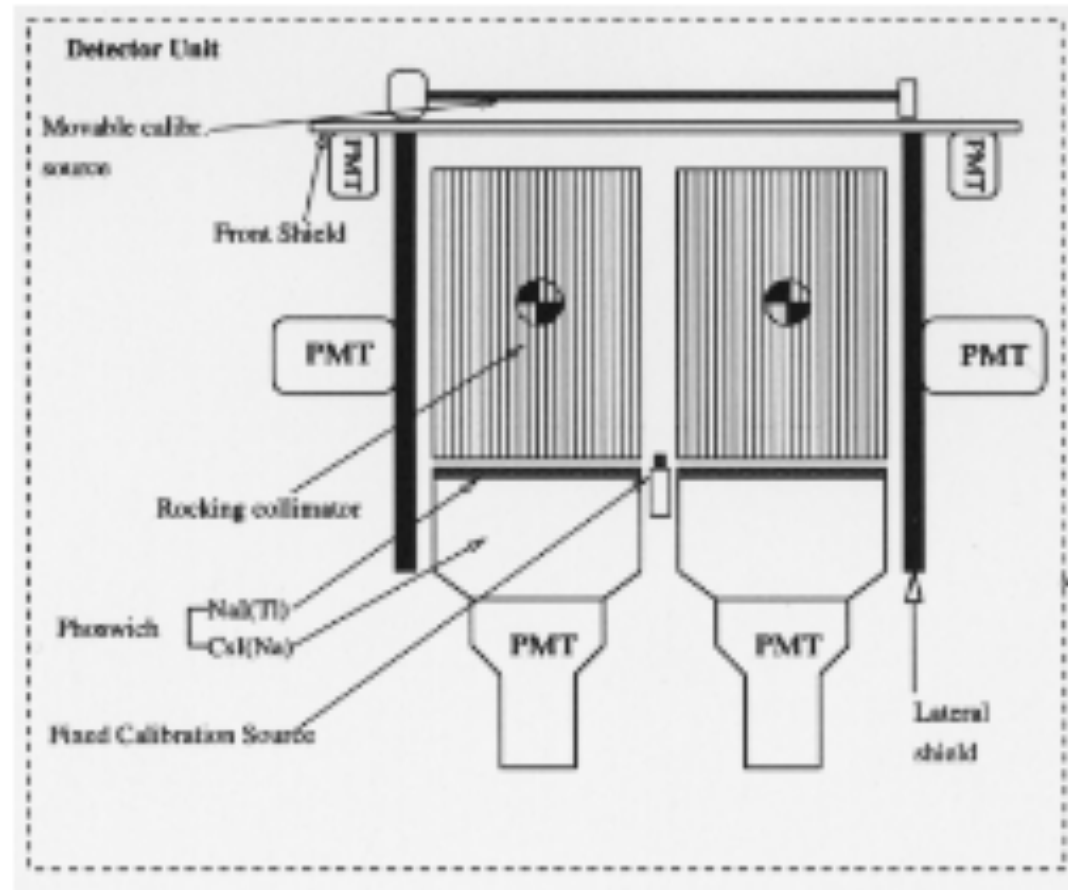
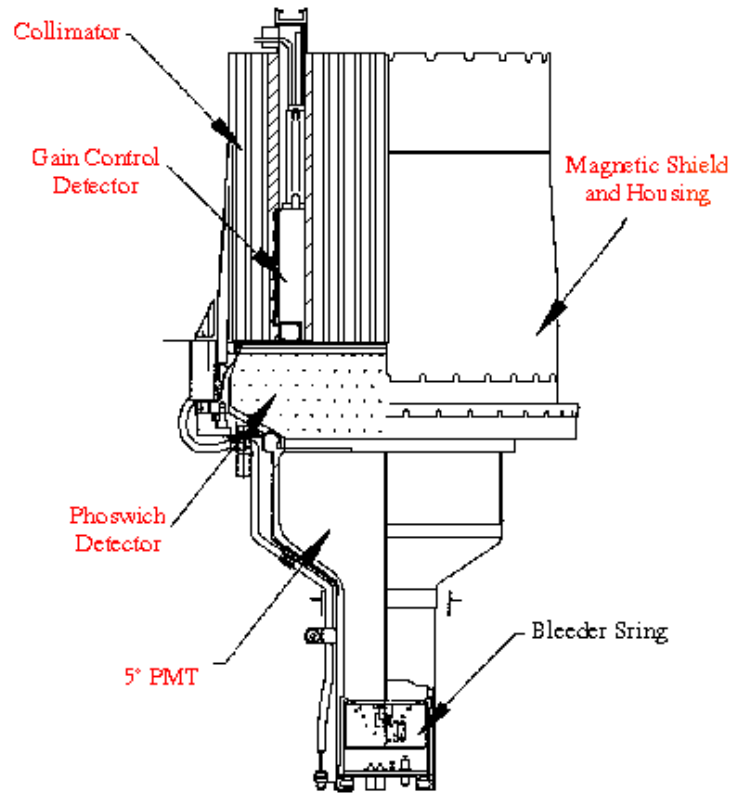
- 0.05-10 MeV
- e^+e^- annihilation, solar flares

OSSE detector



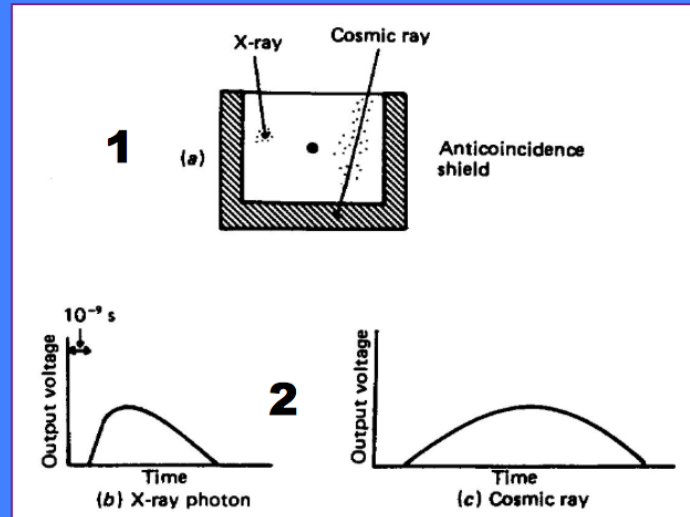
The Oriented Scintillation [Spectrometer](#) Experiment (OSSE) measured the distribution of the energy emitted from a number of gamma-ray sources, and as such studied nuclear lines in solar flares, radioactive decay of nuclei in [supernova](#) remnants, and [matter](#)-antimatter annihilation taking place near the center of our [galaxy](#). OSSE consisted of four NaI scintillation crystals, and was [sensitive](#) to gamma rays with energies ranging from 50 keV to 10 MeV. Each of the detectors could be pointed individually. For most instances, observations of a gamma ray source were alternated with observations of nearby blank sky so as to be able to determine the background gamma ray emission.

Phoswich detectors



Two scintillators with different decay times. Pulse analysis can distinguish. Back scintillator used as shield at low energy, as detector at high energies.

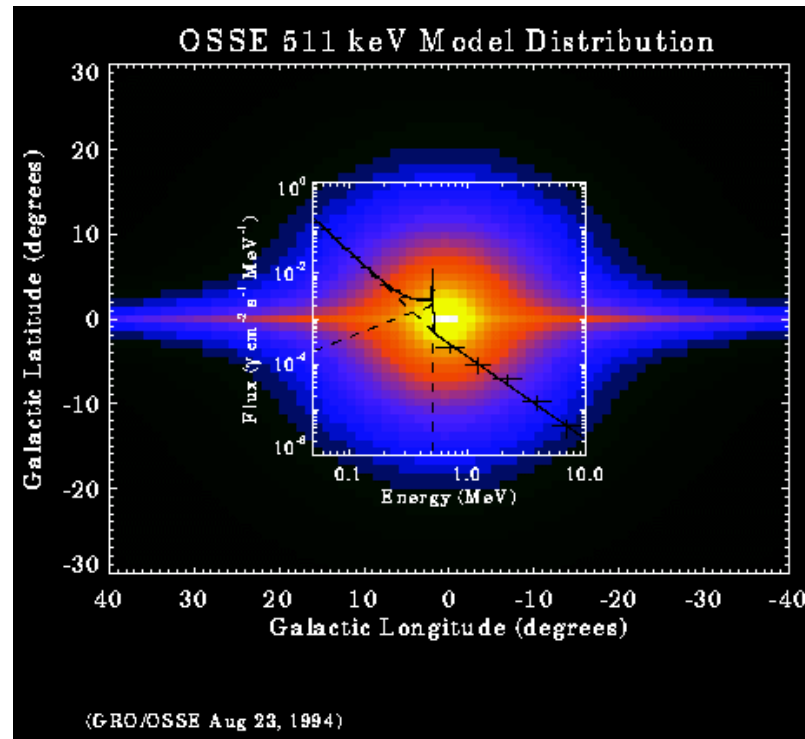
Tecniche di schermaggio



From M.S. Longair,
“High Energy Astrophysics”
(Vol. 1)

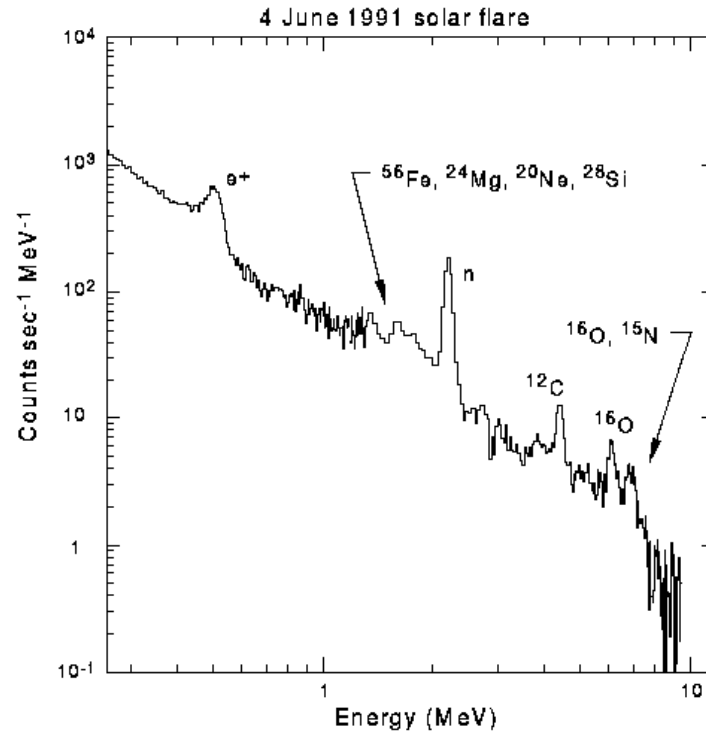
- 1. Anti-coincidence detectors:** any event triggering both the counter and the scintillating material can be safely rejected as cosmic ray (CR)
- 2. Rise-time or pulse-shape discrimination:** a fast particle (CR) or electron produces a tail of ionization and, consequently, results in a broad pulse, whereas an X-ray photon produces a sharper pulse.
- 3. Technique using a phoswich detector:** the detector consists of alternate layers of material having different responses as scintillator detectors for photons and CR. While the first material is sensitive to photons, the following is not. A photon produces only a pulse, while a CR results in a double pulse in a certain time interval.

The Compton Gamma Ray Observatory



Intensity of gamma-ray emission from [positron-electron annihilation](#) in the plane of our Galaxy near the Galactic center. The emission is at 511 keV, which is the rest-mass energy of the electron and positron. The map is of a model that fits the OSSE 511 keV observations. OSSE has discovered that the radiation is mostly contained in a region of about 10 degrees diameter centered on the center of the Galaxy. The line plot superimposed on the map represents an OSSE observation of the 511 keV emission line.

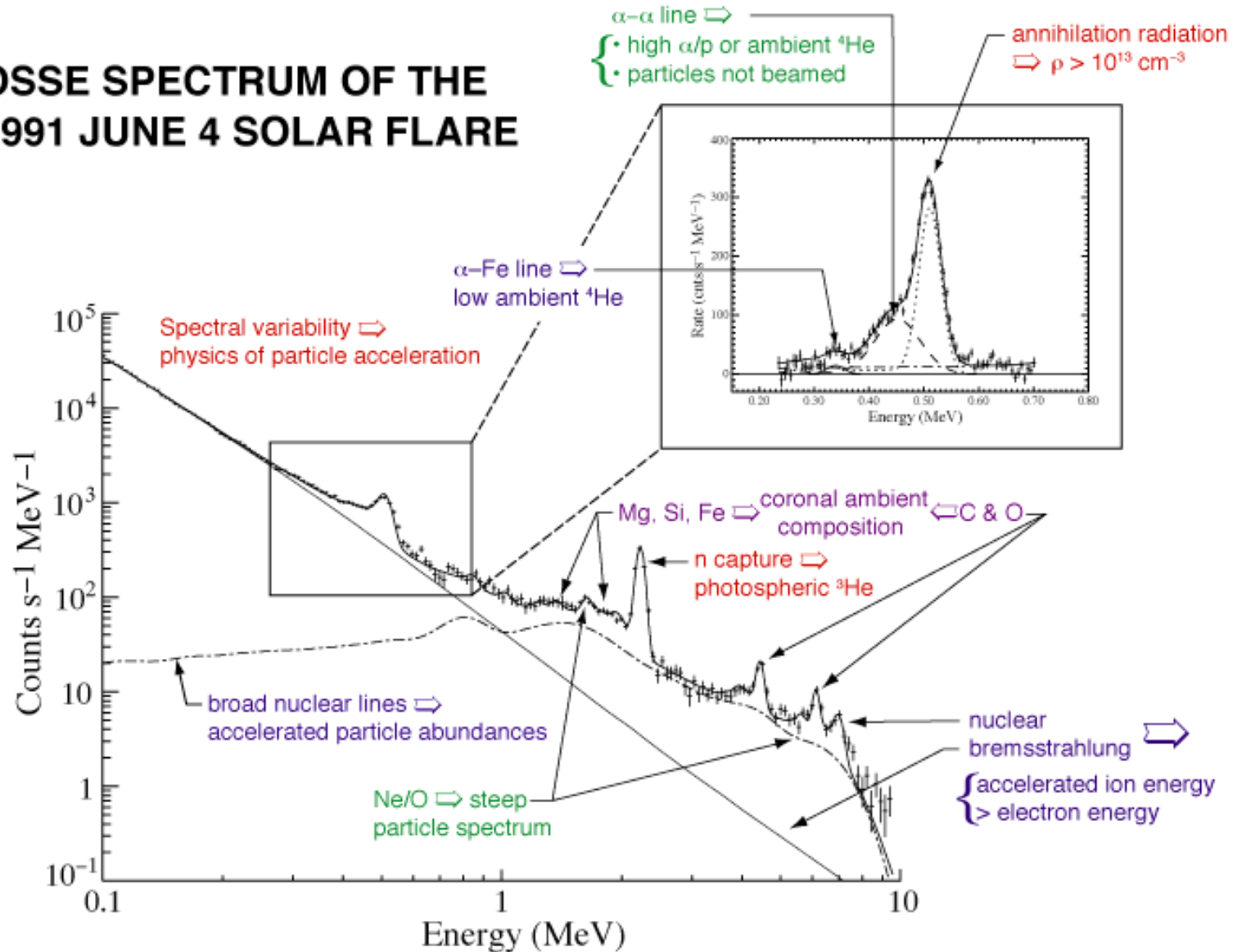
The Compton Gamma Ray Observatory



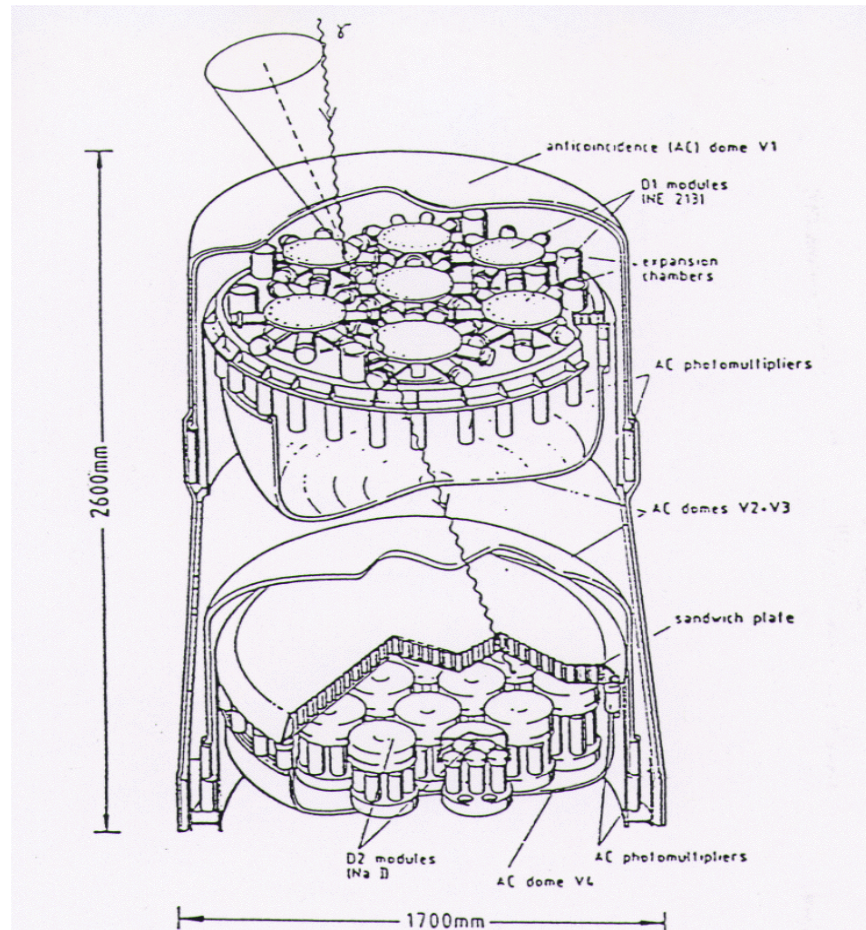
On June 4, 1991, the OSSE instrument observed a bright [high-energy flare](#) from an intensely active region of the sun. The energy spectrum of the flare shown in this slide indicates that solar flares accelerate particles to extremely high energies causing interactions which produce nuclear emission lines from excited atomic nuclei of Fe, Mg, Ne, Si, C, O, and N, along with emission lines from the formation of deuterium by neutron capture (labeled "n" in the slide) and electron-positron annihilation (labeled "e+").

Solar Flares lines

OSSE SPECTRUM OF THE 1991 JUNE 4 SOLAR FLARE



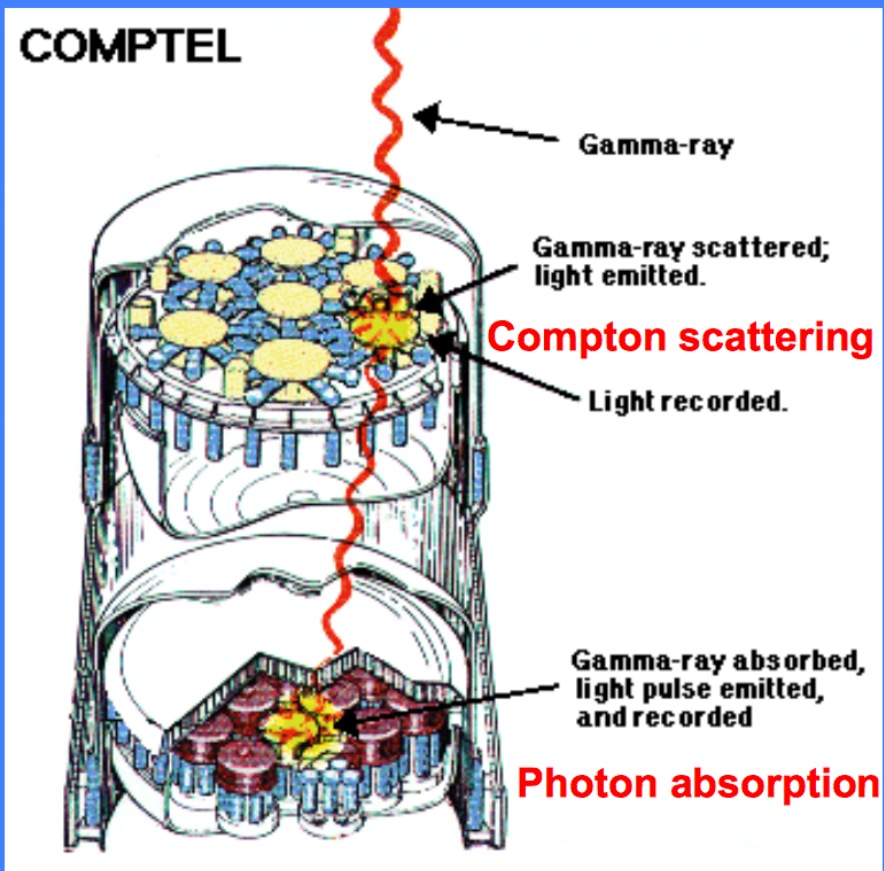
The Compton Gamma Ray Observatory



COMPTEL

- 0.05-30 MeV
- Radioactive elements map, pulsars, a few flaring black hole candidates, blazars, solar flares

Telescopi Compton



Two-level instruments:

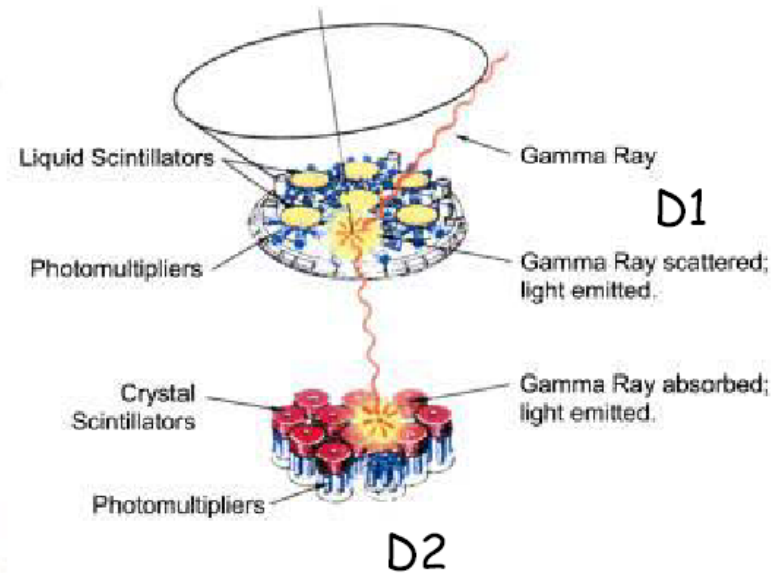
1st level: the γ -ray Compton scatters off an electron in a **liquid scintillator**. The scattered photon enters into a **2nd level scintillator** (NaI) and is absorbed. Phototubes can determine the interaction points at the two layers and record the amount of energy deposited in each layer.

It is possible to reconstruct the angle of incidence the photon made wrt the original direction using the Compton scattering law, linking this angle and the energy of the scattered photon (2nd level) and the scattering electron (1st level).

“Event circle” (ring on the sky), poor angular resolution (but multiple photons can help to reconstruct the position)

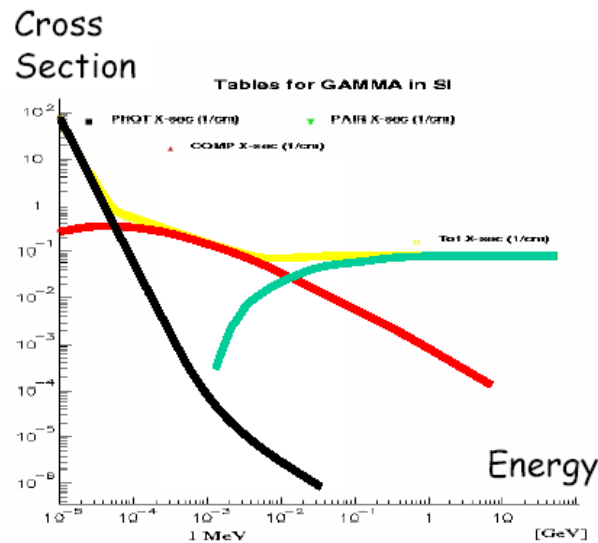
Compton Imaging

COMPTEL on CGRO



Compton Imaging

Detection of Gamma Radiation



Photoeffect (< 100 keV)

Photons effectively blocked and stopped

Telescopes:

Collimators
 Coded Mask Systems

Pair Creation (> 10 MeV)

Photons completely converted to e^+e^-

Telescope:

Tracking chambers to visualize the pairs

Compton Scattering (0.2-10 MeV)

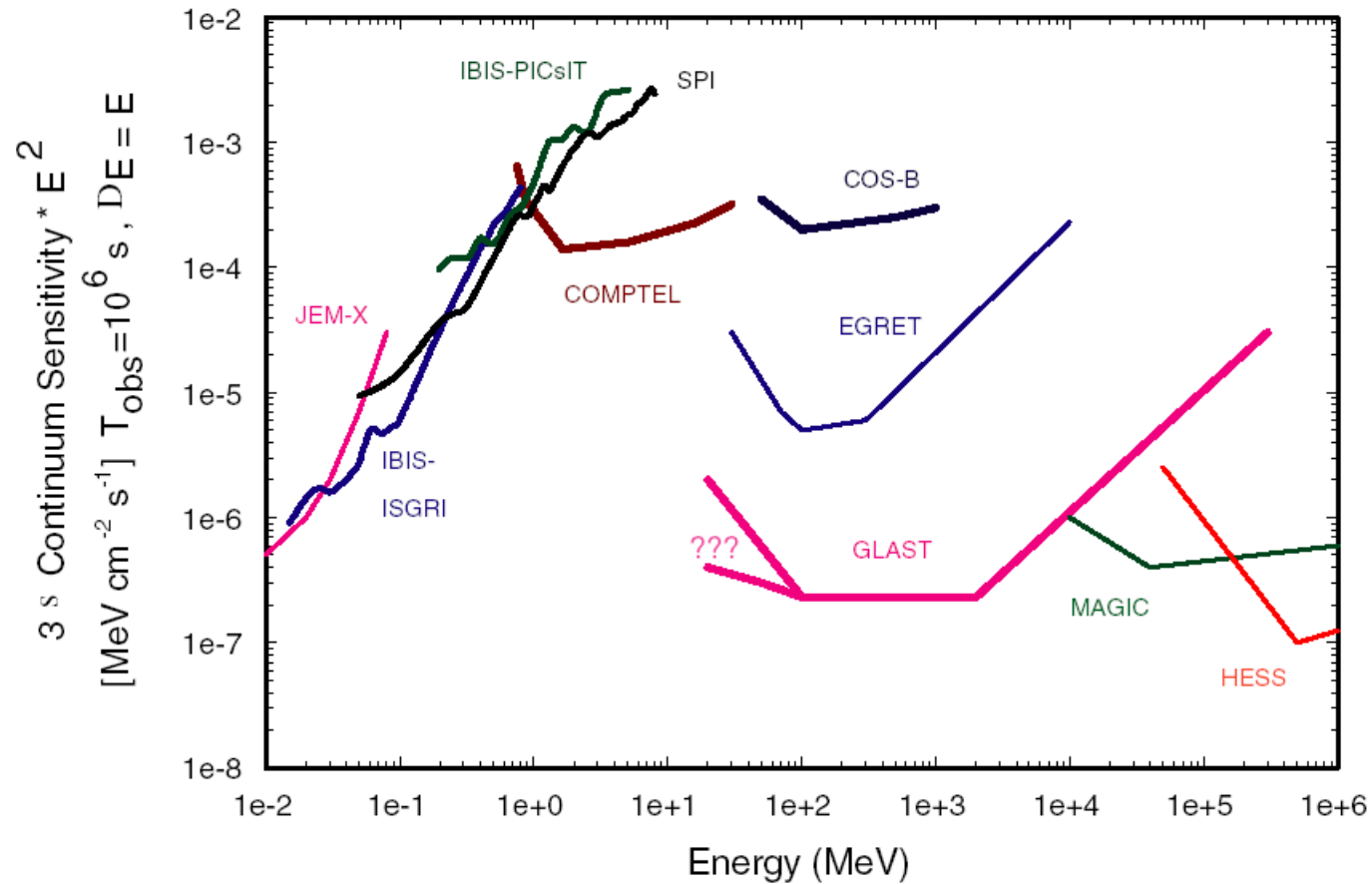
Photon Cross-section Minimum
 Scattered photons with long range

Telescope:

Compton Camera Coincidence System

Sensitivity

G. Kanbach et al. / New Astronomy Reviews 48 (2004) 275–280



Compton Imaging

Low to **M**edium **E**nergy **G**amma-Ray
Astronomy

or

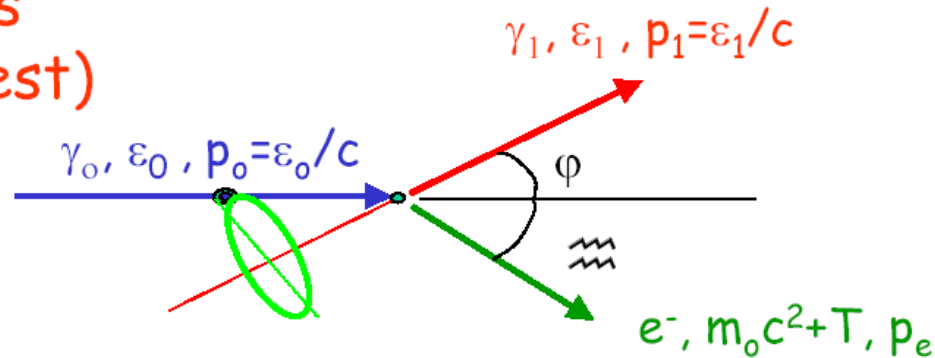
what is the promise and hope for
astrophysics in the energy range

" few 100 keV to ~ 50 MeV "

???

Compton Imaging

Kinematics
(target at rest)



Energy: $\varepsilon_0 = \varepsilon_1 + T$

Momentum:

$$\varepsilon_0 = \varepsilon_1 \cos \varphi + pc \cos \vartheta$$

$$\text{where } pc = \sqrt{T(T + 2m_0c^2)}$$

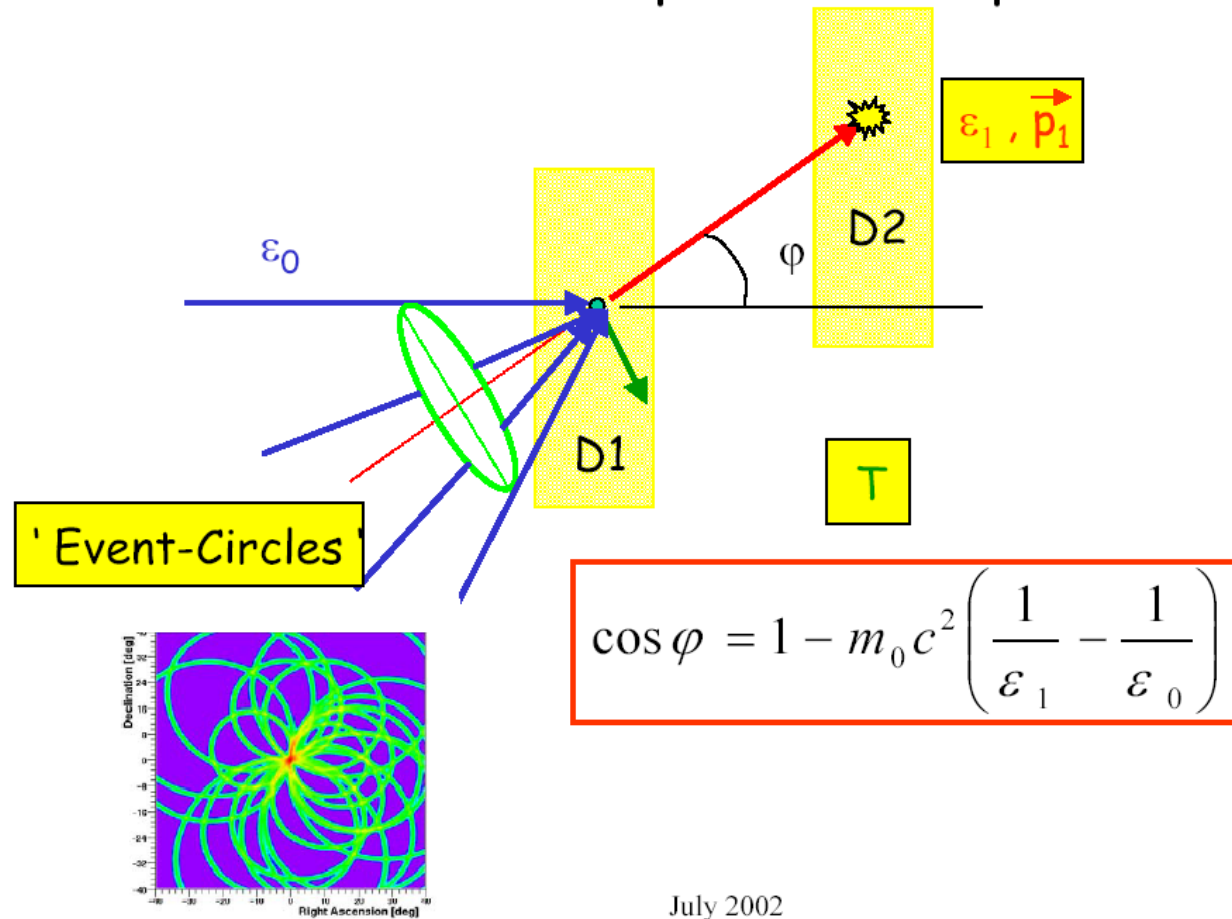
$$\varepsilon_1 \sin \varphi = pc \sin \vartheta$$

Compton Equation:

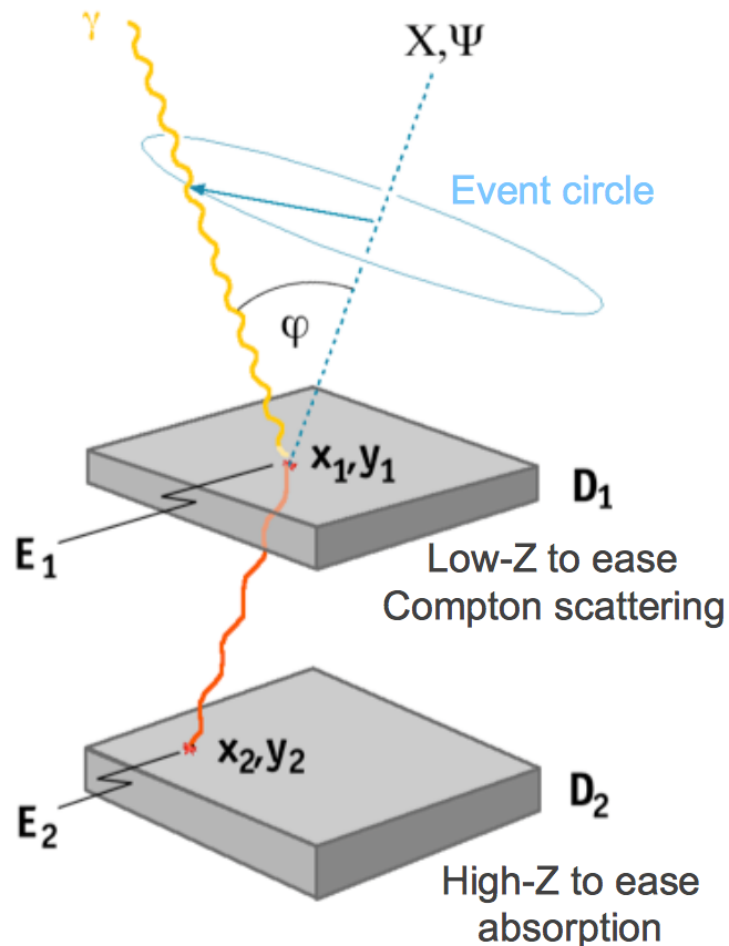
$$\cos \varphi = 1 - m_0c^2 \left(\frac{1}{\varepsilon_1} - \frac{1}{\varepsilon_0} \right)$$

Compton Imaging

The ,classical' Compton telescope



July 2002



measured parameters :

- x_1, y_1 : interaction location in D_1
- E_1 : energy deposit in D_1
- x_2, y_2 : interaction location in D_2
- E_2 : energy deposit in D_2
- $t, \Delta t$: arrival time, TOF D_1 - D_2

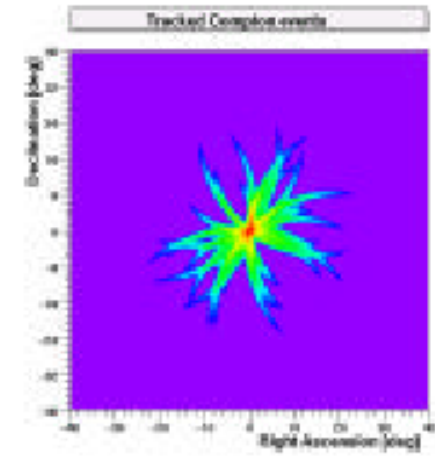
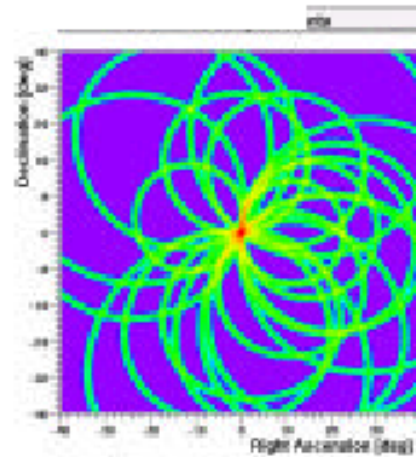
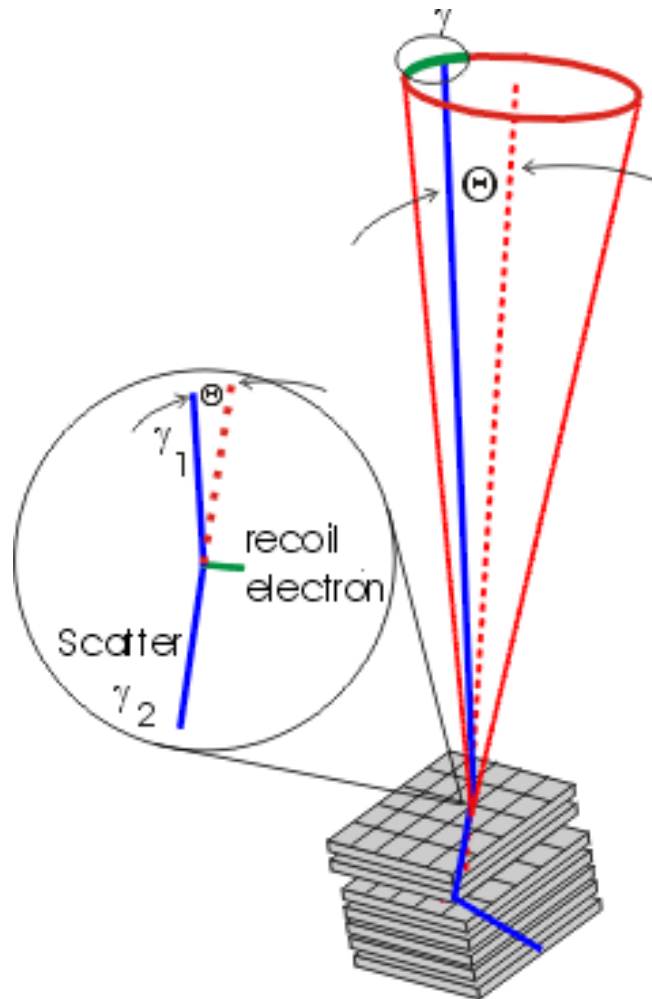
derived parameters :

- $x_1, y_1, x_2, y_2 \Rightarrow \chi, \psi$
- $E_1, E_2 \Rightarrow \bar{\varphi}$

$$\cos \phi = 1 - m_e c^2 \left(\frac{1}{E_2} - \frac{1}{E_1} \right)$$

encoding of the two dimensional source distribution into a 3-D dataspace (X, Ψ, φ)

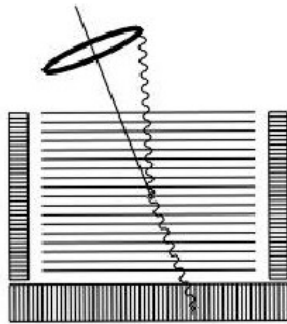
Compton Imaging



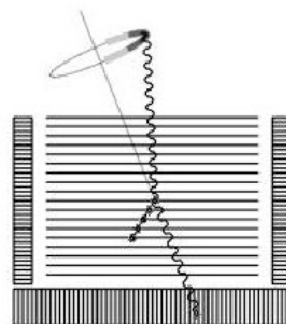
Compton Imaging

Coincidence Detector Schematics

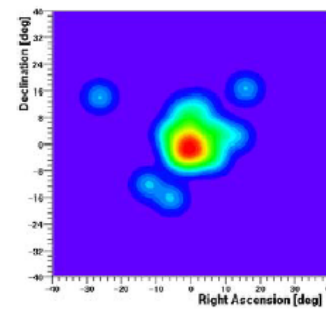
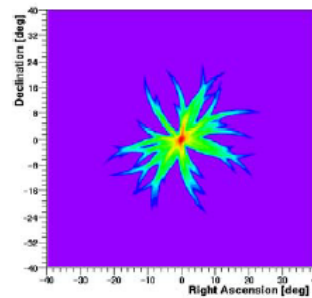
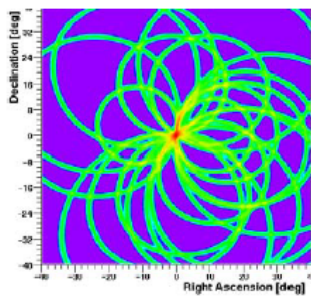
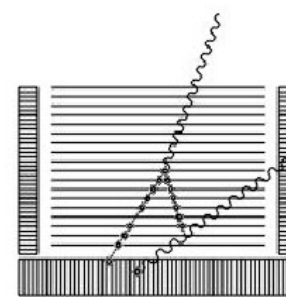
Classical Compton
Event Circles
(no electron tracking)



Reduced Compton
circles of events
with electron track



Direct imaging of pair-
creation events

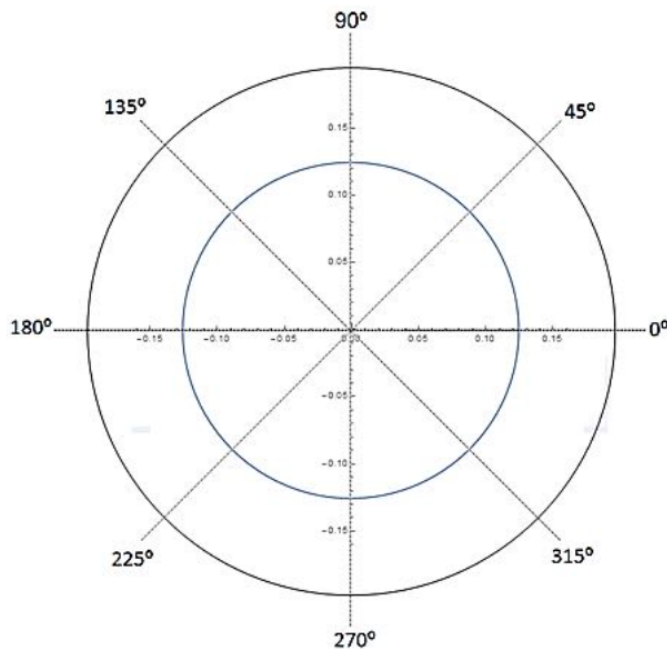


Compton Polarimetry

Compton Polarimetry

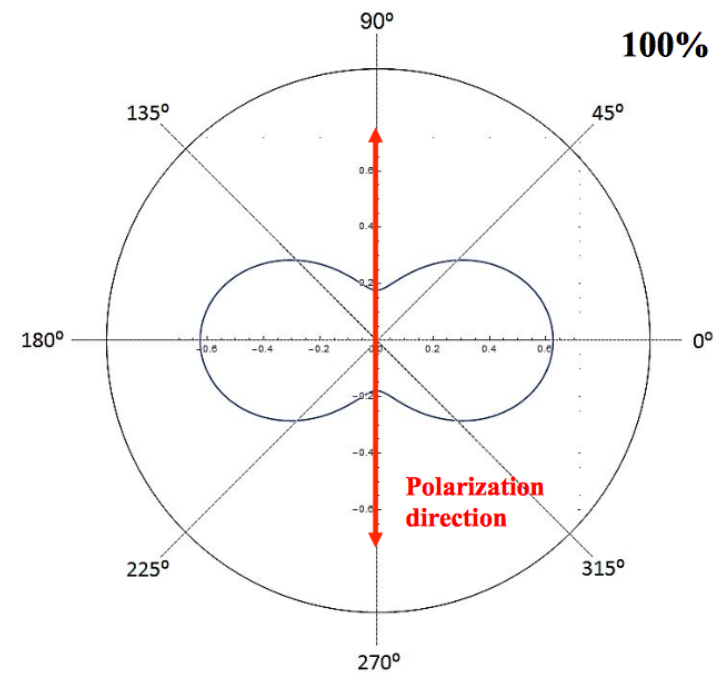
Unpolarized Beam

$$\frac{d\sigma_{KN,U}}{d\Omega} = \frac{1}{2} r_0^2 \varepsilon^2 [\varepsilon + \varepsilon^{-1} - \sin^2 \theta]$$



Polarized Beam

$$\frac{d\sigma_{KN,P}}{d\Omega} = \frac{1}{2} r_0^2 \varepsilon^2 [\varepsilon + \varepsilon^{-1} - 2 \sin^2 \theta \cos^2 \eta]$$



Compton Polarimetry

Compton Polarimetry

Polarization modulation factor

Klein-Nishina cross-section for linearly polarized photons:

$$\frac{d\sigma}{d\Omega} = \frac{r_0^2}{2} \left(\frac{E'}{E} \right)^2 \left[\frac{E'}{E} + \frac{E}{E'} - 2 \sin^2 \theta \cos^2 \varphi \right]$$

$$Q = \frac{N_{\perp} - N_{\parallel}}{N_{\perp} + N_{\parallel}} \quad Q = \frac{d\sigma(\varphi = 90) - d\sigma(\varphi = 0)}{d\sigma(\varphi = 90) + d\sigma(\varphi = 0)}$$

$$Q = \frac{\sin^2 \theta}{\frac{E'}{E} + \frac{E}{E'} - \sin^2 \theta}$$



Minimum Detectable Polarization 3σ

$$MDP = \frac{4.29}{A \cdot \varepsilon \cdot \phi_s \cdot Q_{100}} \sqrt{\frac{A \cdot \varepsilon \cdot (\phi_s + \phi_B)}{T}}$$

ϕ_s – source flux

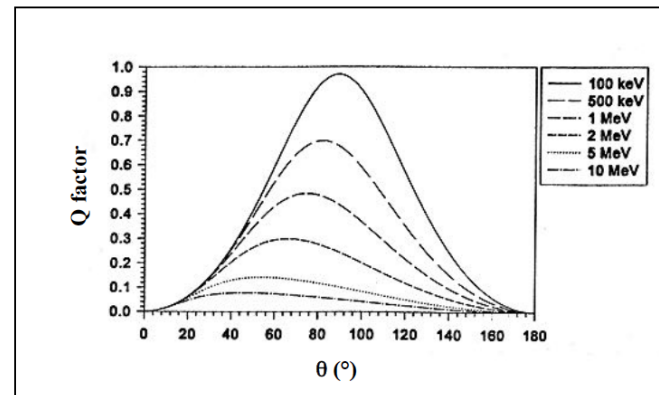
ϕ_B – background flux

Q_{100} – polarimetric modulation factor for 100% radiation

ε – detector double event efficiency

A – detector area

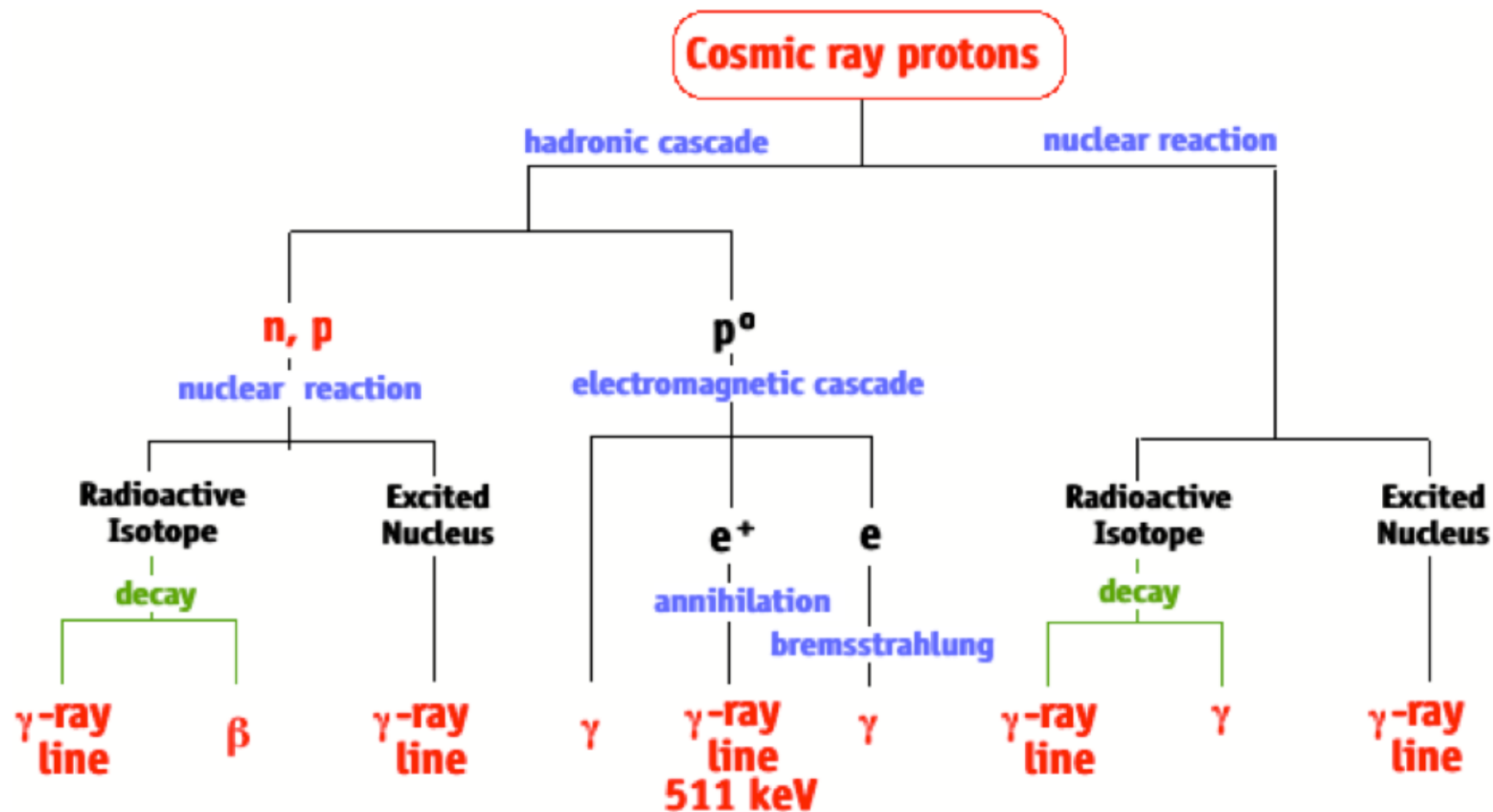
T – observation time



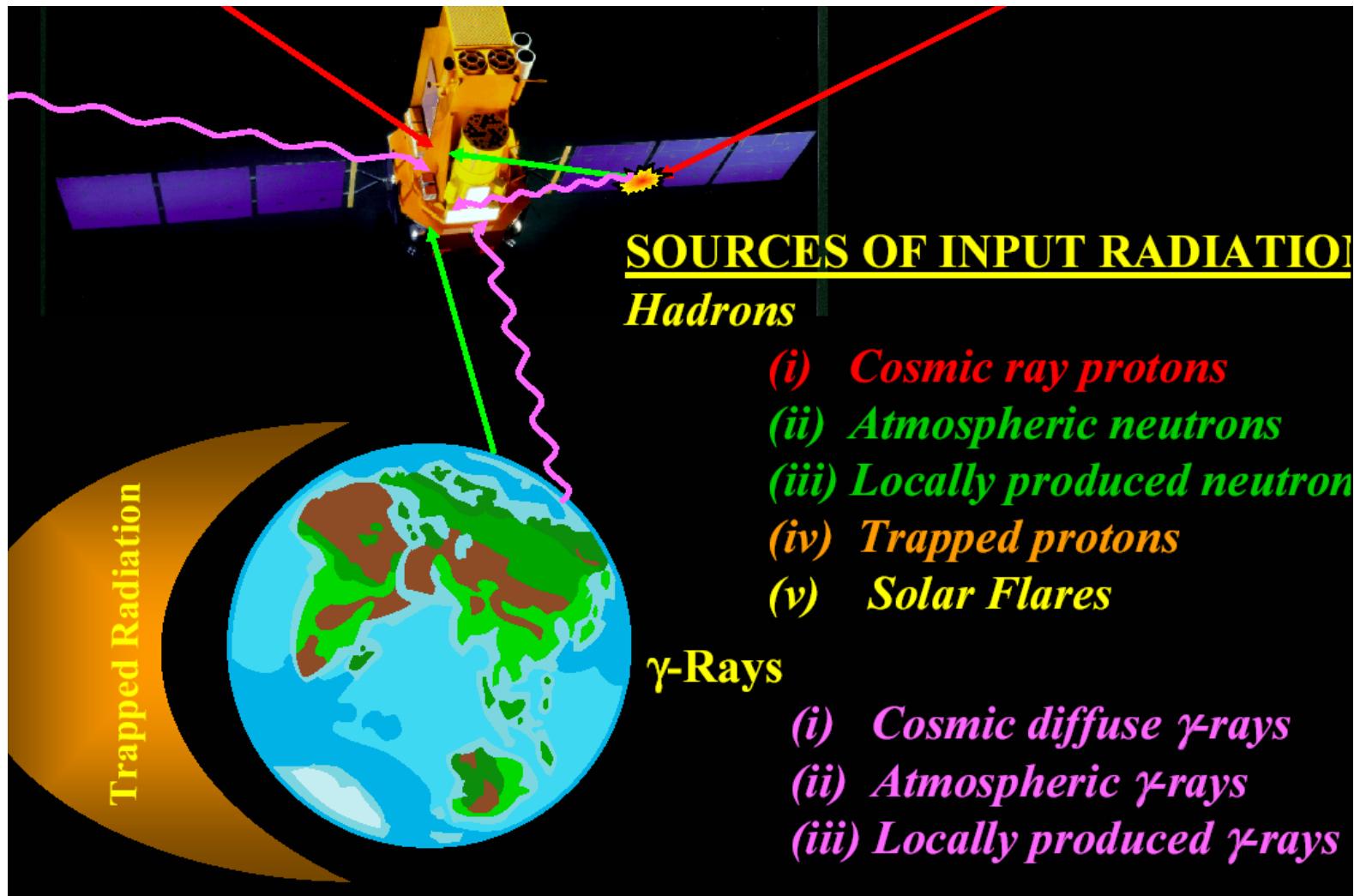
Il background- 1

- **Il fondo di un telescopio X e gamma consiste dei segnali misurati dal rivelatore NON dovuti alla sorgente osservata**
- **Parametro fondamentale nel calcolo della sensibilità**
- **Difficilmente calcolabile con precisione PRIMA della operatività in orbita del telescopio:**
 - **Simulazioni MC**
 - **Valutazioni geometriche**
 - **Environment dello spacecraft**
 - **Orbita**
 - **Attività solare**
 - **Geometria dello strumento e del telescopio**

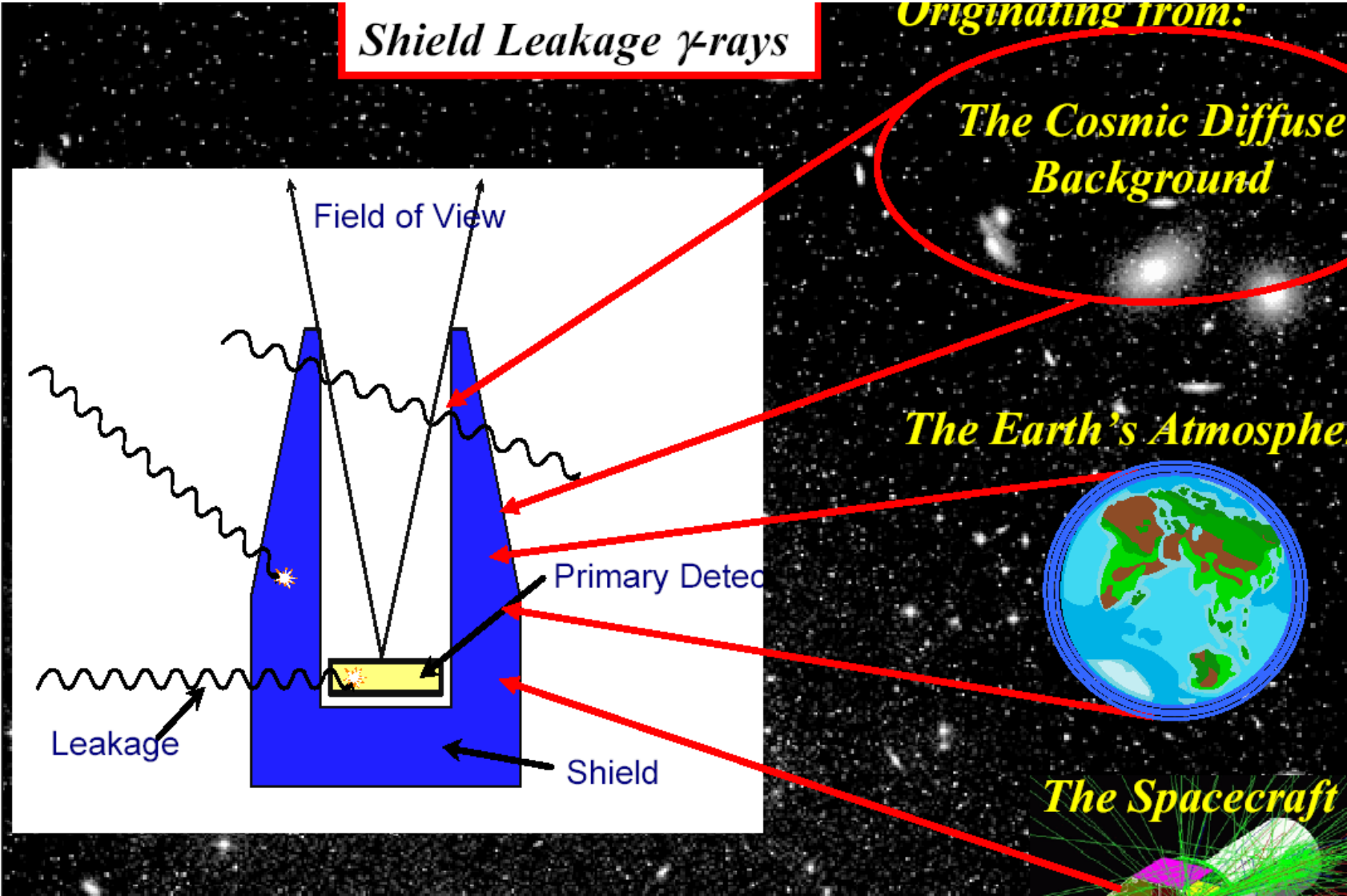
Cosmic Ray interactions and γ -ray background



Background

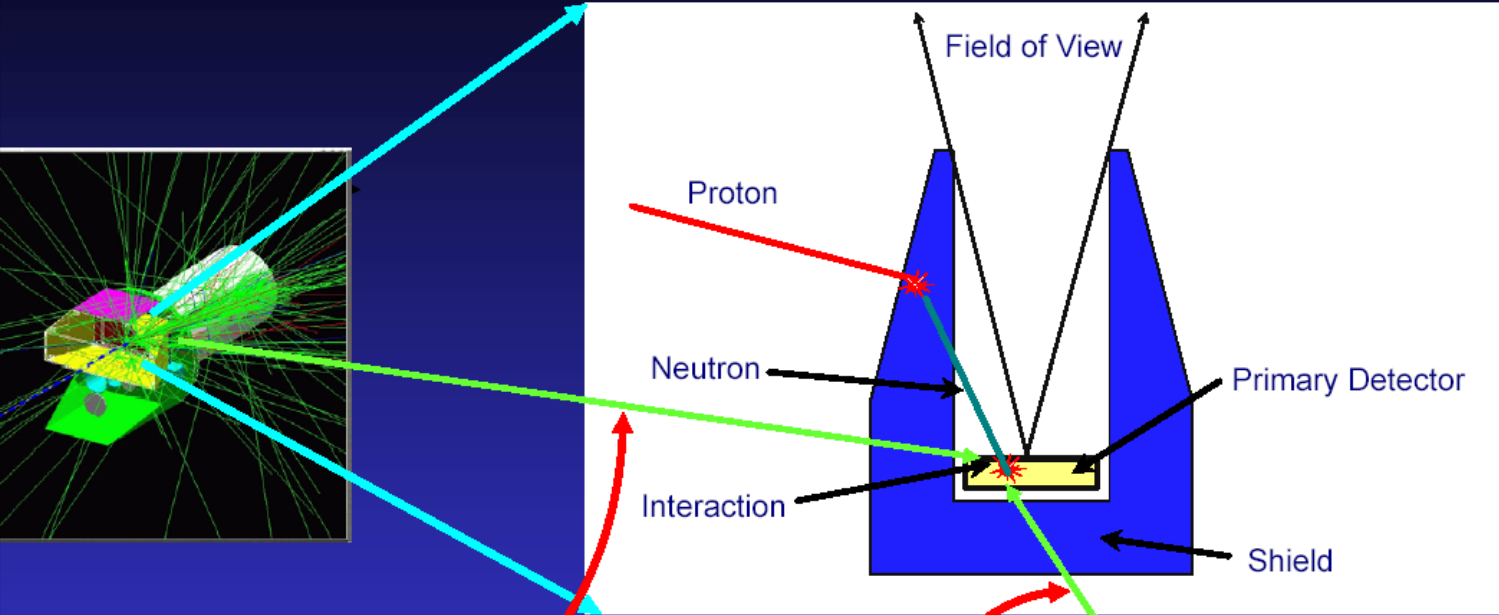


Background



Background

Neutron Induced Background



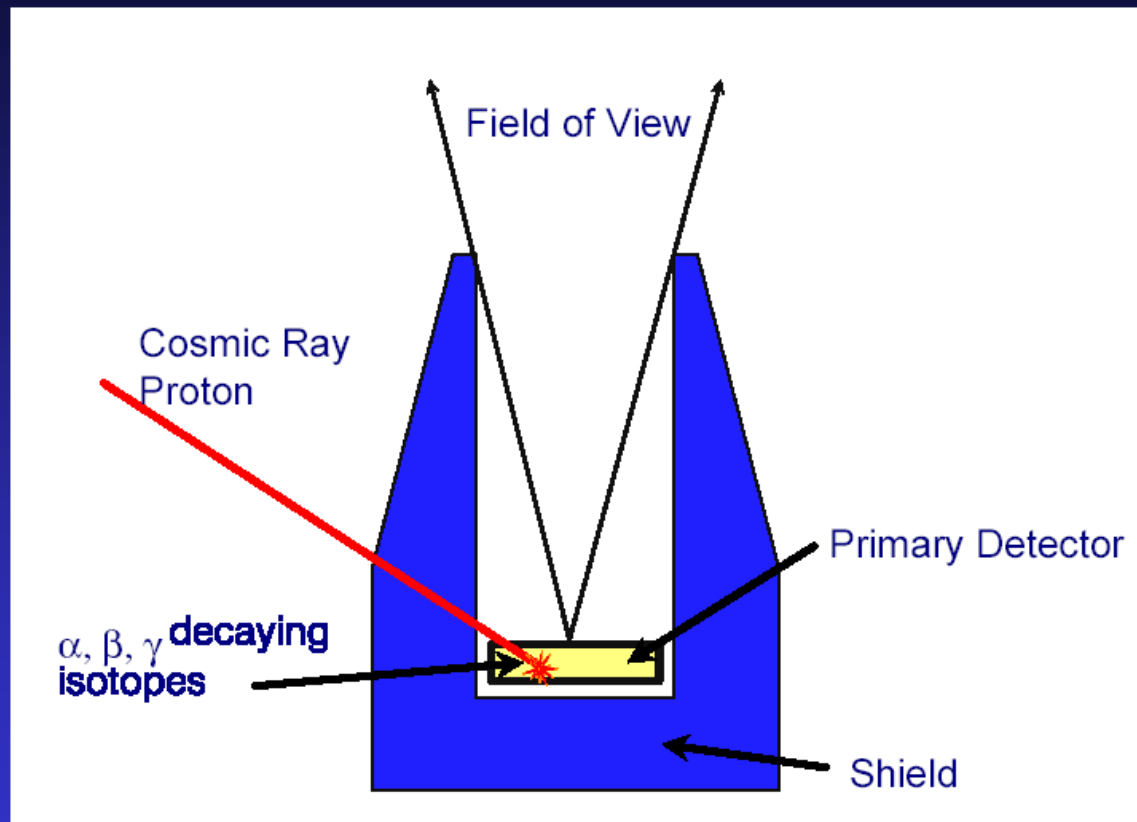
Neutron from another part of the spacecraft

Neutron from the Earth's atmosphere



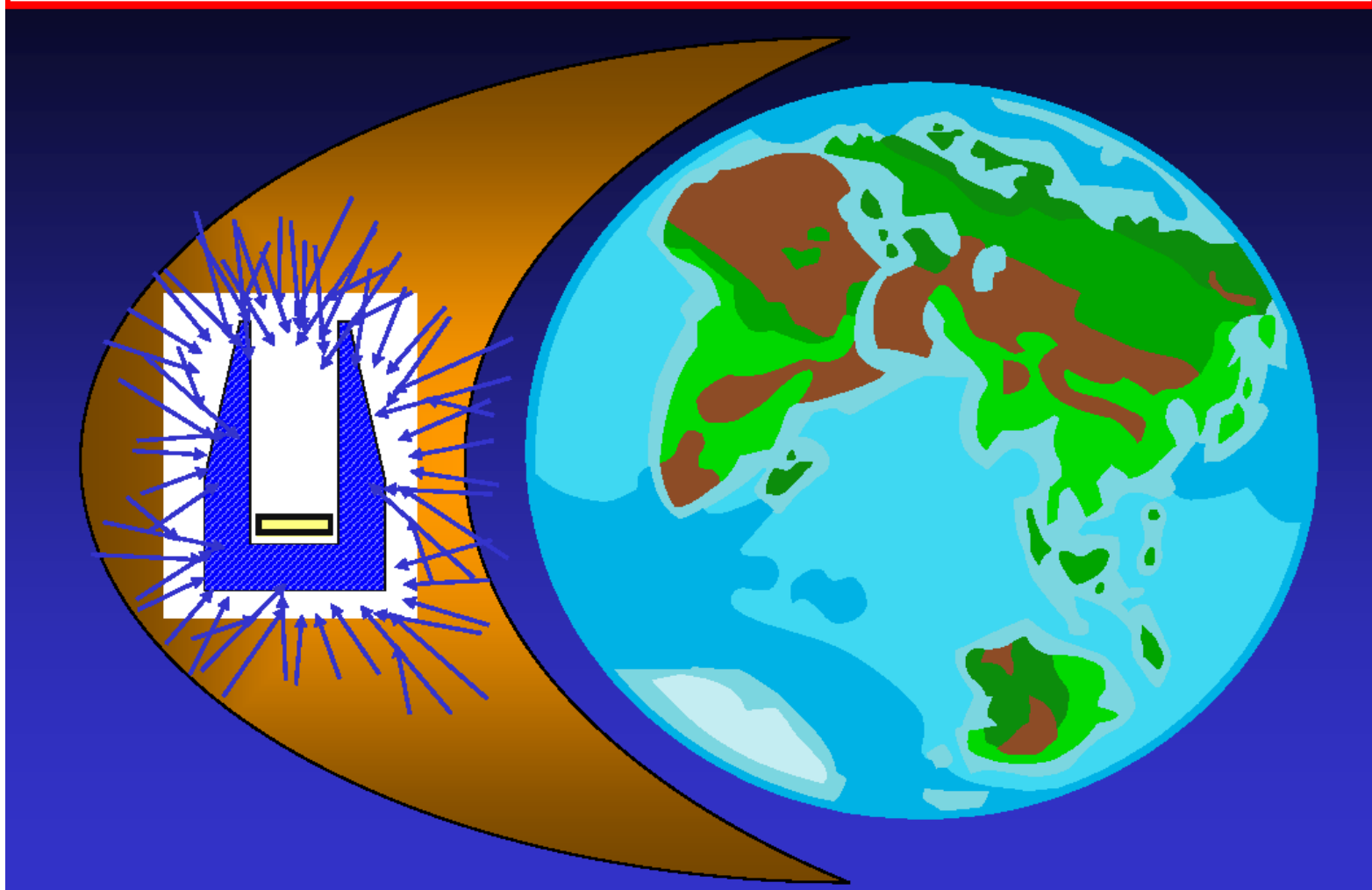
Background

Spallation Induced Background

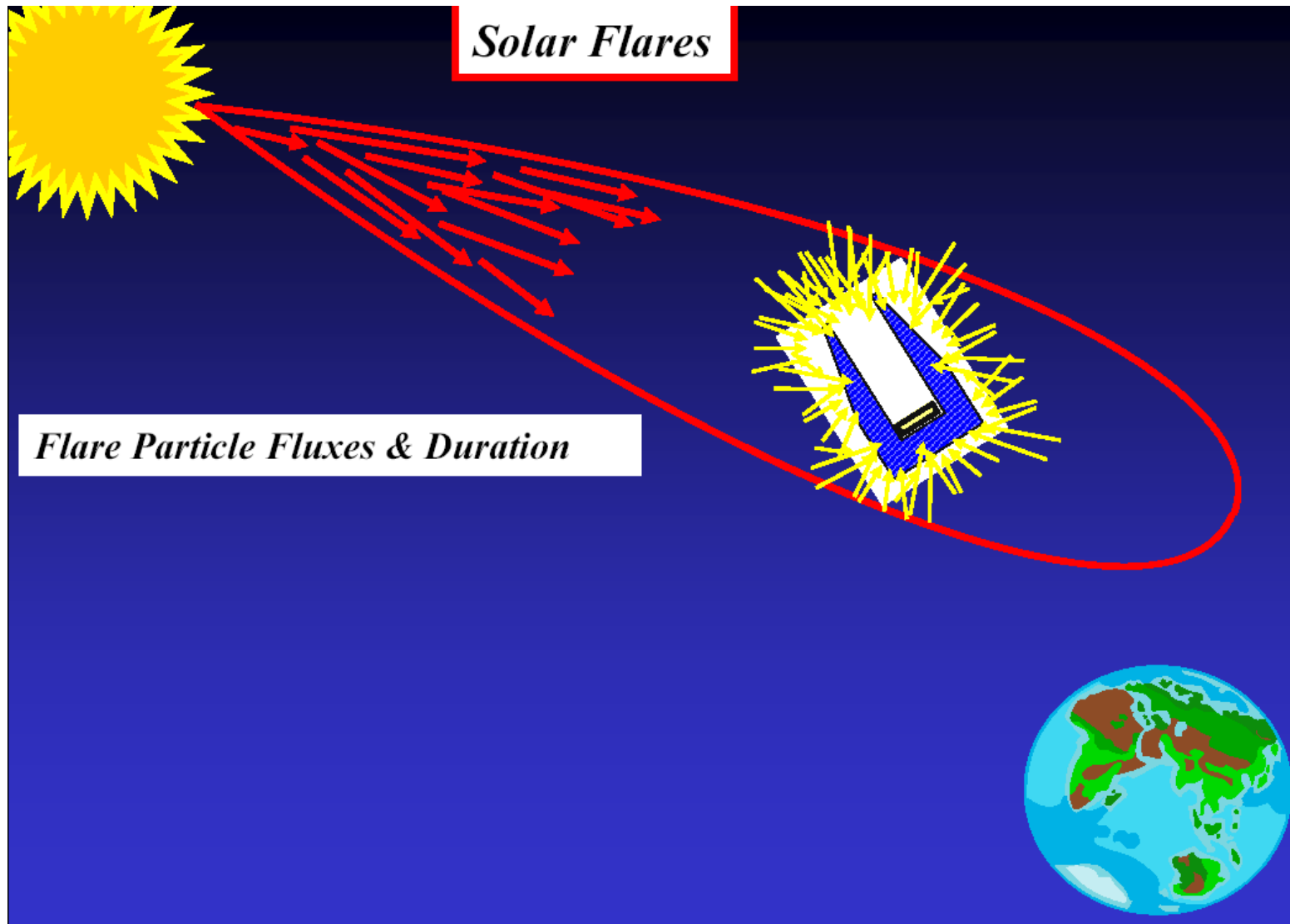


Background

Radioactivity Caused by Particle Bombardment in the Trapped Radiation Belts



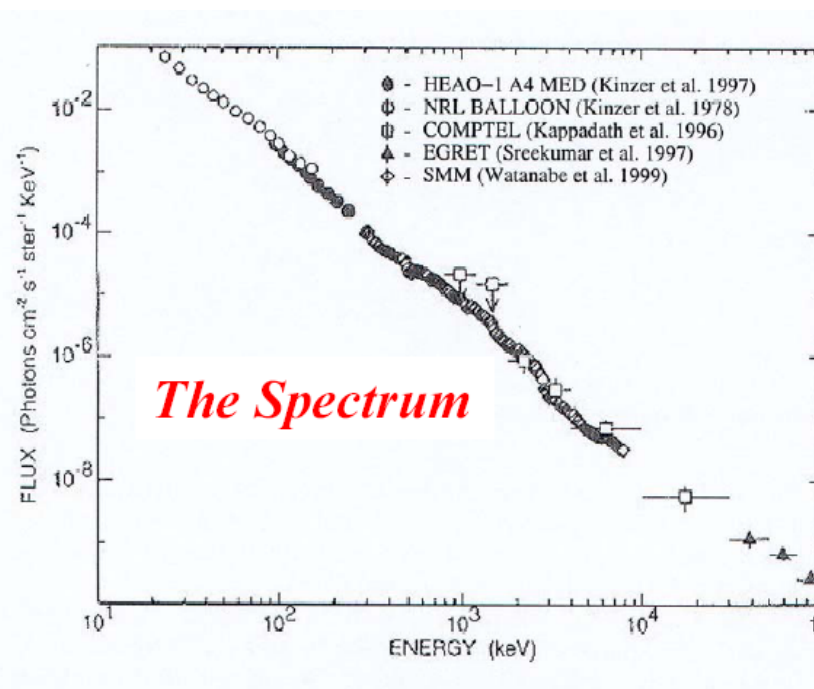
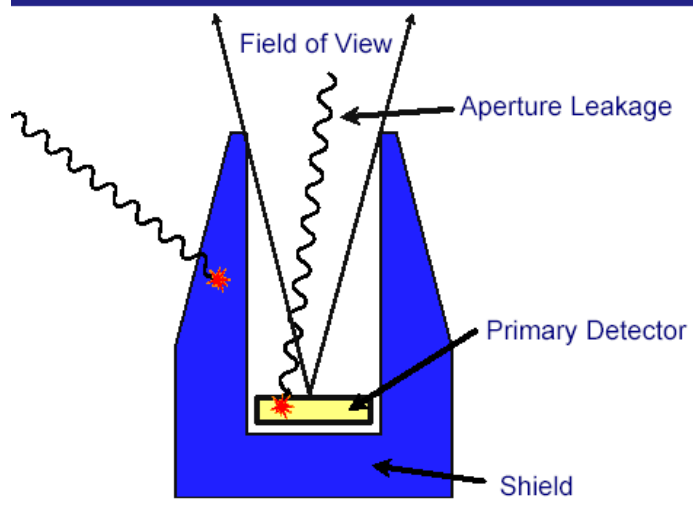
Background



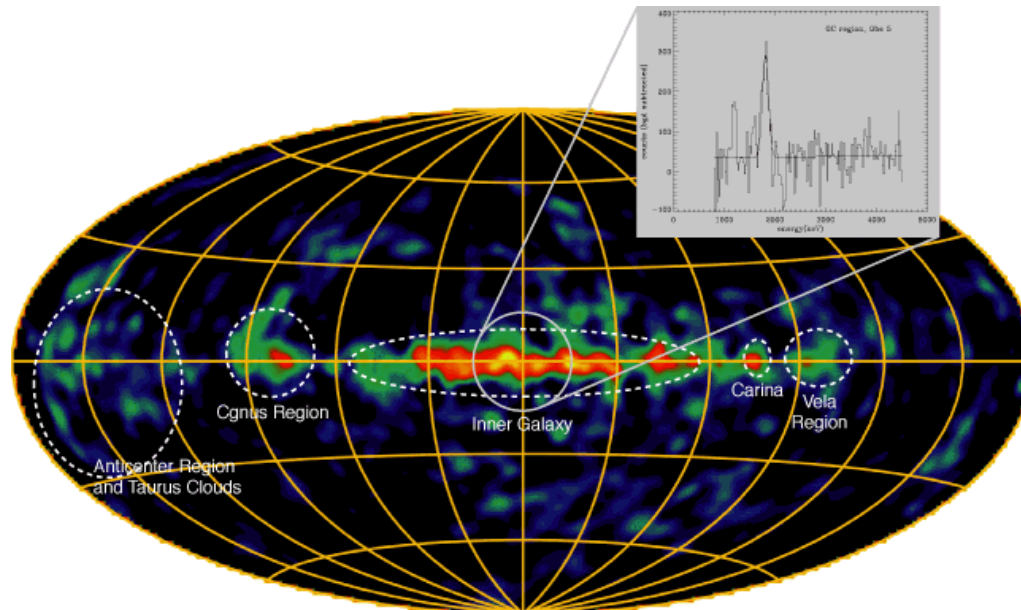
Background

Cosmic Diffuse γ -rays

These γ -rays enter directly through the aperture of the telescope

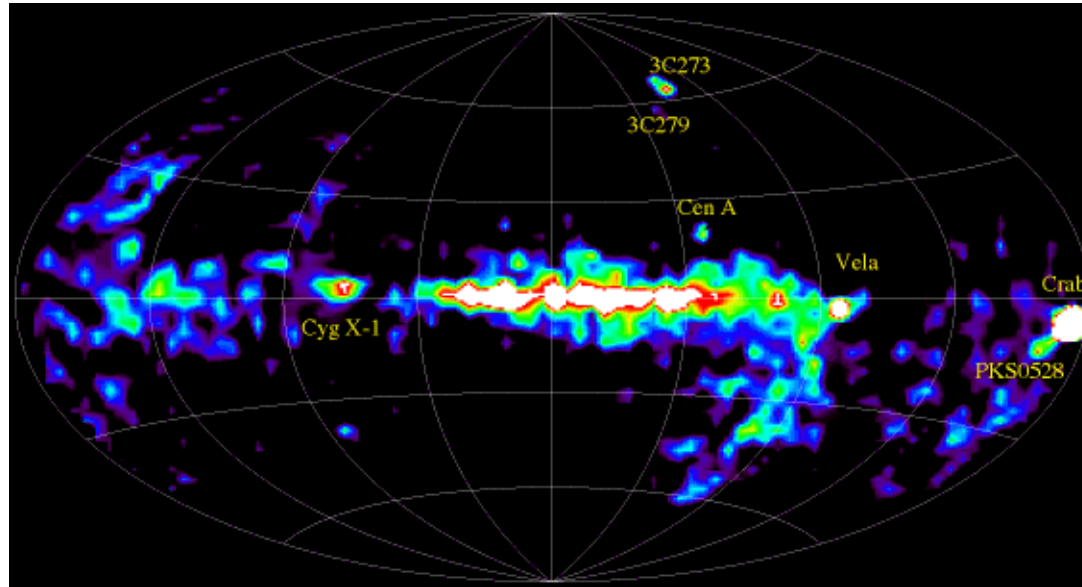


The Compton Gamma Ray Observatory



This COMPTEL image is taken at energy of **1.809 MeV**, which corresponds to the gamma-ray line produced by the radioactive decay of the ^{26}Al isotope. ^{26}Al has a decay time of a million years, and is produced along with other elements in trace quantities at cosmic sites of **nucleosynthesis**. Therefore, the sky image in these gamma-rays integrates nucleosynthesis events over millions of years and shows the spatial distribution of these events. From the above image we learn that ^{26}Al -producing events are predominantly Galactic sources. Several localized regions appear prominent (Inner Galaxy, Cygnus, Vela), suggesting that massive stars (via their Wolf-Rayet winds and core-collapse supernovae) are the true sources. The insert shows the spectral information captured by COMPTEL. The ^{26}Al line at 1.809 MeV is clearly seen above the large instrumental background. COMPTEL is the first imaging instrument with a spatial resolution of roughly degrees, and thus made possible this all-sky survey of ^{26}Al radioactivity. The Galaxy is transparent to gamma-rays, therefore this image has, for the first time, shown us the locations of nucleosynthesis and **massive stars** throughout the Galaxy.

The Compton Gamma Ray Observatory



The COMPTEL 1 to 30 MeV all-sky map in continuum gamma radiation represents the results of the first-ever survey of the sky at these energies. The concentration of the emission along the **Galactic plane** is the most striking aspect of the map. The plane stands out clearly against the rest of the sky indicating that most of the measured gamma-ray fluxes come from regions or objects inside the Galaxy. The dominant Galactic continuum emission seems to come from interstellar space and is visible as diffuse Galactic radiation. Superimposed on the large-scale Galactic emission are **point-like sources** (like Crab, Vela, Cyg X-1), but many of the Galactic point sources remain unidentified at this time. A significant contribution of unresolved point sources to the apparently diffuse Galactic emission cannot be excluded. At medium and high Galactic latitudes, a few of the gamma-ray blazars, discovered by EGRET, are visible in the COMPTEL map as well. Examples are 3C 273, 3C 279, and PKS 0528+134. The radio galaxy Cen A is also visible at MeV gamma rays. Some of the extragalactic objects detected by COMPTEL are not visible in this map, because they flare up only occasionally: on average they are too weak to be visible in this time-averaged all-sky map.

Compton Astrophysics

Astrophysics of low/medium Energy γ - rays

The energy range from a few 100 keV to several 10 MeV is scaled by the electron rest mass $m_e c^2 = 0.511$ MeV

- continuous γ -ray spectra from sites of high-energy particle acceleration are mostly produced in e-m interactions:
Bremsstrahlung, inverse Compton scattering, Synchrotron
Many of these sources have their maximum Luminosity at MeV energies

and by the nuclear energy levels

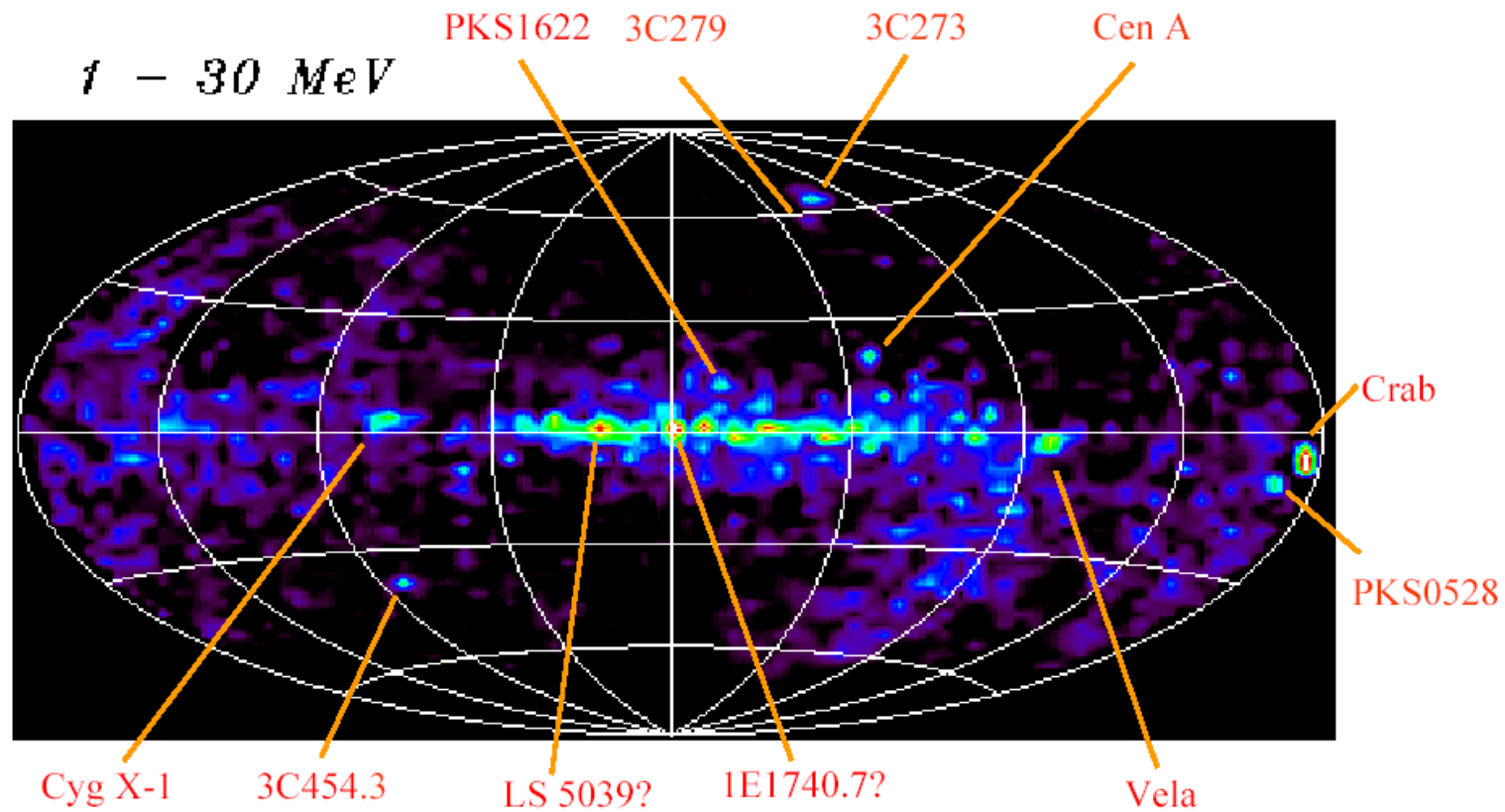
- Signatures of cosmic radioactivity through γ -ray lines: the direct observation of nucleosynthesis, i.e. the creation of the elements,

Compton Astrophysics

Sky Survey

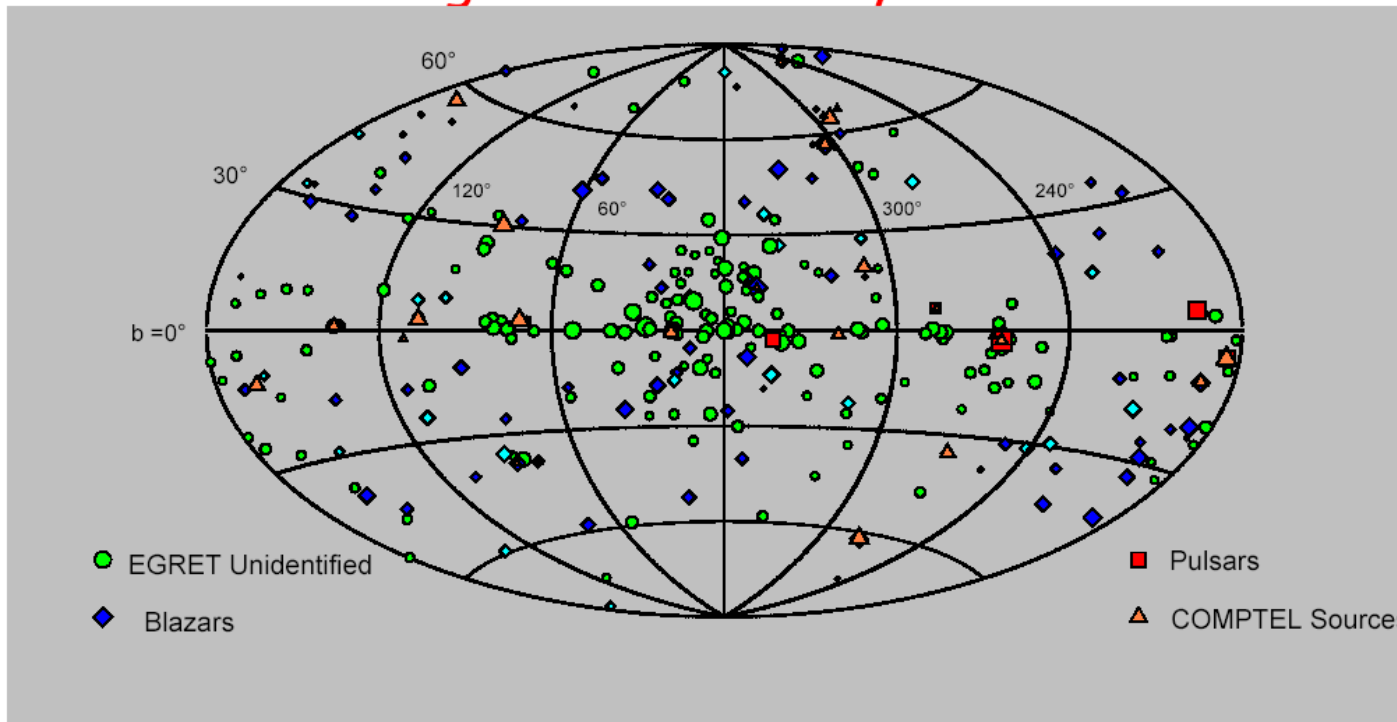
COMPTEL

1 - 30 MeV



Compton Astrophysics

Catalog of Gamma-Ray-Sources



3. EGRET Catalog:
(3EG)
Hartman et al, 1999
ApJS, 123, 79

271 Sources
80-90 AGN
6-8 PSR
~170 Unid..

1. COMPTEL Katalog:
Schönfelder et al., 2000
A&AS, 143, 145

32 constant Srces.
39 transient
11 AGN
3 PSR
4 EGRET Unid.

July 2002

~

Compton Astrophysics

Cosmic Accelerators:

- **Accretion on compact objects (relativistic jets):**

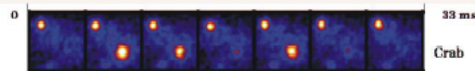
AGN, μ Blazars, Binaries



- **Explosions and Shocks:**

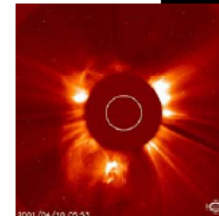
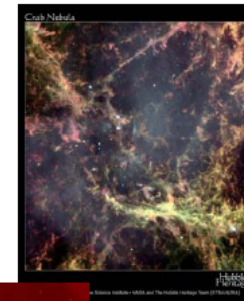
GRBs, SNRs, mass. stellar winds, ISM
Novae, Supernovae

- **Rotation of NS: pulsars**



-

electro-magnetic dissipation: solar flares



July 2002

Compton Astrophysics

Origin and characteristics of astrophysically important γ -ray lines

Isotope	Energy	$t_{1/2}$	origin
^{57}Ni	1378 keV	2.14 d	SN
^{56}Ni	812 keV	8.5 d	SN
^{56}Co	847 keV 1238 keV	111.5d	SN
^{22}Na	1275 keV	3.8 yr	Novae
^{44}Ti	1157 keV	79 yr	SNR
^{26}Al	1809 keV	1Myr	AGB and massive stars (O & WR), Novae, core-collapse SNe
$^{12}\text{C}^*$ $^{16}\text{O}^*$	4.4 MeV 6.1 MeV	prompt	cosmic ray induced ISM lines, flares
e^+, e^-	511 keV		β^+ activity, jet sources, PSR, Novae, flares etc.
$n+p \rightarrow d$	2.21 MeV		flares, flare stars?

Compton Imaging

Sensitivities

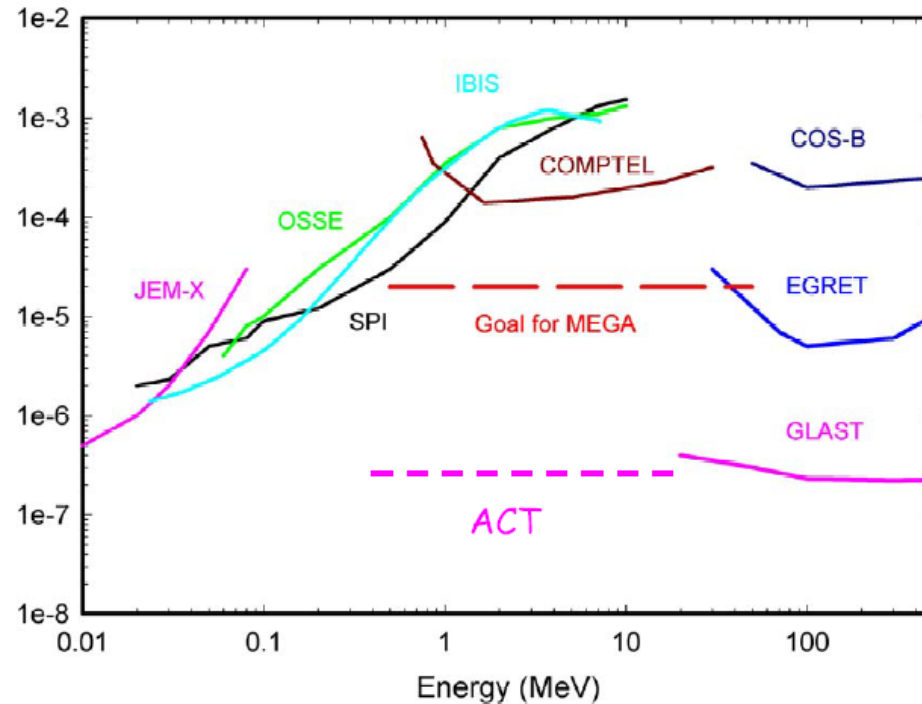
Generations of γ -ray Missions:

1. COMPTTEL \leftrightarrow COS-B

2. MEGA (~2006) \leftrightarrow EGRET

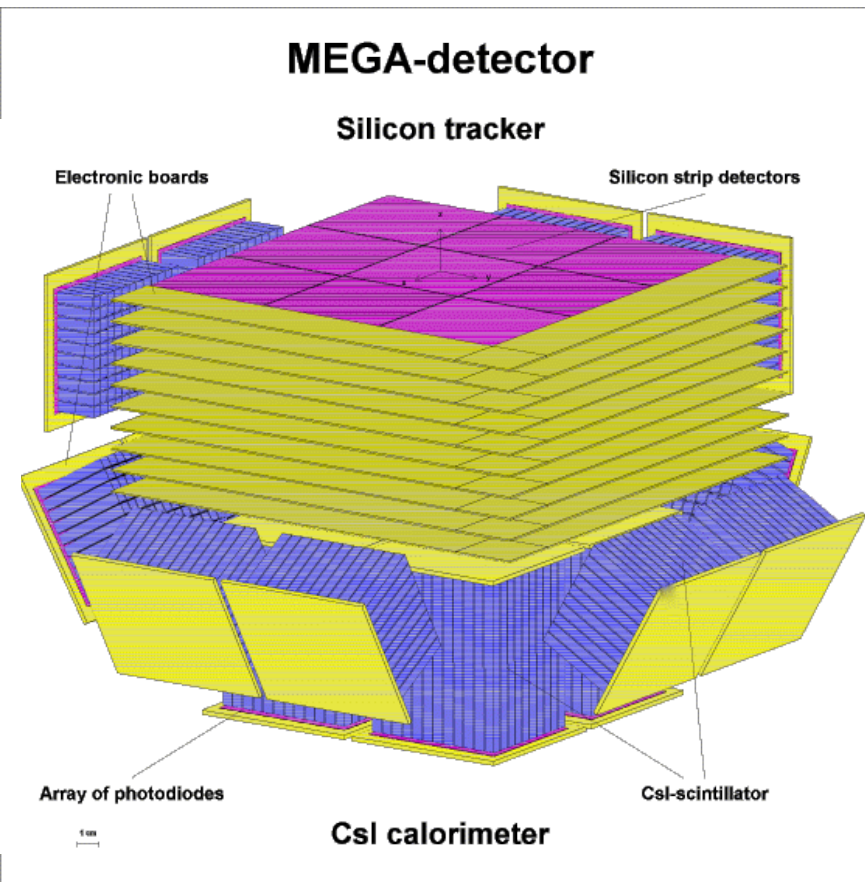
3. Advanc^d Compton \leftrightarrow GLAST
(ACT, ~2012) (~2006)

Continuum Sensitivity * E^2
[MeV cm⁻² s⁻¹] $T_{\text{obs}}=10^6$ s, $\Delta E = E$



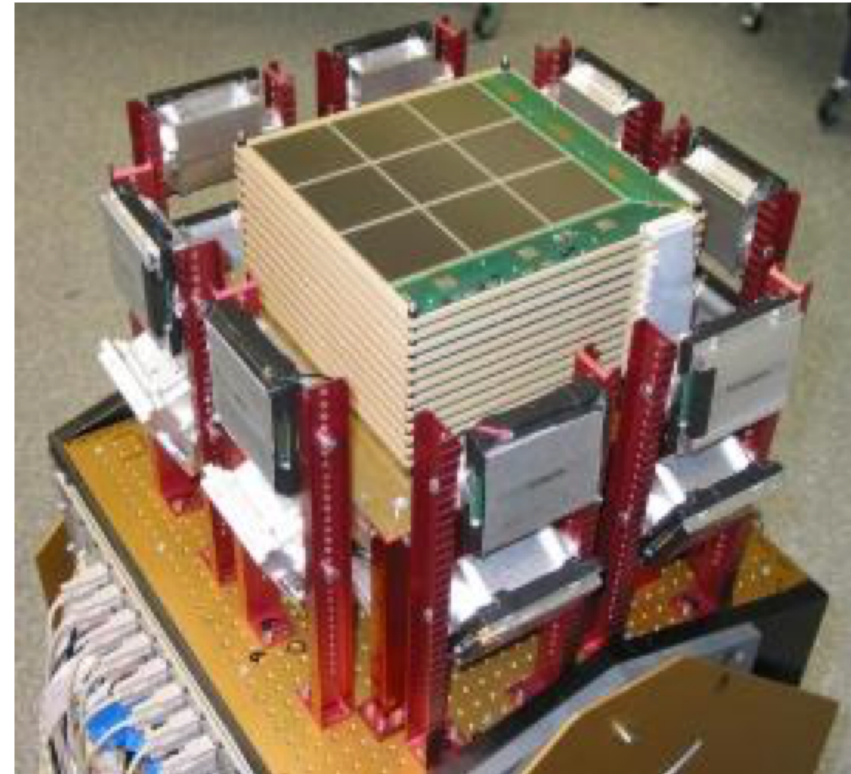
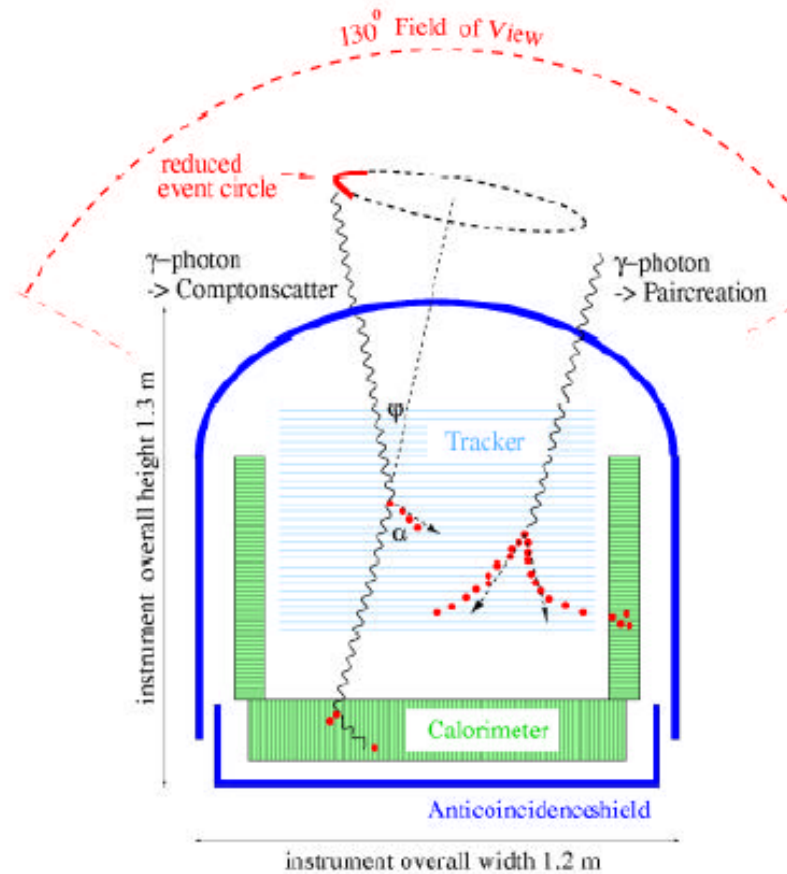
MEGA

MEGA is planned as a telescope for **Medium Energy Gamma-Ray Astronomy** in the energy range between 400 keV and 50 MeV. In this energy range MEGA exploits the two dominating interaction mechanisms for gamma rays: Compton scattering and Pair creation. MEGA has two detectors: A tracker, consisting of double-sided silicon strip detectors, and a calorimeter, consisting of highly segmented CsI(Tl) bars. In the tracker the Compton and Pair interactions take place and the direction and energy of the participating electrons and positrons is measured. In the calorimeters the Compton scattered gamma rays are stopped and thus their energy and direction is determined.



<http://www.gamma.mpe-garching.mpg.de/MEGA/mega.html>

MEGA



<http://www.gamma.mpe-garching.mpg.de/MEGA/mega.html>

ACT project

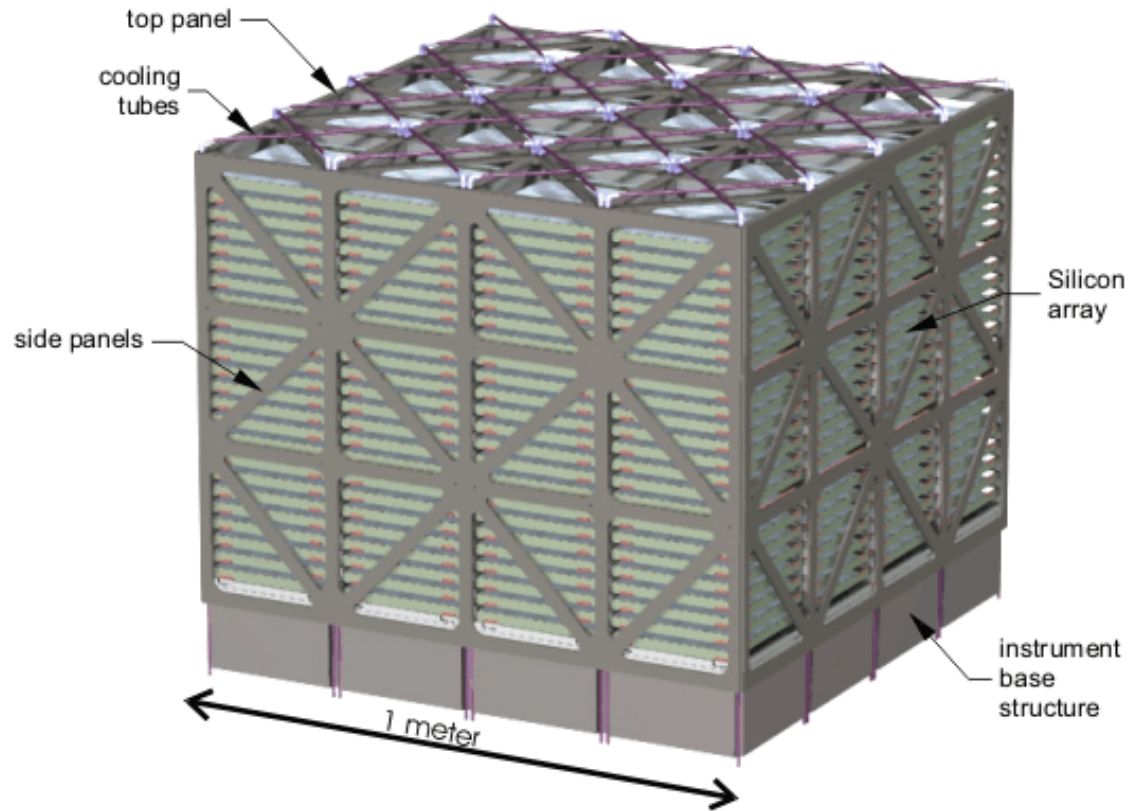
Energy Range	0.2 - 30 MeV Compton mode
Energy Resolution	$\leq 10\text{keV FWHM @ } 1\text{ MeV}$
Field of View	> 4 steradian
Angular Resolution	1 deg
Source Localization	5 arcmin for bright sources
Line Sensitivity in 1.0E6 sec	1.0E-7 ph/(cm ² s) (narrow) 5.0E-7 ph/(cm ² s) (broad)
Continuum Sensitivity	1.0E-5 ph/(cm ² sMeV) @ 0.5 MeV
Polarization Sensitivity	1%, 2.0E-3 ph/(cm ² sMeV) 10%, 2.0E-4 ph/(cm ² sMeV)

These science requirements are expected to translate to an instrument with effective area on the order of 1000-3000 cm², a position resolution in the detectors of 1mm³, energy resolution of 1% (0.5-2.0 MeV) or better, and possibly recoil electron tracking capabilities for electron energies < 0.5 MeV. The concept study will look at a variety of possible detector technologies for implementing such a Compton telescope. Candidate detectors include, but are not limited to, CZT strip detectors, Si strip detectors, Ge strip detectors, liquid Xe, and gaseous Xe (or Ar) microwell detectors.

<http://boggs.ssl.berkeley.edu/act/index.html>

<https://arxiv.org/abs/astro-ph/0608532>

ACT project



The baseline instrument (pictured above) is built from thick Silicon(Li) detectors, and measures roughly 1 m x 1 m in frontal area. The individual detectors are ~ 7 mm thick, and measure 10 x 10 cm in area using technology in crystal growth and lithium drifted silicon, or Si(Li). Detectors are assembled in tower structures, each containing a small 4x4 array of detectors and stacked 24 layers deep. Readout electronics for the detectors are distributed along the four side walls of each tower.

New MeV concepts



National Aeronautics and Space Administration
Goddard Space Flight Center

Astrophysics Science Division • Sciences and Exploration

Home Registration Directions/Hotel Program Participants

Future Space-based Gamma-ray Observatories

March 24-25, 2016
Goddard Space Flight Center
Building 34, Rooms W150 & W120A/B

The medium energy γ -ray band accessible from space contains a wealth of scientific promise from the study of γ -ray bursts and active galaxies, dark matter annihilation and decay, particle acceleration and cosmic ray production in Galactic and extragalactic sources, cosmic ray interactions in the Milky Way, rotation powered pulsars and magnetars, acceleration processes in the Sun and more. Our appetite for this science has been whetted by many recent exciting results from Fermi (at higher energies) and NuSTAR (at lower energies) and is based on studies of the MeV sky by CGRO/COMPTEL and INTEGRAL. Progress in this exciting field has been limited largely by the challenges of building sufficiently capable instruments to detect these γ rays as they interact by Compton scattering and pair production. The detailed scientific questions within these areas are addressed by a range of different performance optimizations such as flux and polarization sensitivity, angular and energy resolution, photon counting statistics, background rejection, and field of view. Different technical and hardware approaches result in different optimization of these performance parameters.

We will meet March 24-25 at Goddard Space Flight Center in Greenbelt, MD to discuss the Science Drivers for new space-based gamma-ray missions, as well as technologies and instruments concepts for new gamma-ray experiments. This workshop is a continuation of the discussions from the [previous Future Gamma-ray workshop](#).

<http://asd.gsfc.nasa.gov/conferences/fgo2/>

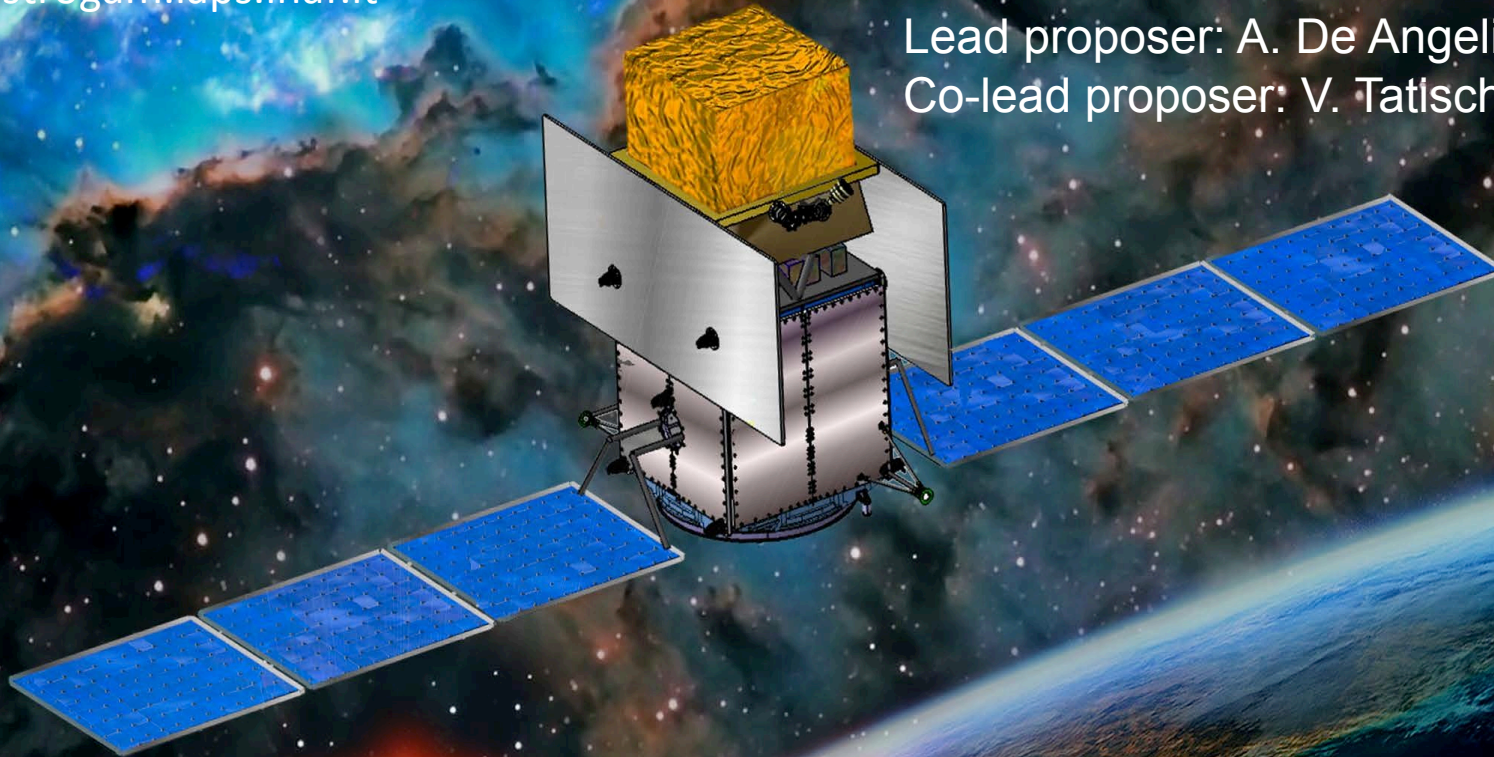
e-ASTROGAM

at the heart of the extreme Universe

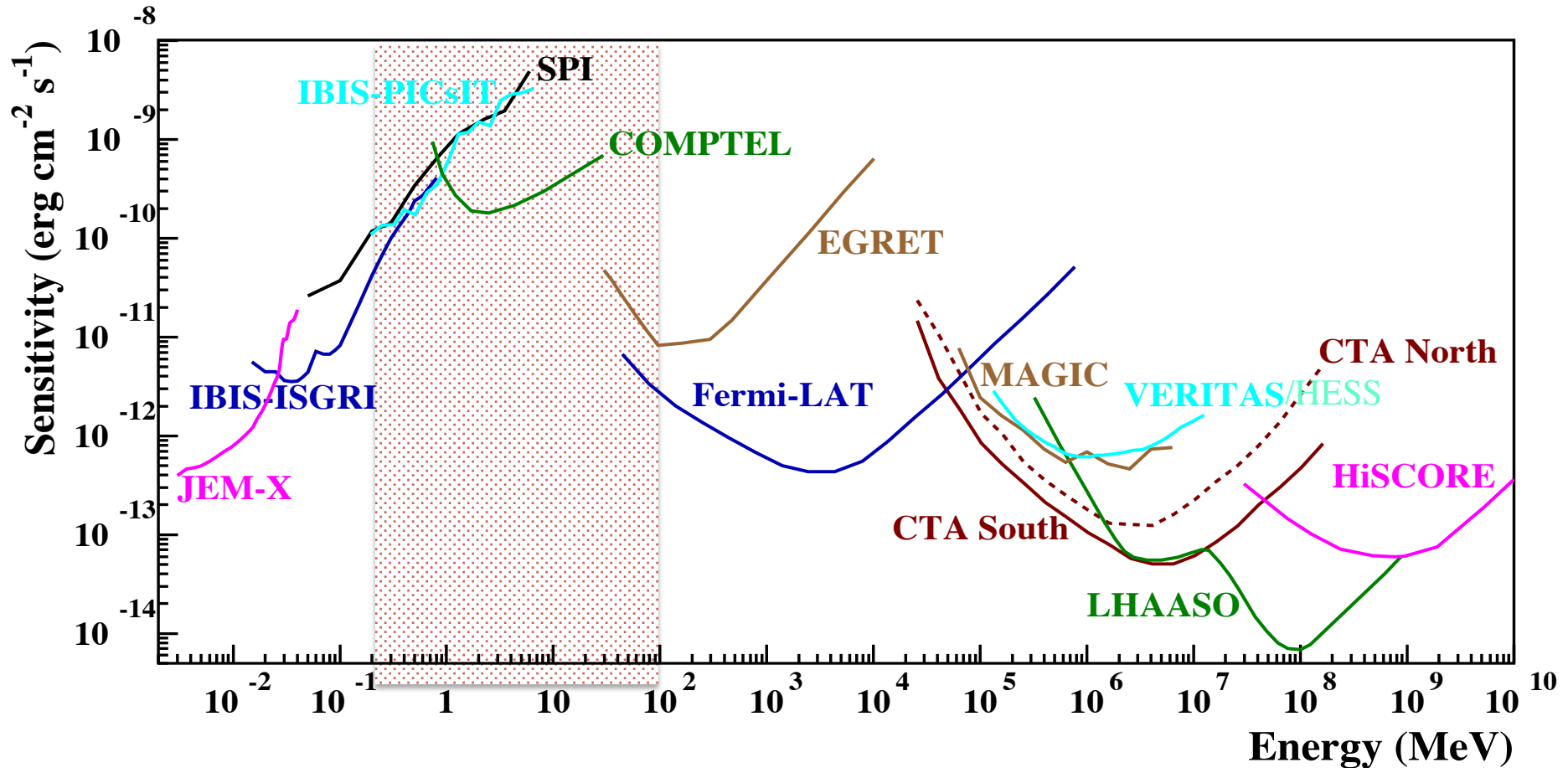
<http://eastrogam.iaps.inaf.it>

An observatory for gamma rays
In the MeV/GeV domain

Lead proposer: A. De Angelis
Co-lead proposer: V. Tatischeff

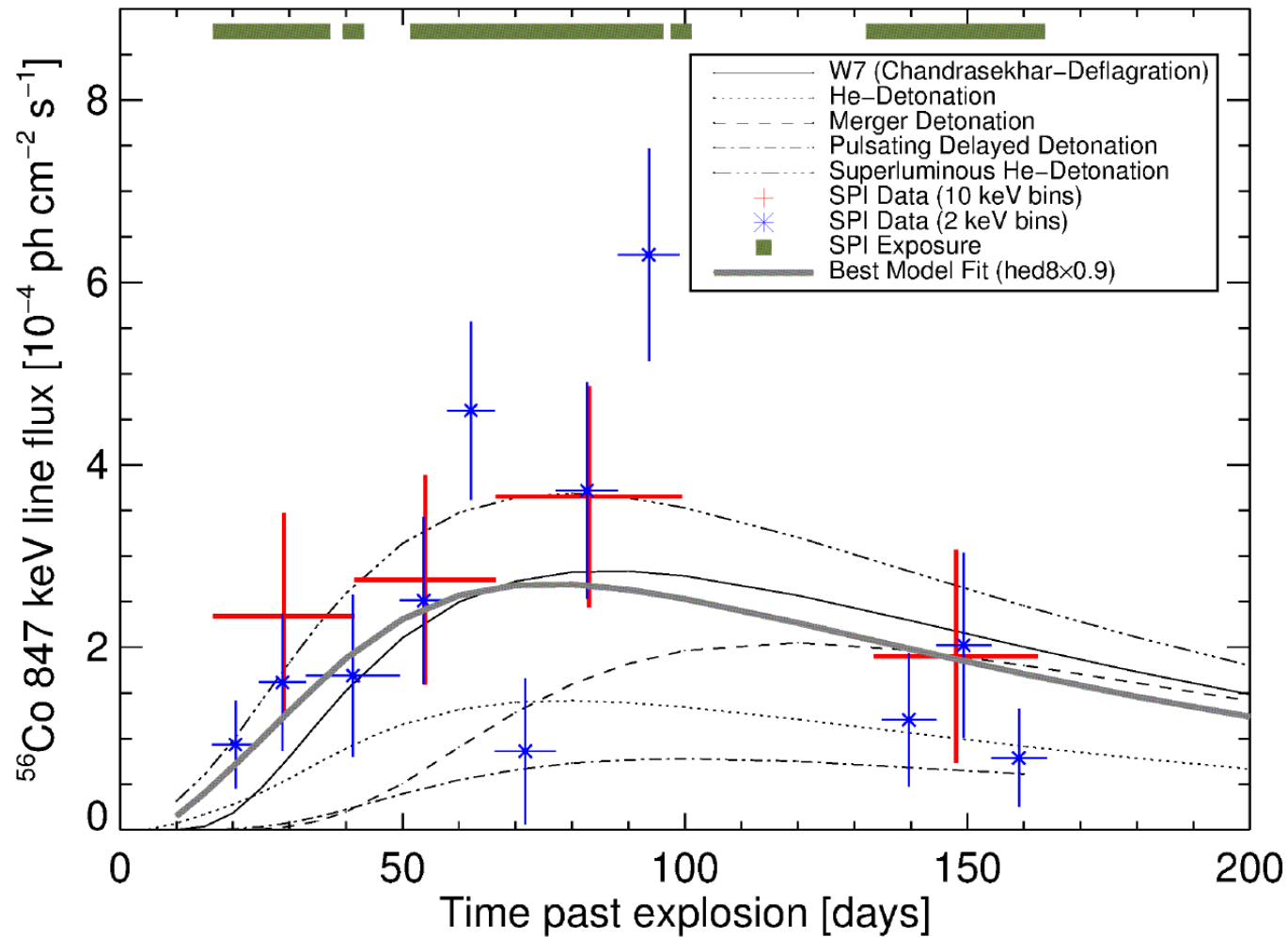


The MeV/GeV domain



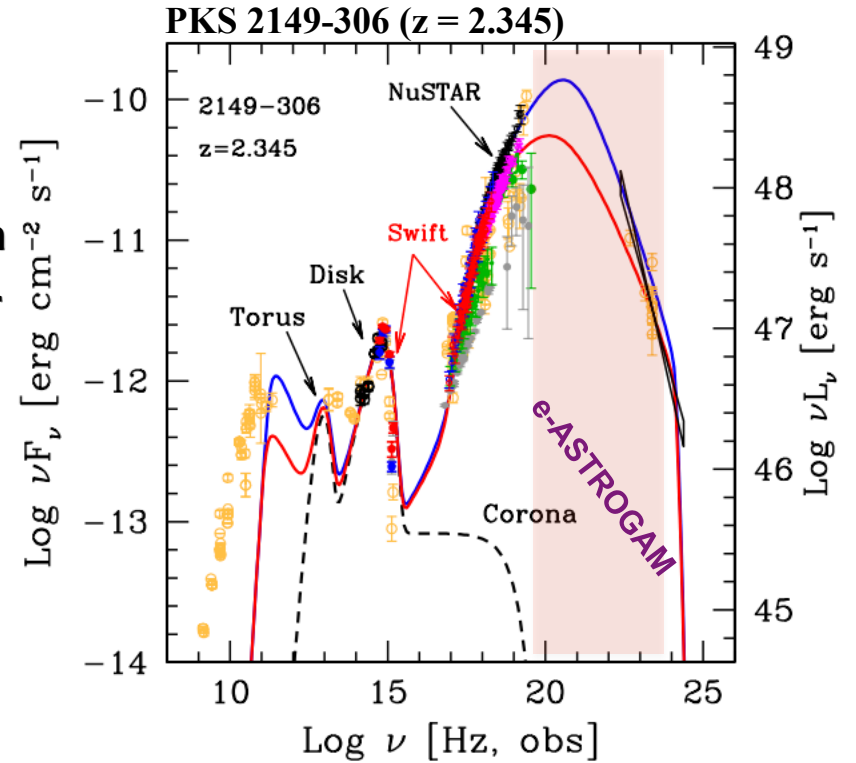
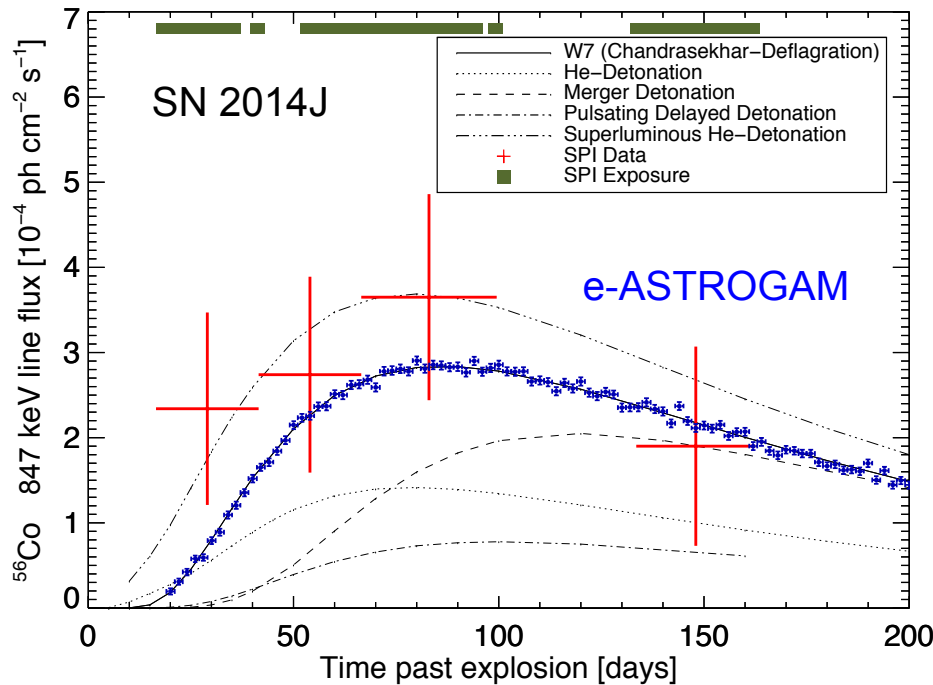
- **Worst covered part of the electromagnetic spectrum** (only a few tens of steady sources detected so far between 0.2 and 30 MeV)
- Many objects have their peak emissivity in this range (GRBs, blazars, pulsars...)
- Binding energies of atomic nuclei fall in this range, which therefore is as important for HE astronomy as optical astronomy is for phenomena related to atomic physics

SPI gamma-ray observations of SN2014 J



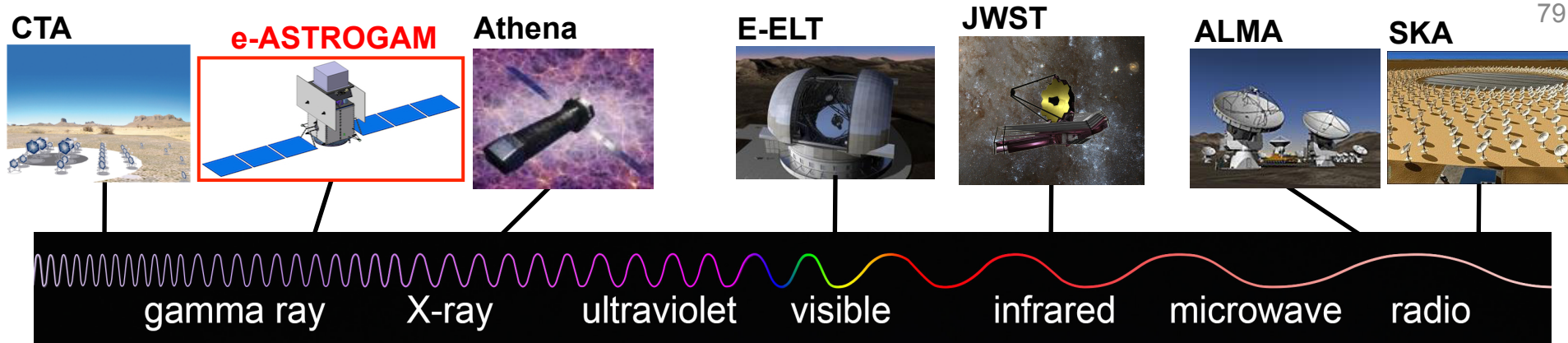
Core science motivations for a γ -ray mission in the MeV/GeV

1. Processes at the heart of the extreme Universe (AGNs, GRBs, microquasars): prospects for the Astronomy of the 2030s
2. The origin and impact of high-energy particles on galaxy evolution, from cosmic rays to antimatter



3. Nucleosynthesis and the chemical enrichment of our Galaxy

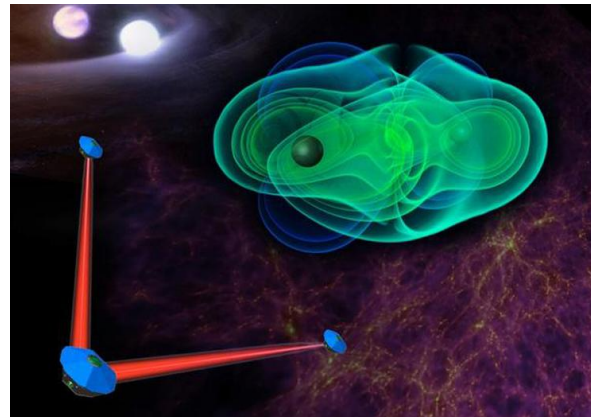
e-ASTROGAM: γ -ray astronomy in context



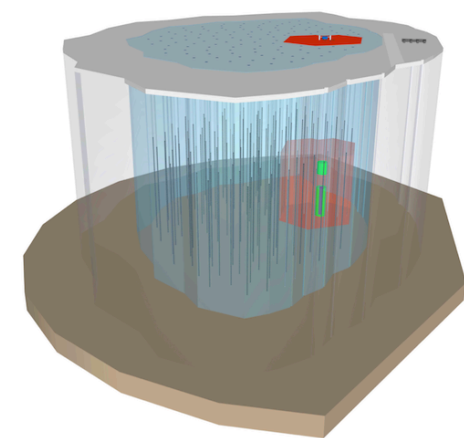
79

New Astronomies:
gravitational waves
neutrinos

eLISA – Gravitational waves



Km3Net/IceCube-Gen2 - ν



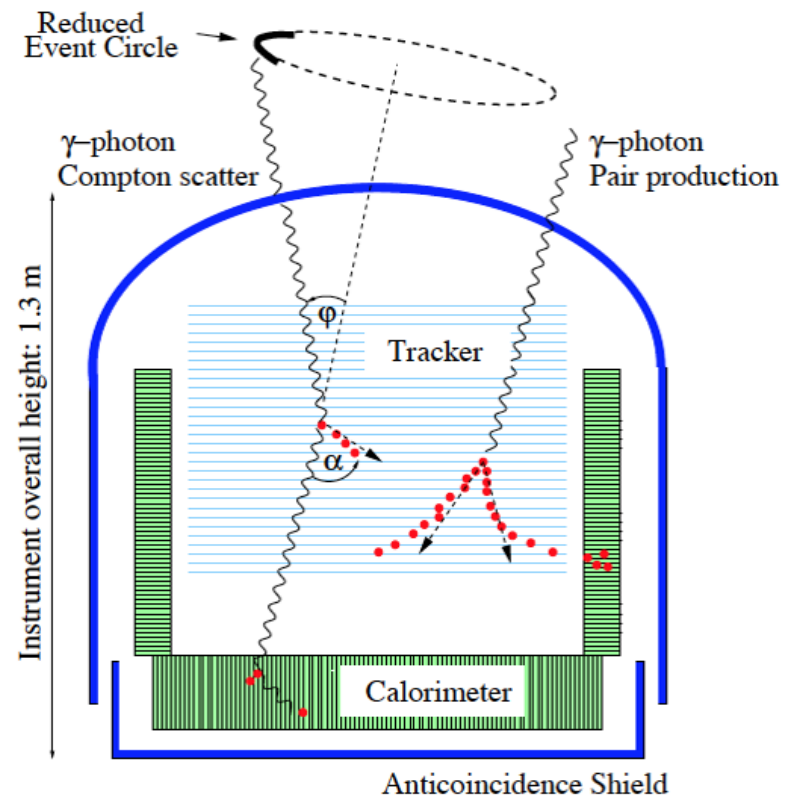
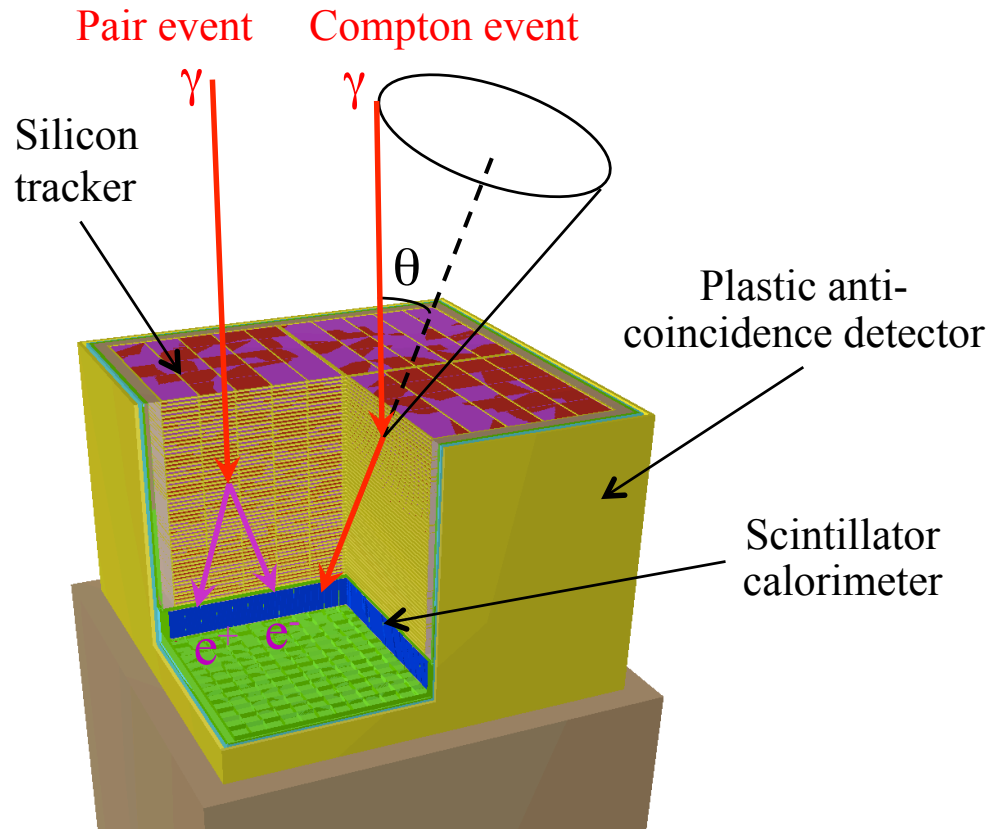
- e-ASTROGAM will be a **sensitive, wide-field γ -ray space observatory** operating at the same time as facilities like SKA and CTA, as well as eLISA and neutrino detectors, to get a coherent picture of the **transient sky** and the sources of **gravitational waves** and **high-energy neutrinos**

e-ASTROGAM scientific requirements

80

1. Achieve a **sensitivity** better than that of INTEGRAL/CGRO/COMPTEL by a factor of 20 - 50 - 100 in the range 0.2 - 30 MeV
2. Fully exploit gamma-ray **polarization** for both transient and steady sources
3. Improve significantly the **angular resolution** (to reach, e.g., $\sim 10'$ at 1 GeV)
4. Achieve a very large **field of view** (~ 2.5 sr) \Rightarrow efficient monitoring of the γ -ray sky
5. Enable sub-millisecond trigger and **alert capability** for transients

How to measure gamma rays in the MeV-GeV?

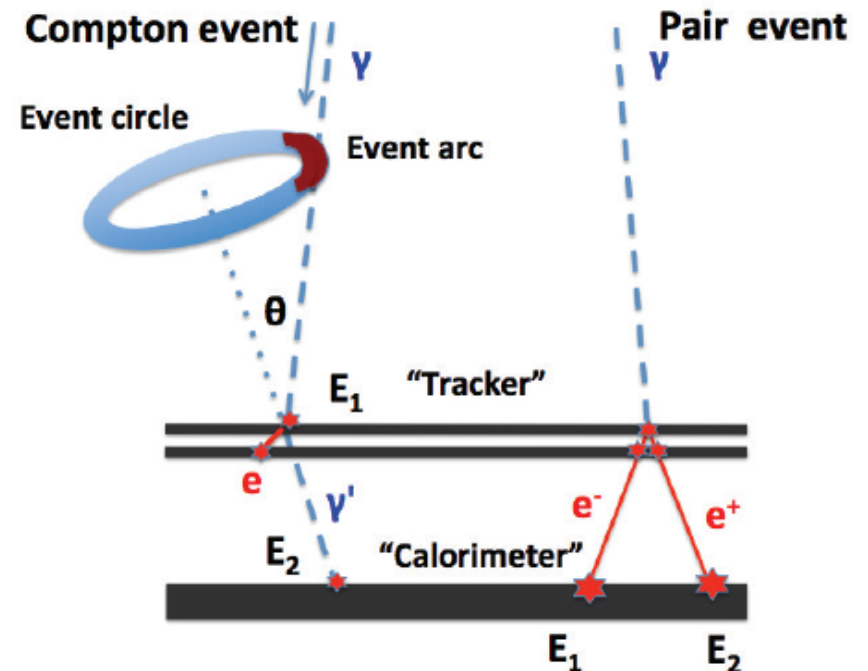


- **Tracker** – Double sided Si strip detectors (DSSDs) for excellent spectral resolution and fine 3-D position resolution (1m^2 , $500\ \mu\text{m}$ thick, $0.3 X_0$ in total)
- **Calorimeter** – High-Z material for an efficient absorption of the scattered photon \Rightarrow CsI(Tl) scintillation crystals readout by Si drift detectors or photomultipliers for best energy resolution. 8 cm ($4.3 X_0$)
- **Anticoincidence detector** to veto charged-particle induced background \Rightarrow plastic scintillators readout by Si photomultipliers

Detection of (sub)MeV-GeV gamma-rays

- Compton regime
 - Require excellent 3D-point resolution and energy resolution
 - Event reconstruction with 2 points and 2 energy measurements!
- Pair regime
 - Tracking resolution is most important
 - Dominated by Multiple Scattering effect
 - Main concern is detector layer thickness
- Difficult to be truly optimal in both regimes across the gap with one detector

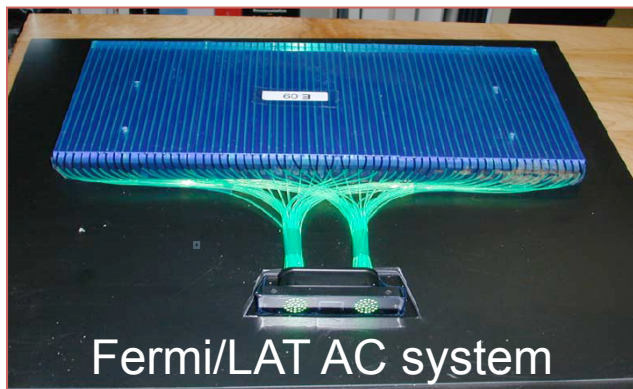
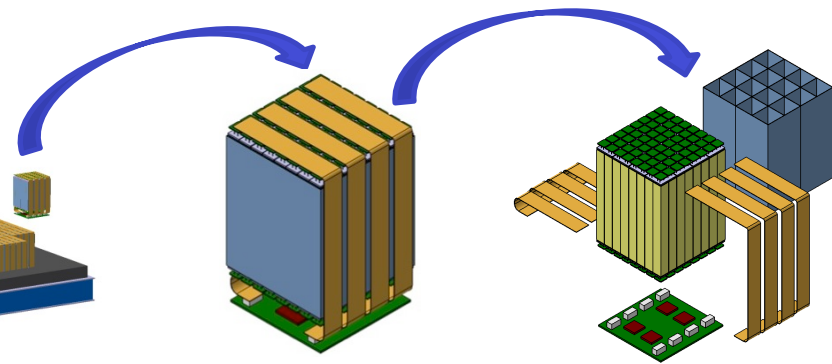
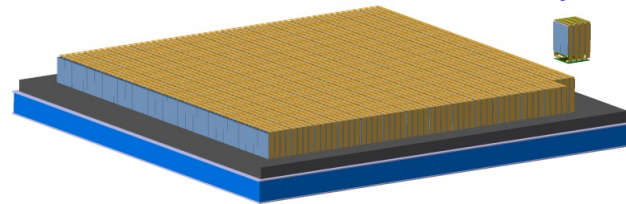
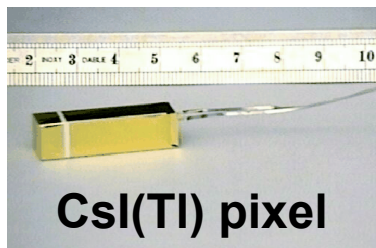
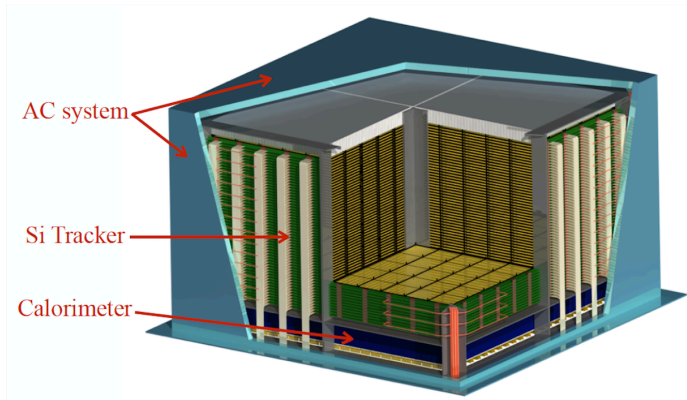
$$\cos \theta = 1 + \frac{m_e}{E_\gamma} - \frac{m_e}{E_\gamma - E_e} = 1 + \frac{m_e}{E_1 + E_2} - \frac{m_e}{E_2}$$



$$\sigma_\theta = \frac{13.6}{\beta p} z \sqrt{\frac{x}{x_0}} \left[1 + 0.038 \ln \left(\frac{x}{x_0} \right) \right] \quad \mathbf{p \text{ in MeV}}$$

e-ASTROGAM: the payload

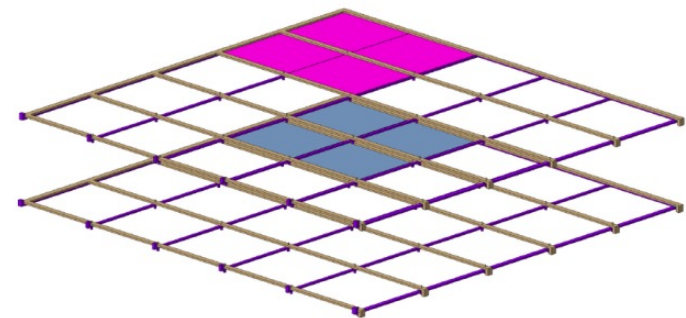
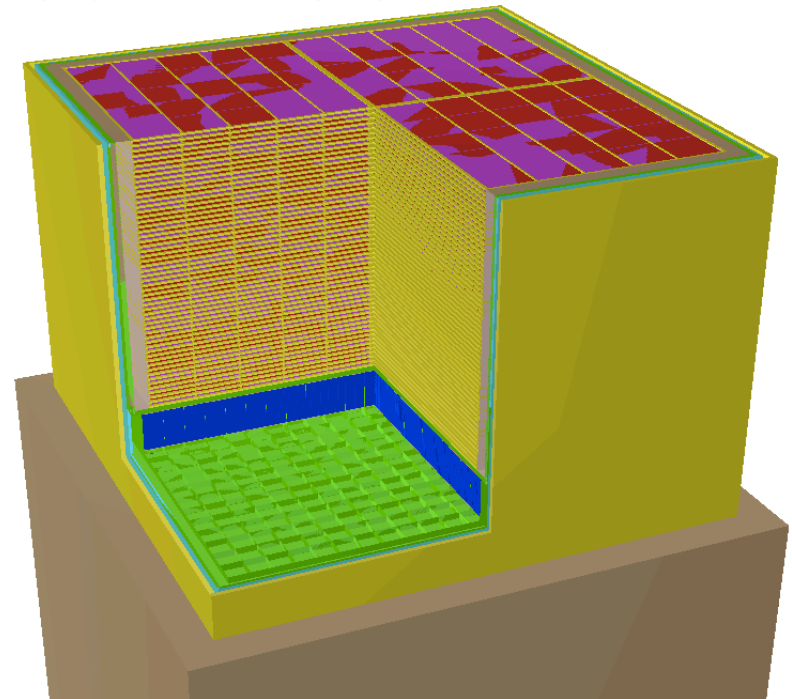
- **Tracker**: 56 layers of 4 times 5×5 DSSDs (5 600 in total) of 500 μm thickness and 240 μm pitch
- DSSDs bonded strip to strip to form 5×5 ladders
- **Light and stiff mechanical structure**
- **Ultra low-noise** front end electronics



- **Calorimeter**: 33 856 CsI(Tl) bars coupled at both ends to **low-noise Silicon Drift Detectors**
- **ACD**: segmented plastic scintillators coupled to SiPM by optical fibers
- **Heritage**: AGILE, Fermi/LAT, AMS-02, INTEGRAL, LHC/ALICE...

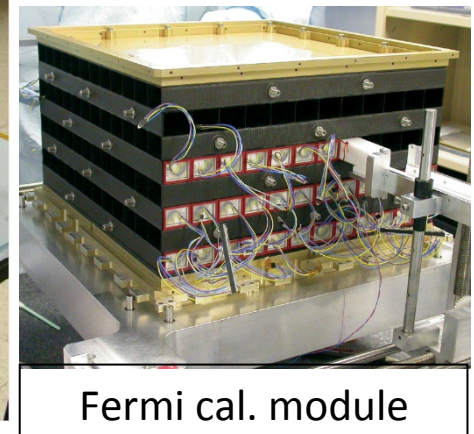
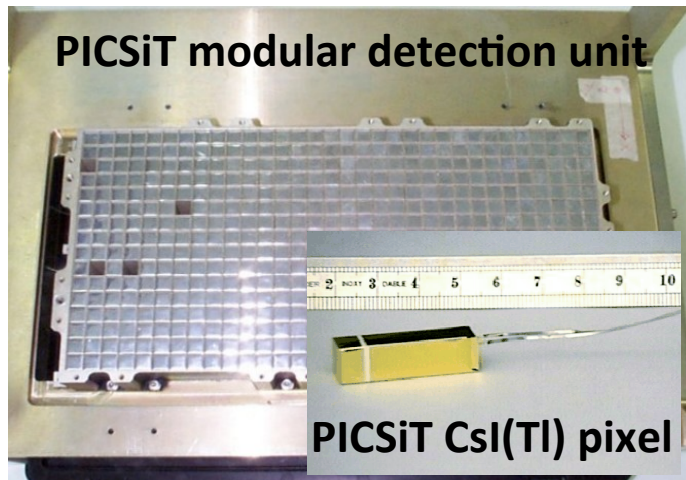
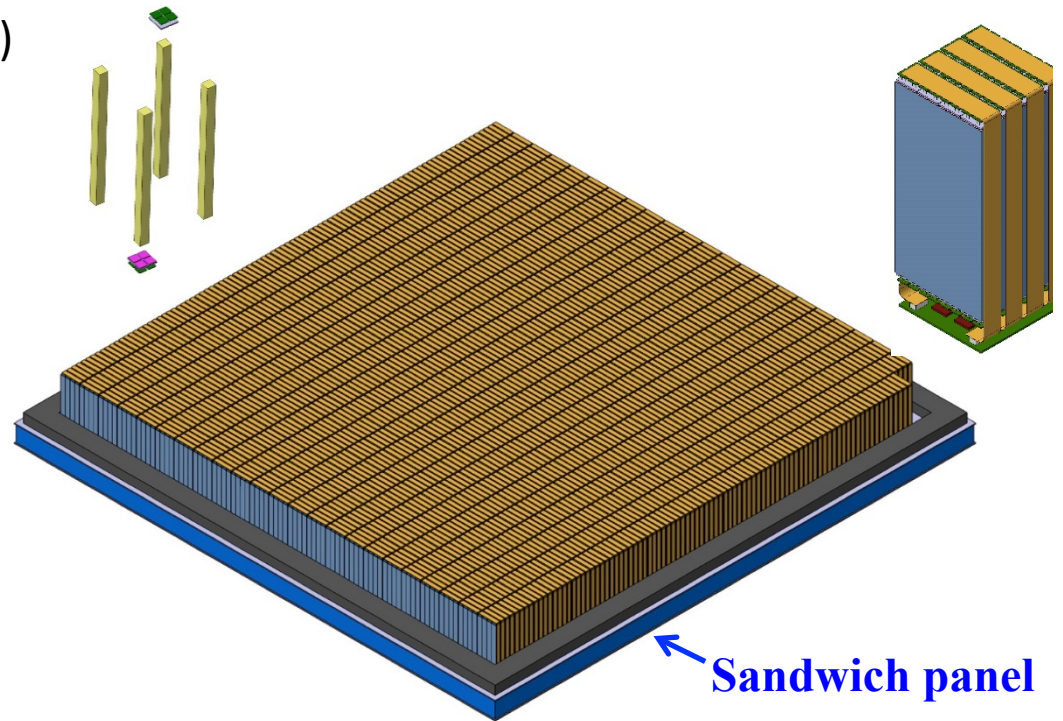
e-ASTROGAM: silicon tracker

- 4 towers, 56 layers of 5×5 double sided Si strip detectors each (5600 DSSDs)
 - Each DSSD has a total area of 9.5×9.5 cm², a thickness of 500 μm and pitch of 240 μm (384 strips per side)
 - The DSSDs are wire bonded strip to strip to form 5×5 2-D ladders
- Spacing of the Si layers: 10 mm
 - Each layer held by a very light mechanical
 - two frames sandwiching the Si detectors
- DSSD strips connected to ASICs through a pitch adapter
 - 26 880 IDeF-X ASICs (32 channels each)
 - 860160 electronic channels
 - 12 IDeF-X ASICs each side
 - The analog output signals of IDeF-X will be converted to digital signals with the OWB-1 ADC
 - 5 OWB-1 ADCs each side
- Power budget = 688 W (800 mW/channel)



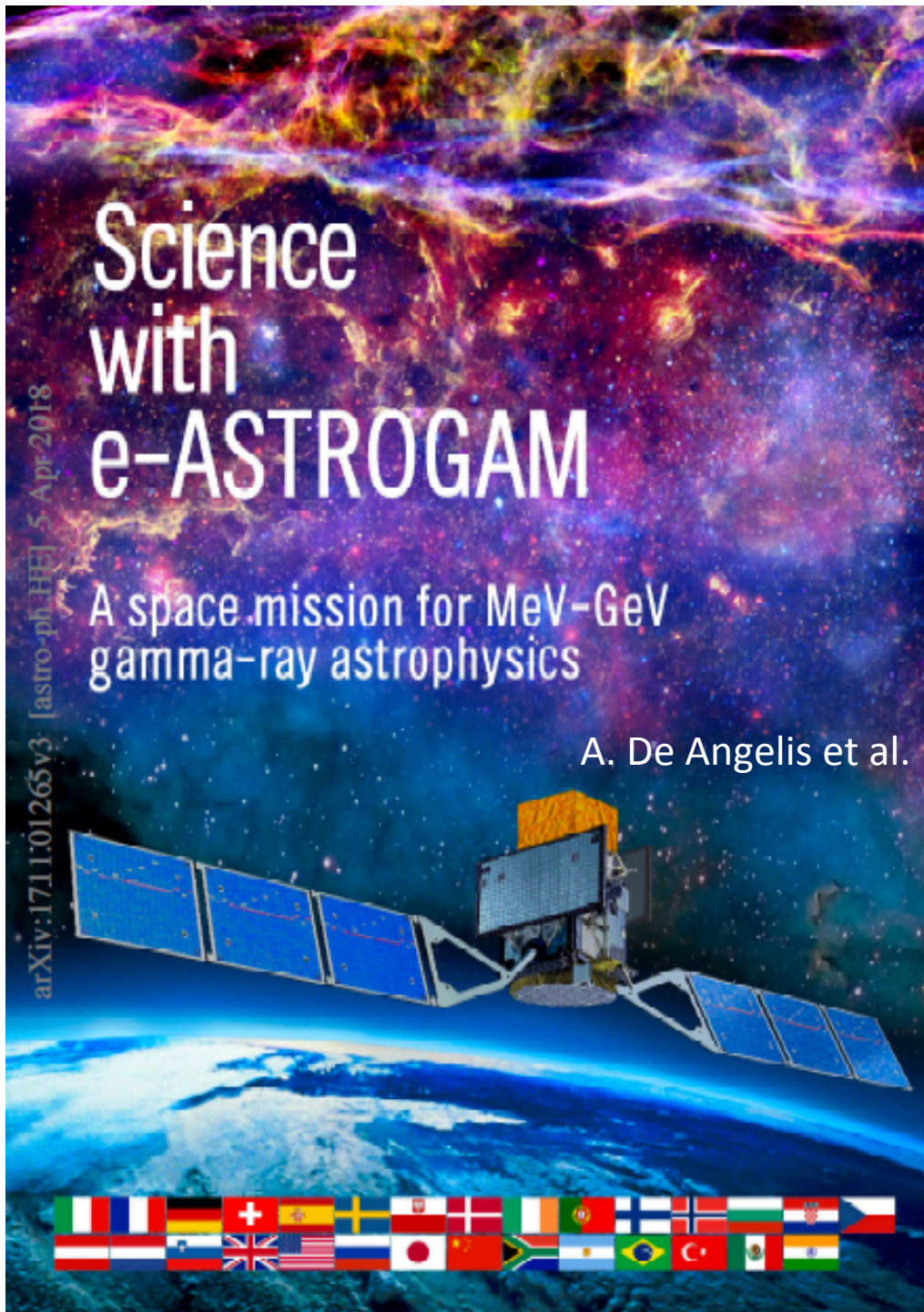
e-ASTROGAM: calorimeter

- Pixelated detector made of 33 856 CsI(Tl) scintillator bars of 8 cm length and 5×5 mm² cross section, glued at both ends to low-noise Silicon Drift Detectors (SDDs)
- Calorimeter formed by the assembly of 529 (23×23) modules
- **Heritage:** INTEGRAL/PICSiT, AGILE, Fermi/LAT, LHC/ALICE
 - FEE ASIC: modified version of the ultra low-noise VEGA ASIC (INFN)



Science with e-ASTROGAM

See <https://arxiv.org/abs/1611.02232>
(Exp. Astronomy)
and <https://arxiv.org/abs/1711.01265>
(JHEAP)

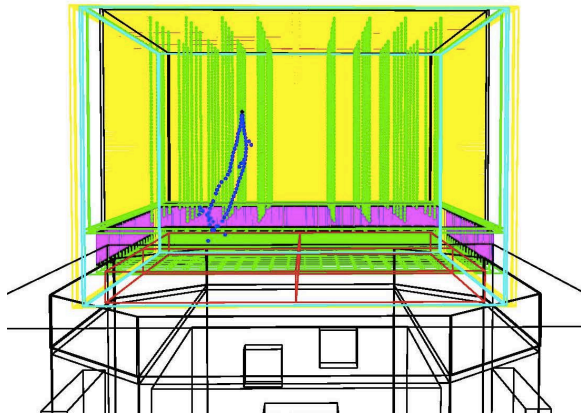
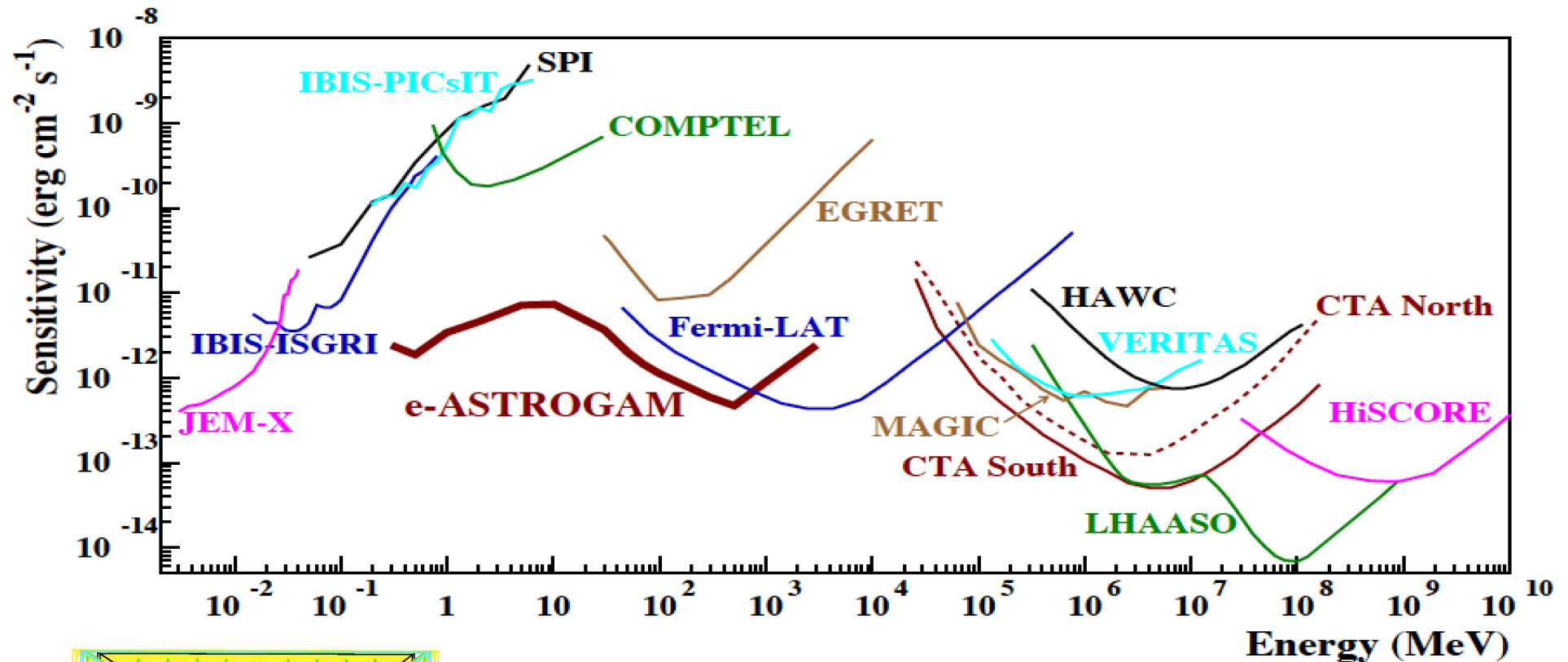


A. De Angelis et al.

A. De Angelis^{1,2,3,4}, V. Tatischeff⁵, I. A. Grenier⁶, J. McEnery⁷, M. Mallamaci¹, M. Tavani^{8,9,10}, U. Oberlack¹¹, L. Hanlon¹², R. Walter¹³, A. Argan¹⁴, P. Von Ballmoos¹⁵, A. Bulgarelli¹⁶, A. Bykov¹⁷, M. Hernanz¹⁸, C. Kanbach¹⁹, I. Kuvvetli²⁰, M. Pearce²¹, A. Zdziarski²², J. Conrad²³, G. Chioselli²⁴, A. Harding⁷, J. Isgrà²⁵, M. Leising²⁶, P. Longo^{27,28}, C. Madsen²⁹, M. Martínez³⁰, M. N. Mazziotta³¹, J. M. Paredes³², M. Pohl³³, R. Rando^{1,34}, M. Razzano^{35,36}, A. Abouan^{34,2}, M. Ackermann³⁷, A. Adlitz³⁸, M. Ajello³⁹, C. Albers⁴⁰, J. M. Álvarez⁴⁰, G. Ambrosi⁴¹, S. Antón^{42,43}, L. A. Antonelli⁴⁴, A. Babic⁴⁵, B. Balbusstov⁴⁶, M. Balbo¹³, I. Baldini^{35,36}, S. Balman⁴⁶, C. Bamba^{38,47}, U. Barres de Almeida⁴⁸, J. A. Barrio⁴⁹, R. Bartels⁵⁰, D. Bastieri^{34,1,51}, W. Bednarek⁵², D. Bernard⁵³, E. Bernardini^{54,37}, T. Bernaboni¹³, B. Bertucci^{41,55}, A. Biland⁵⁶, E. Bissaldi^{57,31}, M. Boettcher⁵⁸, V. Bonvicini⁵⁹, V. Bosch-Ramon²⁵, E. Bottacini^{1,34}, V. Bozhilov⁵⁹, T. Bretz⁶⁰, M. Branchesi^{61,62}, V. Brdar⁶³, T. Brüningmann⁶⁴, A. Broga¹¹, C. Budtz-Jørgensen²⁰, G. Busetto³⁴, S. Buson⁷, M. Buzzo^{41,55}, A. Caeraniga²⁴, S. Camera^{65,66,67,68}, R. Campana⁶⁶, P. Caraveo⁶⁹, M. Cardillo⁸, P. Carlson²¹, S. Celentini⁷⁰, M. Cermeño²⁹, A. Chen⁷¹, C. C. Cheung⁷², E. Churazov^{73,74}, S. Ciprini^{44,41}, A. Coc⁵, S. Colafrancesco⁷¹, A. Coleiro^{75,76}, W. Collmar⁷⁷, P. Coppi⁷⁸, R. Curado da Silva⁷⁹, S. Cutini^{44,41}, F. D'Ammando⁸⁰, B. De Lotto⁸¹, D. de Martino⁸², A. De Rosa⁸, M. Del Santo⁸³, L. Delgado¹⁸, R. Diehl⁷⁷, S. Dietrich⁸⁴, A. D. Dolgov^{85,86}, A. Dominguez⁴⁹, D. Dominis Prester⁸⁷, I. Donnarumma⁸, D. Dornier⁸⁸, M. Doro^{1,34}, M. Dutra⁸⁹, D. Elsaesser⁹⁰, M. Fährizito^{44,91}, A. Fernández-Barral¹, V. Fioretti¹⁶, L. Foffano^{34,1}, V. Formaro⁴¹, N. Fornengo^{65,66}, L. Foschini⁵⁴, A. Franceschini³⁴, A. Franczkowiak³⁷, S. Funk⁶², P. Fuschino¹⁶, D. Gaggero⁵², G. Galassi²⁴, F. Gargano^{31,57}, D. Gasparri^{44,41}, R. Gehrz⁵³, P. Giannicola³¹, N. Giglietto^{57,31}, P. Giommi⁹⁴, F. Giordano³¹, M. Giroletti⁸⁰, C. Ghislandi^{24,95}, N. Godinovic⁹⁶, C. Gouffin⁹⁷, J. E. Grove⁹⁸, C. Hamedache⁵, D. H. Hartmann²⁶, M. Hayashida⁹⁹, A. Hryczuk⁶⁴, P. Jean¹⁵, T. Johnson¹⁰⁰, J. José¹⁰¹, S. Kaufmann¹⁰², B. Kheif¹⁰³, J. Kiener⁵, J. Knöbbseder¹⁵, M. Kole¹³, J. Kopp¹⁰⁴, V. Kozhuharov²⁹, C. Labanti¹⁶, S. Laskowski³⁹, P. Laurent¹⁰⁵, O. Limoustin¹⁰⁶, M. Linares¹⁰⁷, E. Lindfors¹⁰⁷, M. Lindner⁶³, J. Liu¹⁰⁸, S. Lombardi^{44,91}, F. Loparco^{31,57}, R. López-Coto¹, M. López Moya⁴⁹, B. Lott¹⁰⁹, P. Lubrano⁴¹, D. Malyshev¹¹⁰, N. Mankuzhiyil¹¹¹, K. Mannheim⁸⁸, M. J. Marcha¹¹², A. Marengo³⁸, B. Marcote¹¹³, M. Mariotti¹, M. Marisaldi¹¹⁴, S. Meisner¹², S. Mergott⁶⁹, A. Merle¹¹⁵, R. Mignani^{116,117}, G. Minervini⁸, A. Morssev¹¹⁸, A. Morselli¹⁰, F. Moura⁷⁹, K. Nakazawa¹¹⁹, L. Nava^{24,28,120}, D. Nieto⁴⁹, M. Orienti⁸⁰, M. Orto^{121,2}, E. Orlando²⁹, P. Orlandi¹²², S. Palano², R. Paoletti³⁵, A. Papitto⁹¹, M. Pasquato², B. Patricelli^{123,35}, M. A. Pérez-García³³, M. Perse¹²³, G. Piano⁸, A. Pichel¹²⁴, M. Pimenta⁴, C. Pittori^{44,91}, T. Porter²⁹, J. Poutanen¹⁰⁷, E. Prandini^{34,1}, N. Prantzos¹²⁵, N. Produit¹³, S. Profumo¹²⁶, P. S. Quastrol¹²⁷, S. Rainò^{21,57}, A. Raklov⁶⁴, M. Regis^{85,66}, I. Reichardt¹²⁸, Y. Riphael^{129,130}, J. Rieco³⁰, W. Rodejohann⁶³, C. Rodríguez Fernández¹⁰, M. Rossetti¹³¹, L. Roso¹³², A. Rovero¹²⁴, R. Ruffini¹³³, G. Sala¹⁰¹, M. A. Sánchez-Conde¹³⁴, A. Santangelo¹³⁵, P. Saz Parkinson^{136,137}, T. Sbarrato⁹⁵, A. Shearer¹³⁸, R. Shollard⁴⁸, K. Short²⁰, T. Siegert⁷⁷, C. Sigutta^{63,139}, P. Spinnelli²¹, A. Stamerra¹⁴⁰, S. Starrfield¹⁴¹, A. Strong⁷⁷, I. Surimka¹⁴², F. Tavecchio²⁴, R. Taverna²⁴, T. Terzić⁸⁷, D. J. Thompson⁷, O. Tibolla¹⁰², D. F. Torres^{143,144,145}, R. Turolla³⁴, A. Ulyanov¹², A. Ursi⁸, A. Vacchi⁸¹, J. Van den Abeele⁶⁴, G. Vankova-Kirilova⁵⁸, C. Venter⁵⁸, F. Verrecchia^{44,91}, P. Vincini¹⁴⁶, X. Wang¹⁴⁷, C. Weniger²⁰, X. Wu¹³, G. Zaharijatic¹⁴⁸, L. Zampieri², S. Zane¹⁴⁹, S. Zimmer^{150,13}, A. Zoglauer¹⁵¹ and the e-ASTROGAM collaboration

White Book published in arXiv/JHEAP
Wide interest from the scientific community

e-ASTROGAM: performance assessment

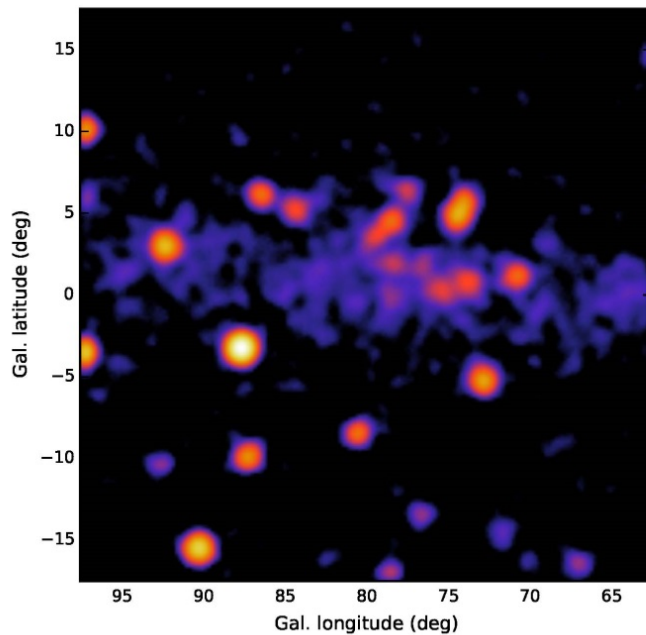
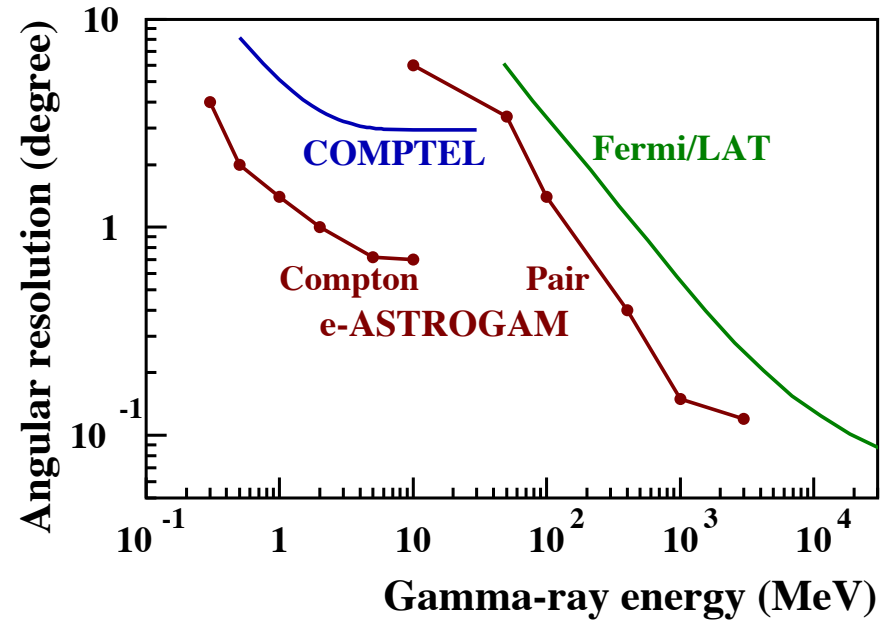


- e-ASTROGAM performance evaluated with **MEGALib** (Zoglauer et al. 2006) and **Bogemms** (Bulgarelli et al. 2012) – both tools based on Geant4 – and a **detailed numerical mass model** of the gamma-ray instrument

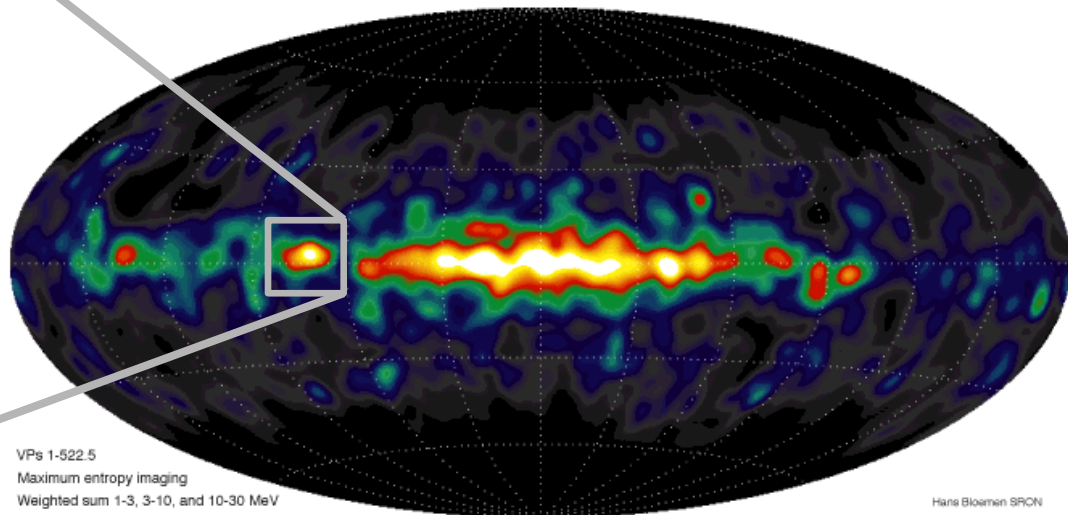
Angular resolution

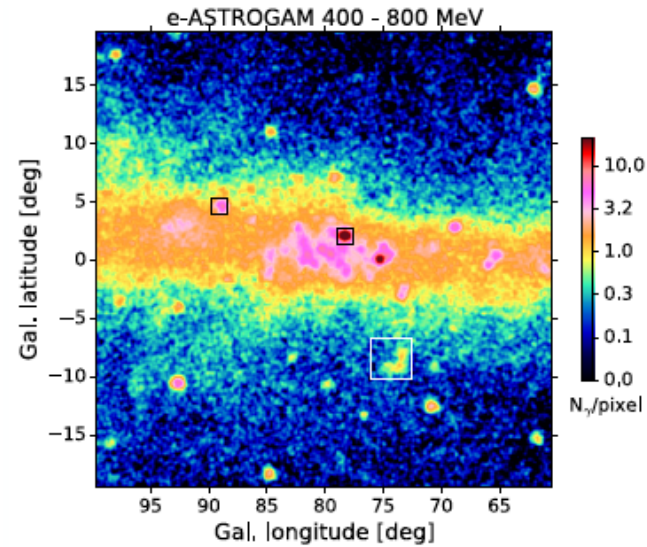
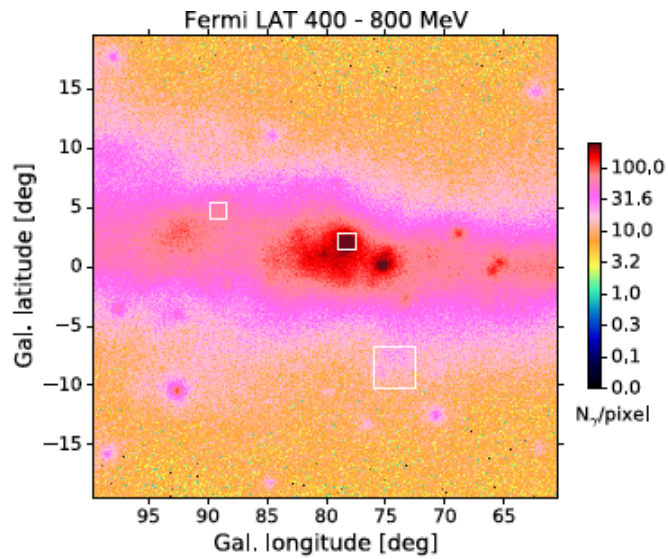
- **Angular resolution** improved close to the physical limits

Cygnus region in the 1 - 3 MeV energy band with the e-ASTROGAM PSF (extrapolation of the 3FGL source spectra to low energies)



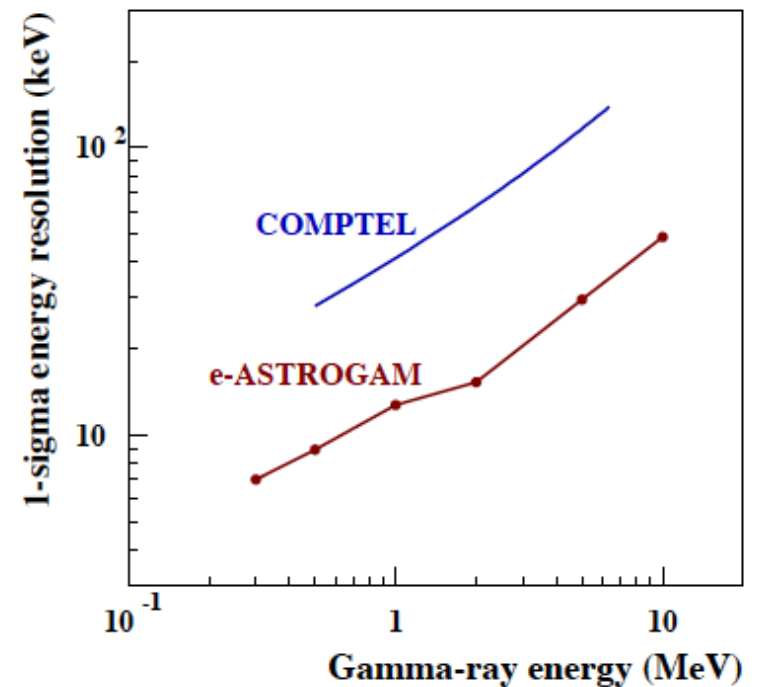
COMPTTEL 1-30 MeV





Energy resolution

$\Delta E/E$ (Gamma-ray imager)	2.5% at 1 MeV 30% at 100 MeV
$\Delta E/E$ (Calorimeter burst)	< 25% FWHM at 0.3 MeV < 10% FWHM at 1 MeV < 5% FWHM at 10 MeV



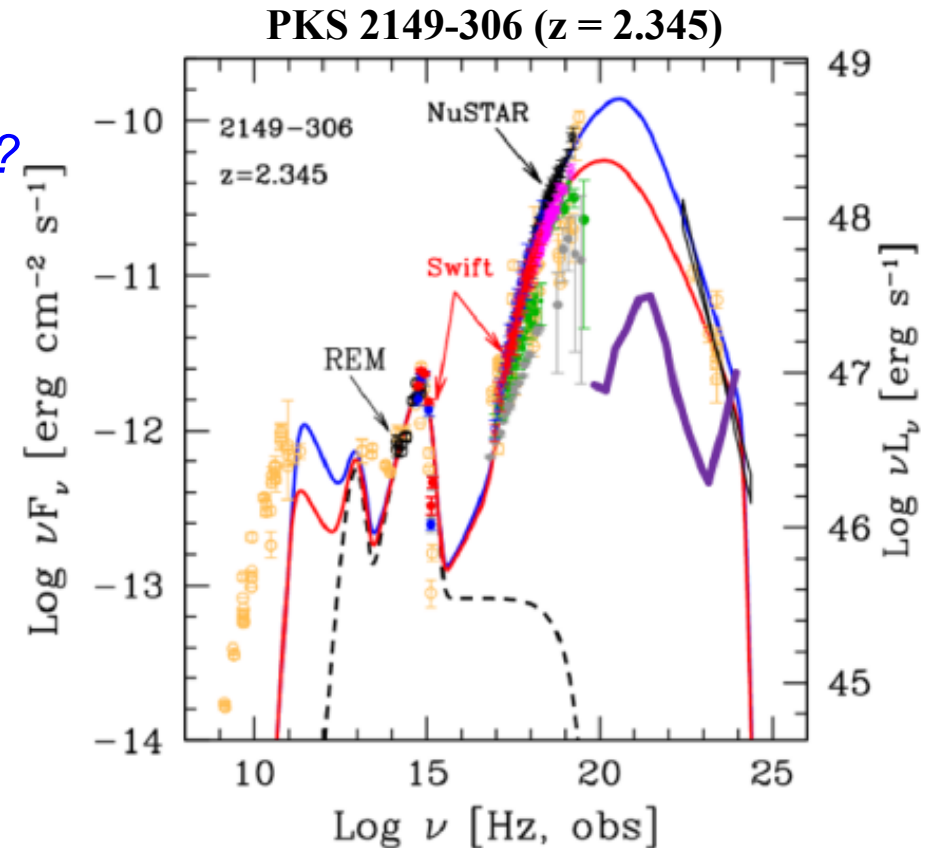
Key instrument characteristics: a summary

- Best PSF in MeV-GeV
 - Resolve sources
- Calorimetric measurements of MeV lines with high resolution:
 - Positron detection (511 keV line)
 - Measurements of isotopic contents, with highest sensitivity
 - Hadronic collisions of LECR with molecular clouds
- Capability of measuring polarization (marks Compton interactions at the sources and magnetic fields)
- SED resolution in the GeV range: allows to reconstruct the “pion bump”, characteristic of the decay $\pi^0 \rightarrow \gamma\gamma$ and thus an indicator of hadronic processes

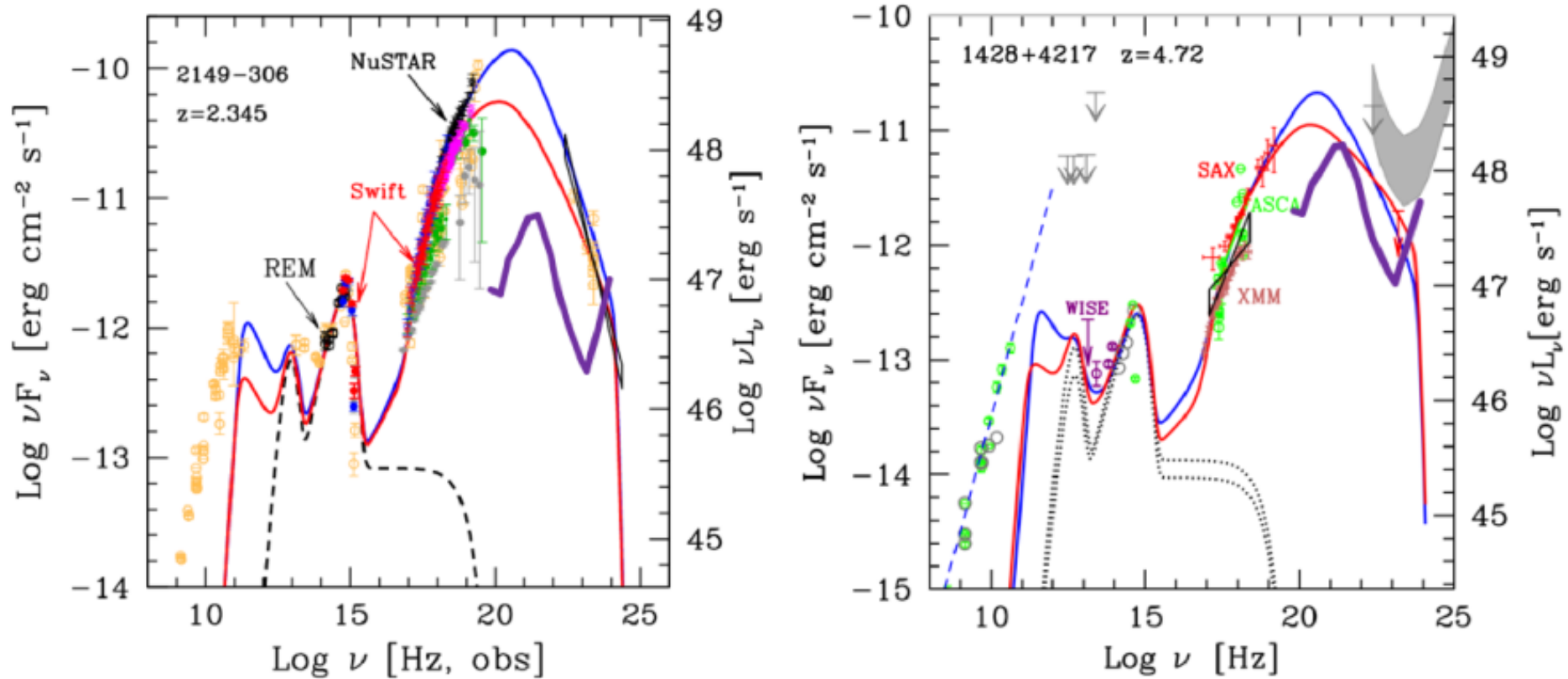
e-ASTROGAM core science topic #1

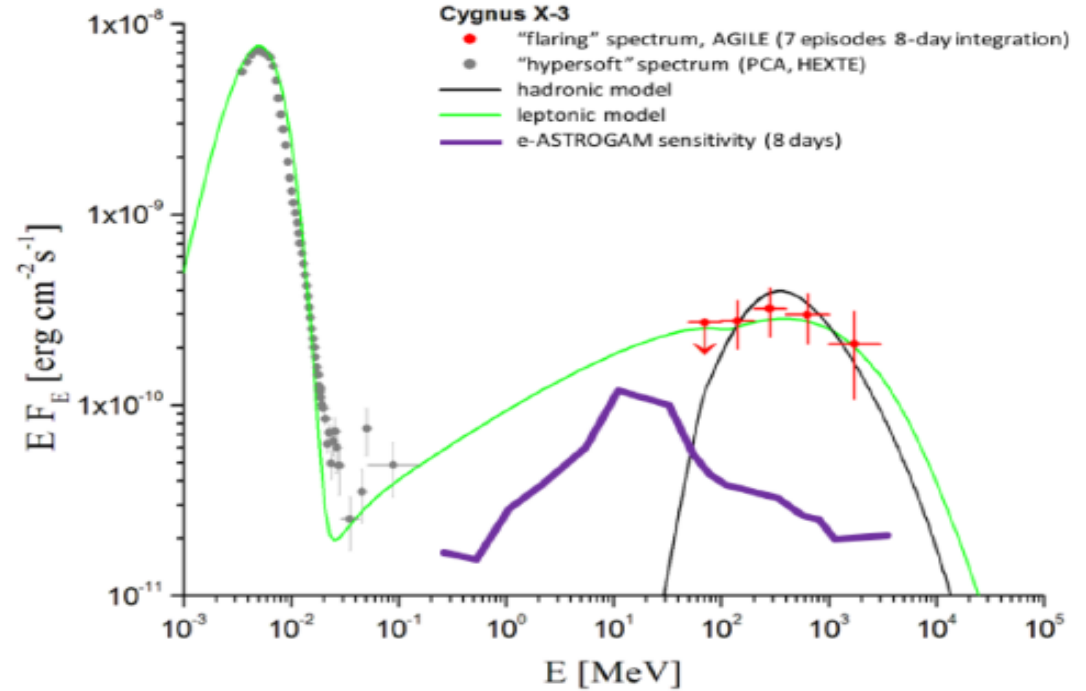
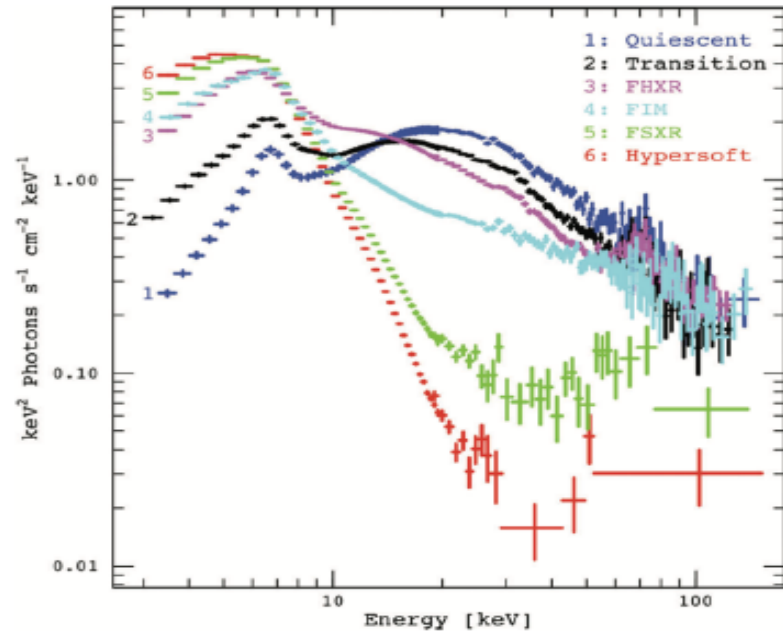
At the heart of the extreme Universe

- *Launch of ultra-relativistic jets in **GRBs**? Ejecta composition, energy dissipation site, radiation processes?*
 - *Can short-duration GRBs be unequivocally associated to **gravitational wave** signals?*
 - *How does the accretion disk/jet transition occur around supermassive black holes in **AGN**?*
 - *Are BL Lac blazars sources of **UHECRs** and high-energy neutrinos?*
- ✓ With its wide **field of view**, unprecedented **sensitivity** over a large spectral band, and exceptional capacity for **polarimetry**, **e-ASTROGAM** will give access to a variety of extreme **transient** phenomena



MeV blazars; cosmology at z up to 4.5





Relativistic jets; flares

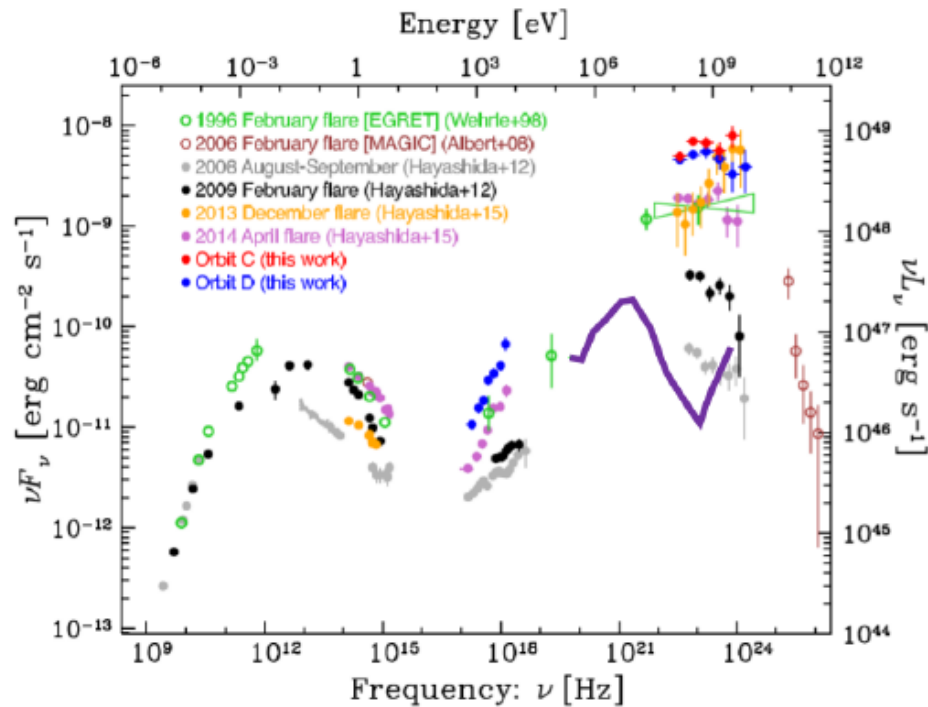


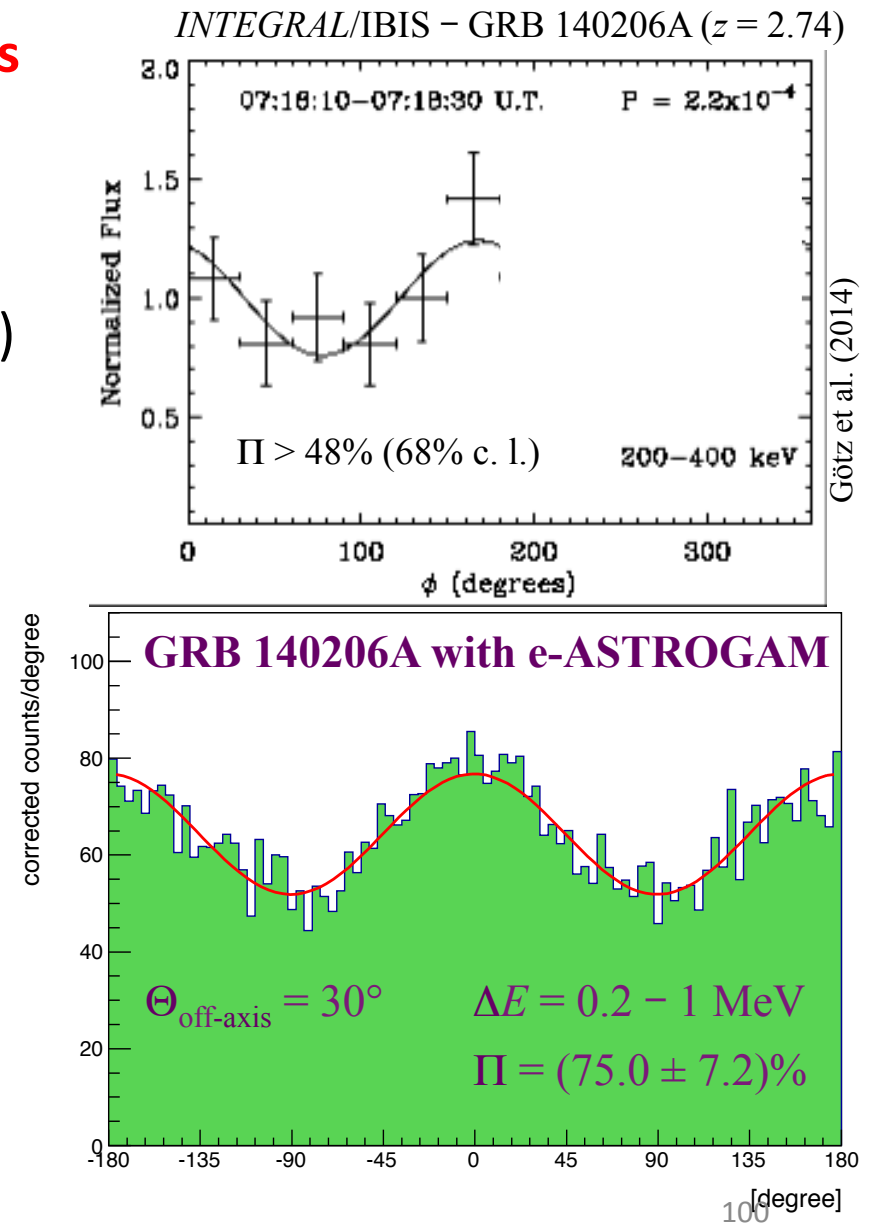
Figure 5: SED from a collection of different spectral states of the FSRQ 3C 279 showing a dramatic gamma-ray flaring activity, including the minute-timescale episode detected by Fermi in June 2015 [13]. The purple solid line is the 3σ e-ASTROGAM sensitivity calculated for a 50 ks exposure.

Gamma-ray bursts; the new Astronomy

- Threshold at 30 keV using the Calorimeter
- 200 GRB/year detected
 - Localized within 0.1-1 deg, and the information can be processed onboard
 - 42 GRBs/year with a detectable polarization fraction of 20%;
- Possible detection of electromagnetic counterparts of impulsive GW events
 - MeV likely to be the threshold (Patricelli et al. 2016)
 - Possible associations GRB/GW
- MeV good target also for the counterparts of neutrino bursts

Gamma-ray polarization

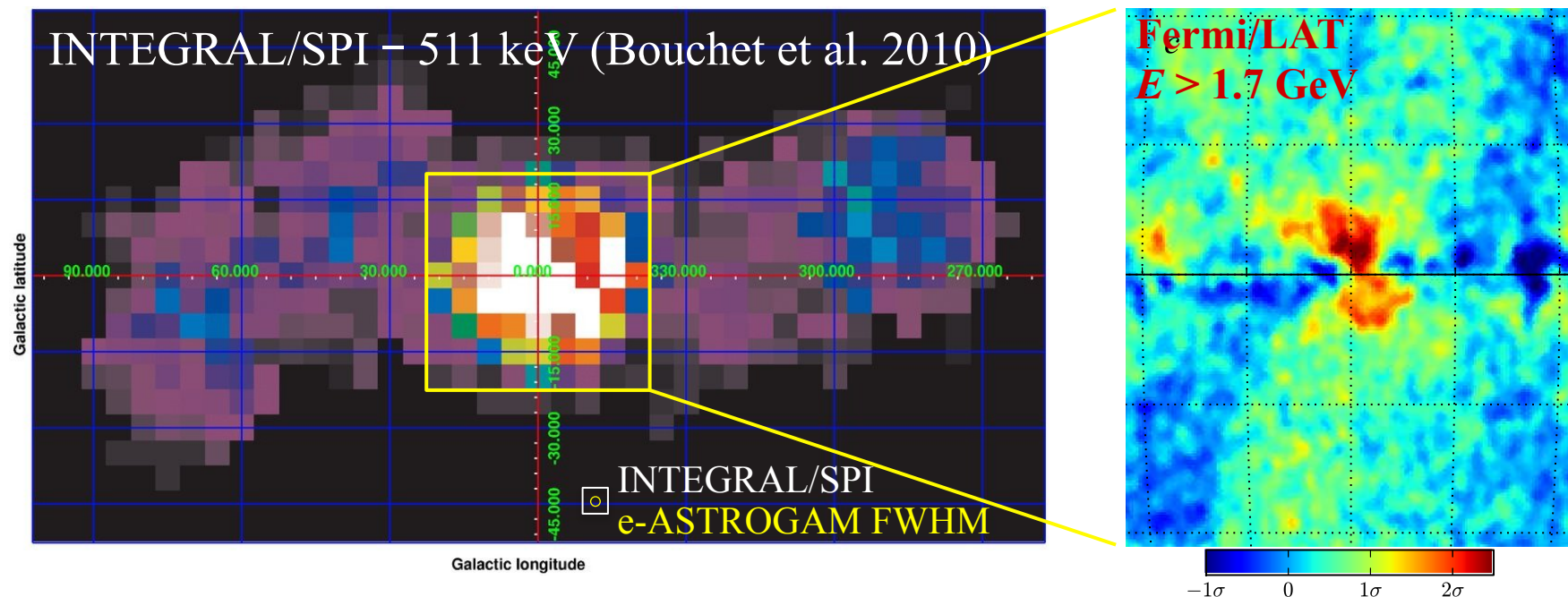
- γ -ray polarization in **objects emitting jets** (GRBs, Blazars, X-ray binaries) or with **strong magnetic field** (pulsars, magnetars) \Rightarrow **magnetization** and **content** (hadrons, leptons, Poynting flux) of the outflows + **radiation processes**
- γ -ray polarization from **cosmological sources** (GRBs, Blazars) \Rightarrow fundamental questions of physics related to **Lorentz Invariance Violation** (vacuum birefringence)
- ✓ e-ASTROGAM will measure the γ -ray polarization of **~ 200 GRBs per year** (promising candidates for highly γ -ray polarized sources)

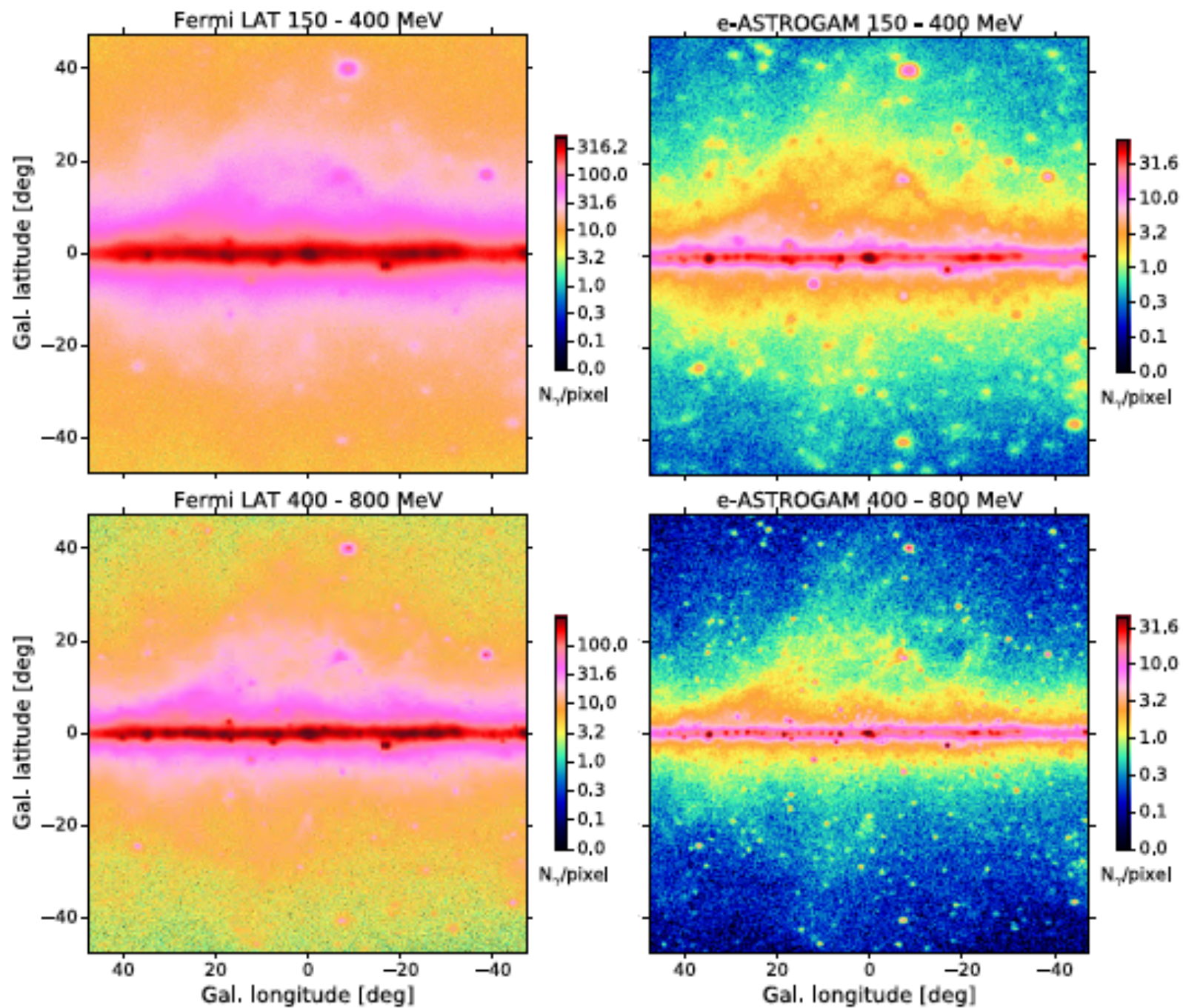


e-ASTROGAM core science topic #2

Origin & impact of HE particles on Galaxy evolution: CR, antimatter, ...

- *Origin of the Fermi Bubbles and of the 511 keV emission from the Galaxy's bulge? Are these linked to a past activity of the central supermassive black hole? What is causing the GeV excess emission from the center region?*
- ✓ With a **sensitivity** and an **angular resolution** in the MeV – GeV range significantly improved over previous missions, **e-ASTROGAM** will enable a detailed **spectro-imaging** of the various high-energy components





Cosmic rays in the Inner Galaxy; acceleration in SNRs

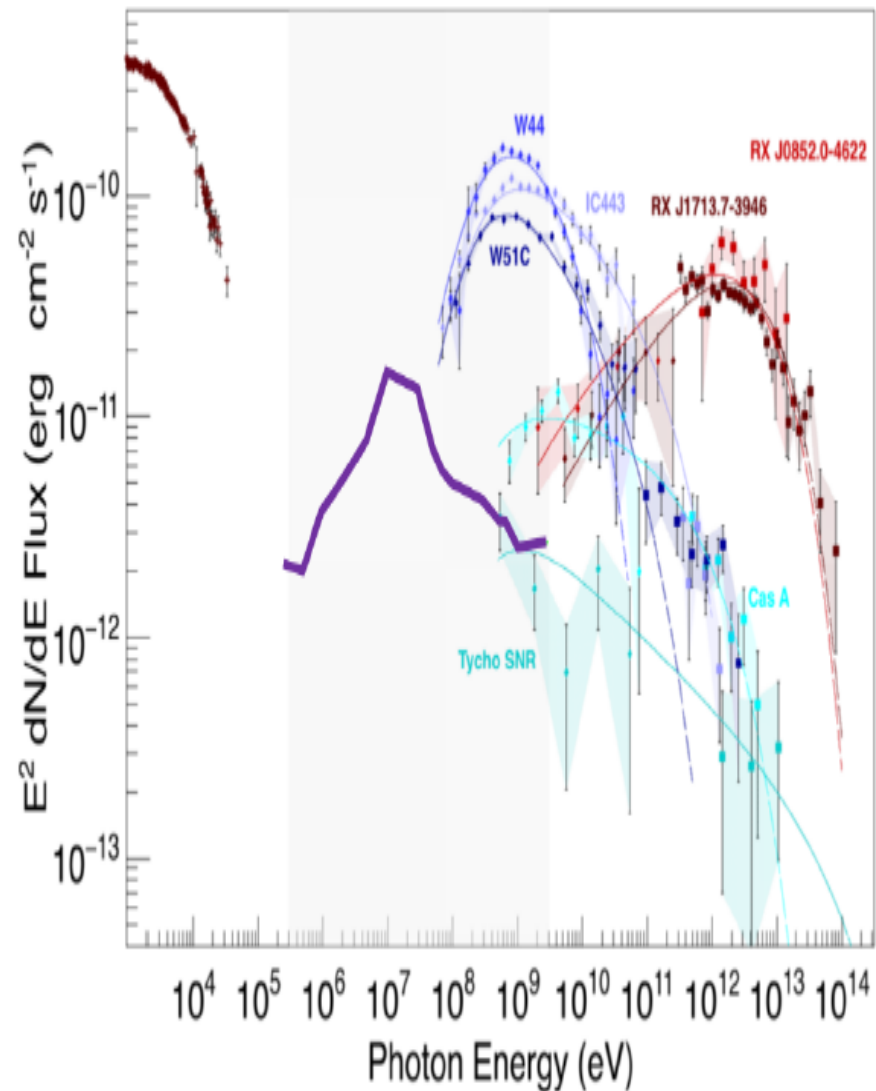
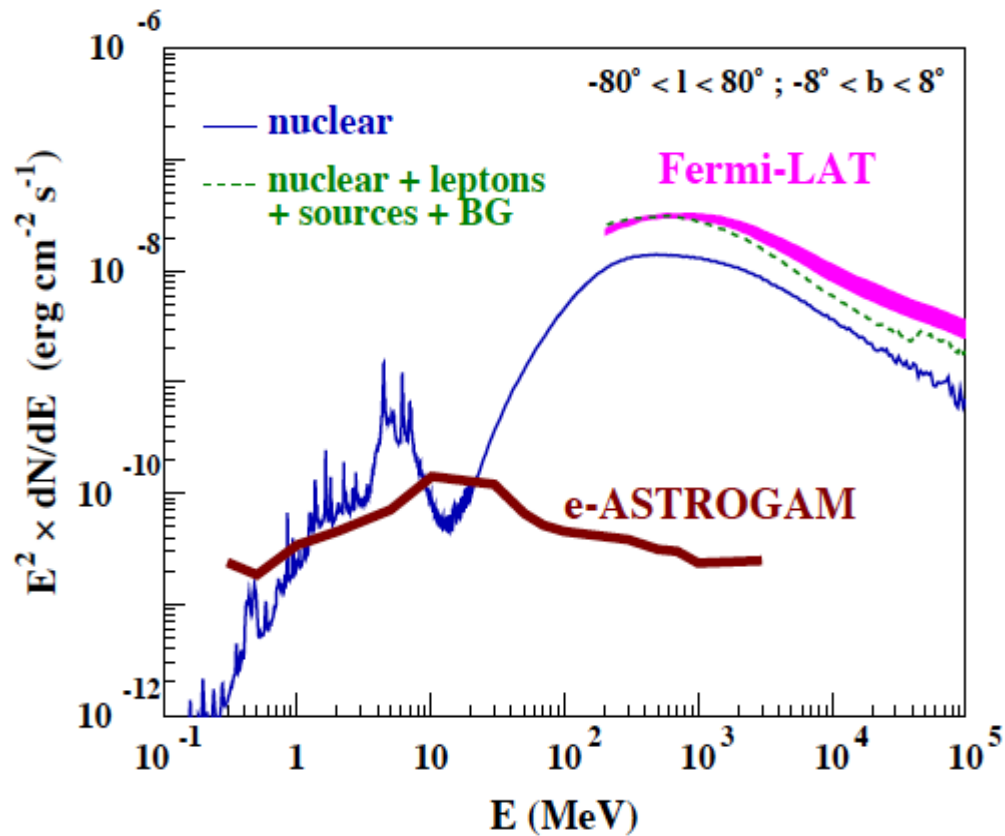


Figure 9: Predicted γ -ray emission due to nuclear interactions of CRs in the Inner Galaxy. The γ -ray line emission below 10 MeV is due to LECRs ([24]). The 1-year sensitivity of e-ASTROGAM (for Galactic background) is superimposed.

Antimatter and Dark Matter

- Unique sensitivity to the 511-keV line
- Sensitivity to many classical positron sources: can constrain the contribution from nearby pulsars in the positron excess seen by PAMELA/AMS-02
- The MeV region is the missing ingredient to determine the photon background from the Inner Galaxy: clarify if there is a photon excess (which might be due to DM, new particles)
- The MeV region is where the bulk of photons from WIMPs below 100 GeV is expected
- In some models, MeV dark matter
 - Plus Axions, ALPs:
 - Sensitivity to photons emitted by SNRs (Meyer et al. 2016)
 - Sensitivity to photon/ALP oscillations (Roncadelli et al. 2011; Hooper et al. 2009)

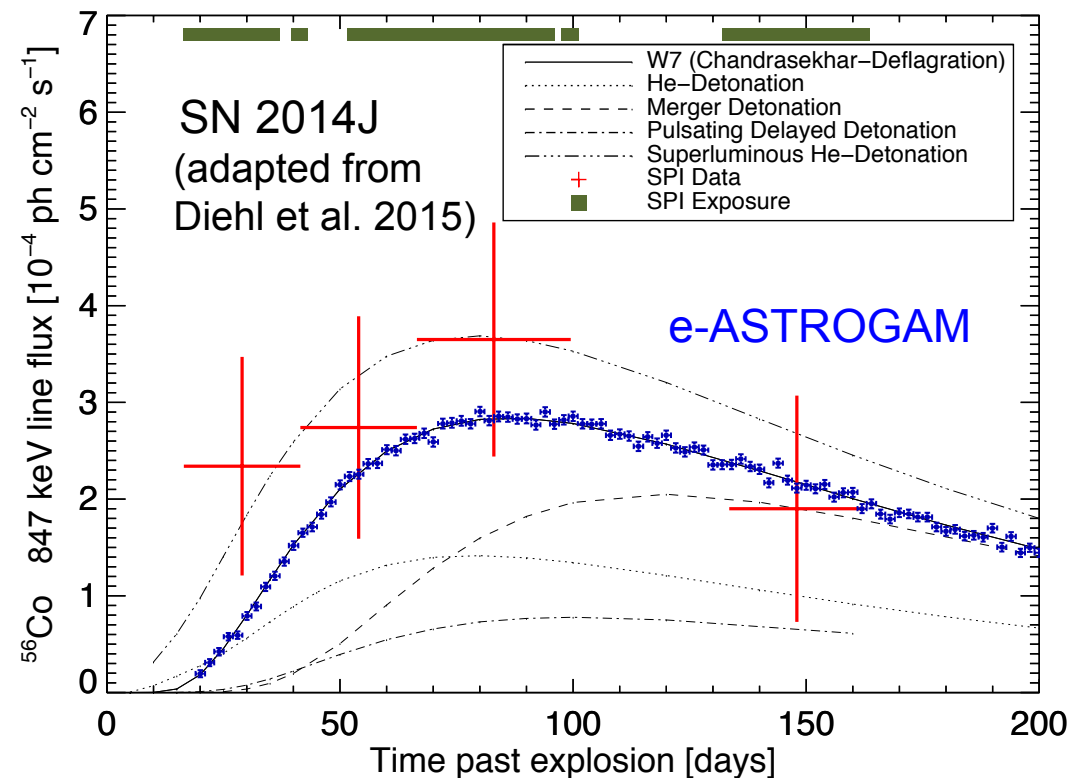
e-ASTROGAM core science topic #3

Supernovae, nucleosynthesis, and Galactic chemical evolution

- *How do thermonuclear and core-collapse SNe explode? How are cosmic isotopes created in stars and distributed in the interstellar medium?*

- ✓ With a remarkable improvement in **γ -ray line sensitivity** over previous missions, **e-ASTROGAM**

should allow us to finally understand the progenitor system(s) and explosion mechanism(s) of **Type Ia SNe** (^{56}Ni , ^{56}Co), the dynamics of **core collapse** in massive star explosions (^{56}Co , ^{57}Co), and the history of **recent SNe** in the Milky Way (^{44}Ti , ^{60}Fe ...)



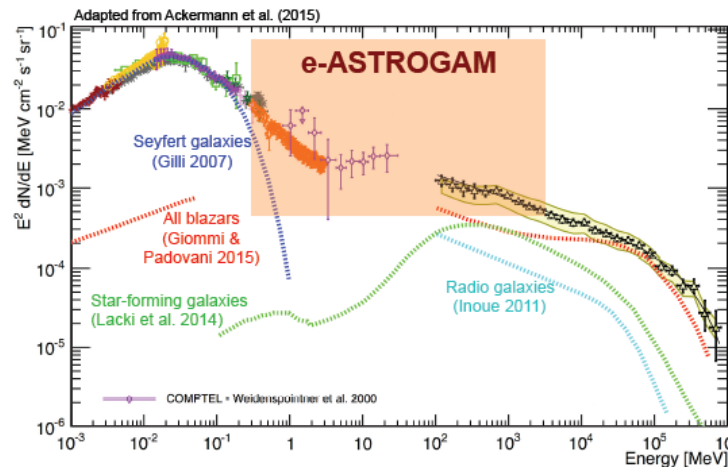
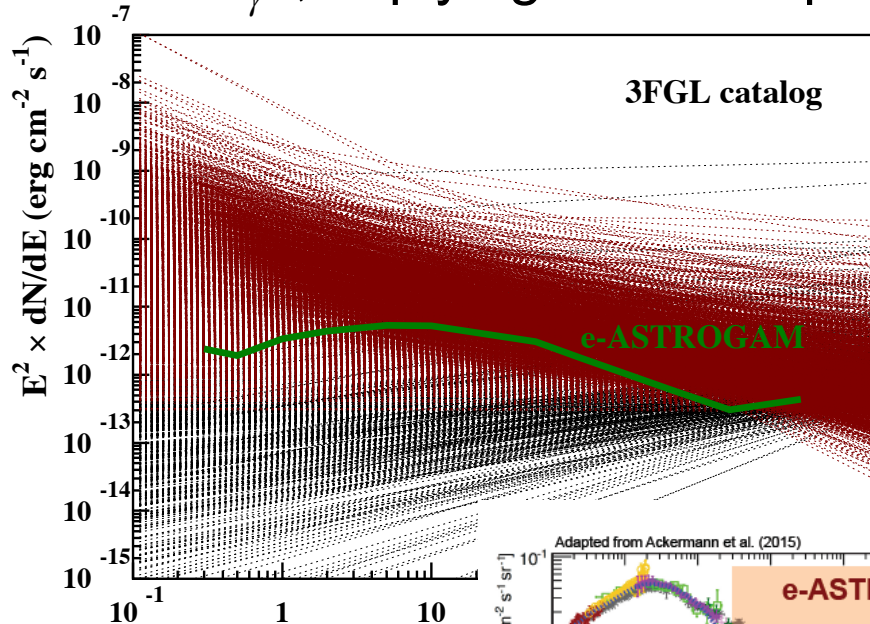
e-ASTROGAM Observatory science

- e-ASTROGAM pointings first focused on core science topics. However a very large number of sources will be detected and monitored.
 - Thousands of sources both Galactic and extragalactic, many new detections. Therefore, a very large community of astronomical users will benefit from e-ASTROGAM data available for multifrequency studies through GI programme managed by ESA.
- Phenomena and sources
 - characterized by rapid and very rapid variability timescales (sub-second, second, minutes, hours): GRB, AGN flares, ...
 - steady
 - **unexpected**

Type	3 yr	New sources
Total	3000 – 4000	~1800 (including GRBs)
Galactic	~ 1000	~400
MeV blazars	~ 350	~ 350
GeV blazars	1000 – 1500	~ 350
Other AGN (<10 MeV)	70 – 100	35 – 50
Supernovae	10 – 15	10 – 15
Novae	4 – 6	4 – 6
GRBs	~600	~600

e-ASTROGAM discovery space

- Over 3/4 of the sources from the 3rd *Fermi*-LAT Catalog (3FGL), **2415 sources** over 3033, have power-law spectra ($E_\gamma > 100$ MeV) steeper than E_γ^{-2} , implying that their peak energy output is below 100 MeV



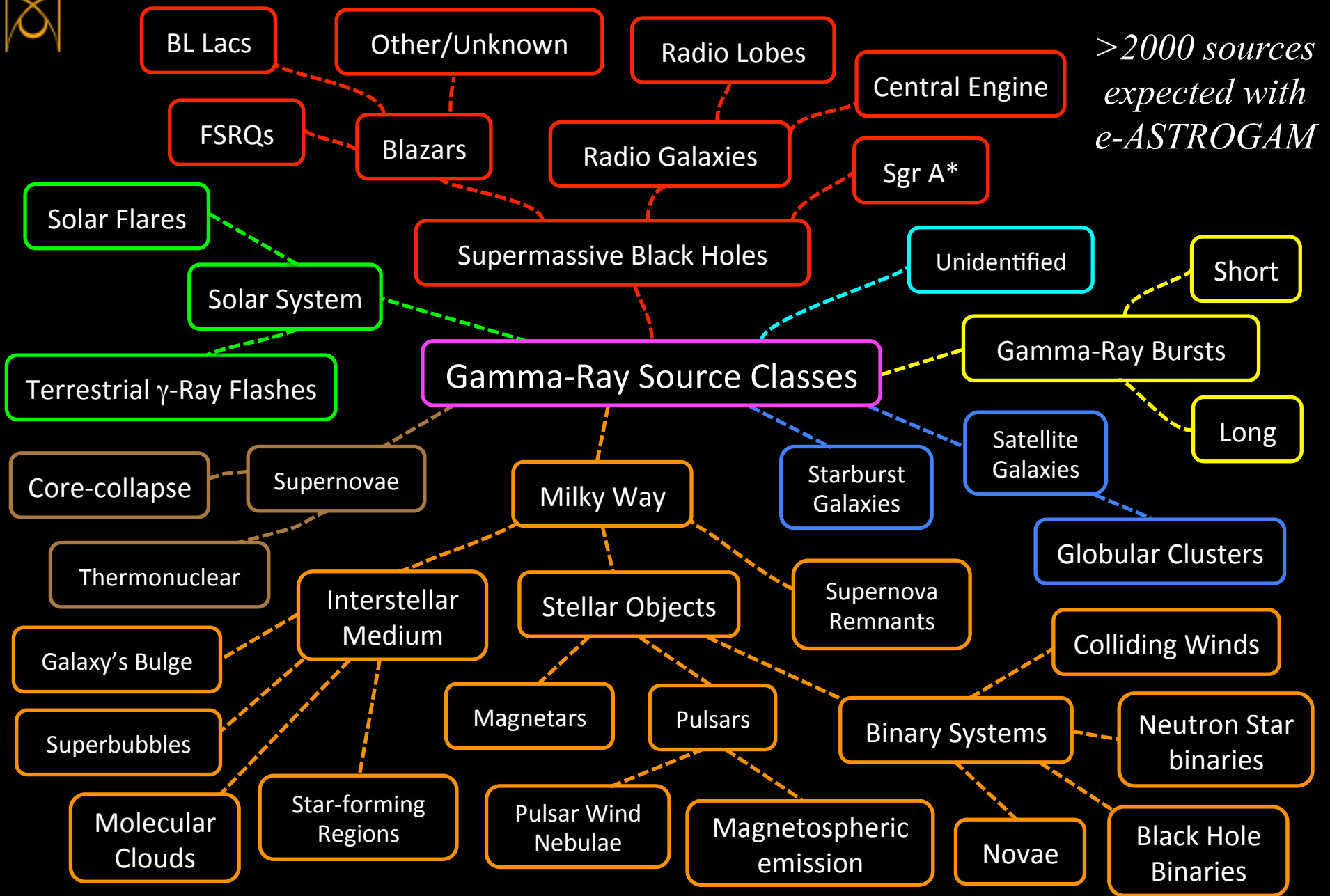
- These includes more than 1200 (candidate) blazars (mostly FSRQ), about 150 pulsars, and nearly **900 unassociated sources**
- Most of these sources will be detected by **e-ASTROGAM** ⇒ **large discovery space** for new sources and source classes
- Observatory science

e-ASTROGAM Observatory science

- Diffuse Galactic gamma-ray background
- Pulsars and millisecond pulsars both isolated and in binaries, whose (pulsed or unpulsed) emission will be observable in a spectral range rich in information to discriminate between different particle acceleration models
- PWNe, for which e-ASTROGAM will obtain crucial data on particle acceleration and propagation
- Magnetars
- Galactic compact binaries, including NS and BHs whose spectral transitions and outbursts will be monitored
- Interstellar shocks
- Propagation over cosmological distances (LIV, ALPs, ...)
- Novae
- Solar flares and terrestrial gamma-ray flashes



>2000 sources expected with e-ASTROGAM



BL Lacs

Other/Unknown

Radio Lobes

Central Engine

FSRQs

Blazars

Radio Galaxies

Sgr A*

Solar Flares

Supermassive Black Holes

Unidentified

Short

Solar System

Gamma-Ray Source Classes

Gamma-Ray Bursts

Long

Terrestrial γ -Ray Flashes

Core-collapse

Supernovae

Milky Way

Starburst Galaxies

Satellite Galaxies

Thermonuclear

Interstellar Medium

Stellar Objects

Supernova Remnants

Globular Clusters

Galaxy's Bulge

Superbubbles

Magnetars

Pulsars

Colliding Winds

Molecular Clouds

Star-forming Regions

Pulsar Wind Nebulae

Magnetospheric emission

Binary Systems

Neutron Star binaries

Novae

Black Hole Binaries

First e-ASTROGAM Science Workshop

- Padova, Feb 28 (start at 13h30)/ Mar 1-2 (end on Mar 2 at 14h)
- Setup a team for a white book (possibly w/ AMEGO)
- Contributed talks & posters on multimessenger astrophysics welcome
- Google “agenda infn e-ASTROGAM workshop”



Second e-ASTROGAM Science Workshop

2nd e-ASTROGAM Workshop, joint to AMEGO Workshop: towards a White Book on MeV Gamma-ray Astrophysics

chaired by Alessandro De Angelis (PD), Riccardo Rando (PD), Julie Mc Enery (NASA Goddard)

from Friday, 13 October 2017 at **10:45** to Saturday, 14 October 2017 at **16:45** (Europe/Rome)
at **Munich (Ambiance Rivoli Hotel)**

Albert-Roßhaupter-Straße 22

Description This scientific workshop, open to contributions, continues the discussion on the e-ASTROGAM (and AMEGO) science: exploration of the Universe in the MeV domain. After the 1st workshop held in Padova in February 2017, we aim at finalizing our "White Book" on the opportunities of astronomy, astrophysics and astroparticle physics from observations of cosmic gamma rays in the MeV domain.

More documentation is available at the homepage <http://eastrogam.iaps.inaf.it>



The conference fee covers breaks and renting the room and the facilities. 30 rooms are pre-booked at the hotel at a preferential rate (specify eASTROGAM in the reservation).

Participants Solen Balman; Juan Abel Barrio; Denis Bernard; Martina Cardillo; Paolo Cumani; Alessandro De Angelis; Domitilla de Martino; Alberto Dominguez; Yongwei DONG; Michele Doro; Fabio Gargano; J. Eric Grove; Elizabeth Hays; Margarita Hernanz; Jordi Isern; Stefan Lalkovski; Manuela Mallamaci; Dmitry Malyshev; Karl Mannheim; Ajello Marco; Manel Martinez; Mario Nicola Mazziotta; Roberto Mignani; Alexander Moiseev; Aldo Morselli; Uwe Oberlack; Josep M. Paredes; Carlotta Pittori; Martin Pohl; Riccardo Rando; Javier Rico; Pablo Saz Parkinson; Andy Strong; Vincent Tatischeff; Marco Tavani; Roberto Turolla; Roland Walter; Silvia Zane; Andrzej Zdziarski

<https://agenda.infn.it/conferenceDisplay.py?confId=13913>



AMEGO

ALL-SKY MEDIUM ENERGY GAMMA-RAY OBSERVATORY

Home

Science

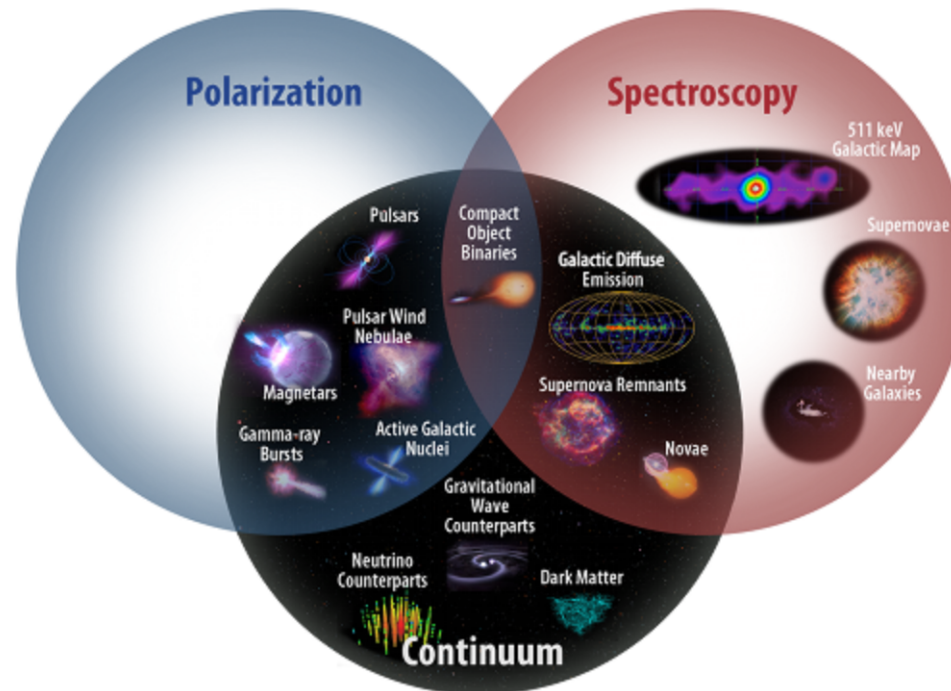
Technical

Team

Talks and News

Internal

AMEGO, the All-sky Medium Energy Gamma-ray Observatory, is an [Astrophysics Probe mission concept](#) designed to explore the MeV sky.



AMEGO



AMEGO Science

Understanding Extreme Environments

Astrophysical Jets

Understand the formation, evolution, and acceleration mechanisms in astrophysical jets

Compact Objects

Identify the physical processes in the extreme conditions around compact objects

Dark Matter

Test models that predict dark matter signals in the MeV band

MeV Spectroscopy

Measure the properties of element formation in dynamic systems



AMEGO

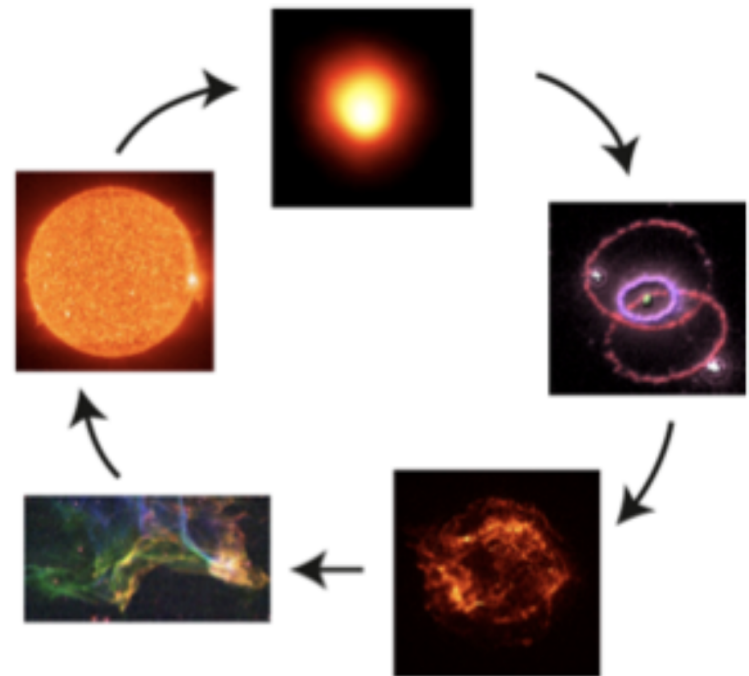


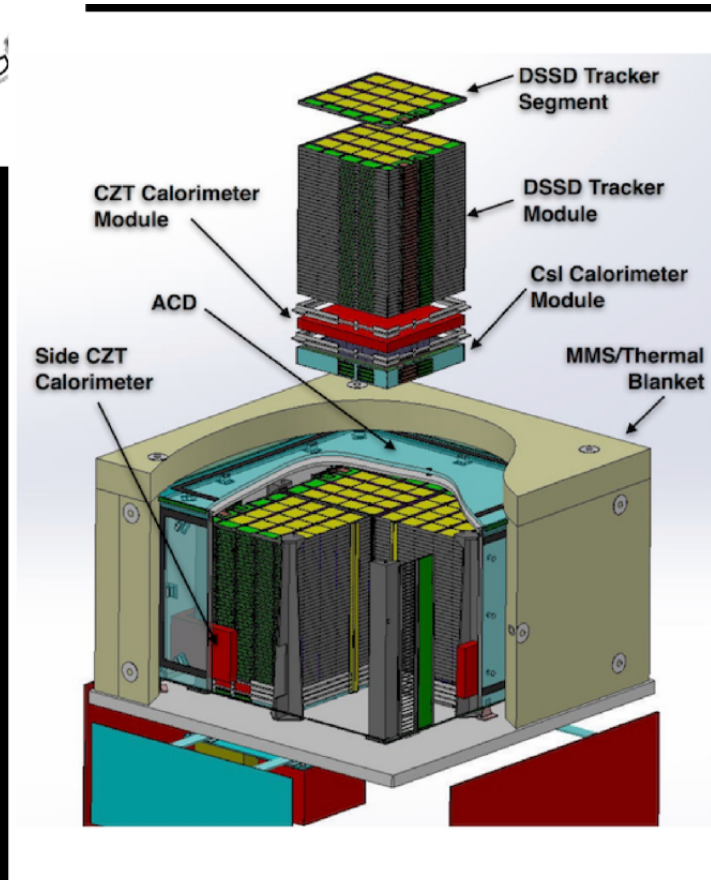
Element Formation in Dynamic Systems

Nuclear lines explore Galactic chemical evolution and sites of explosive element synthesis (SNe)

- Electron-positron annihilation radiation
 - $e^+ + e^- \rightarrow 2\gamma$ (0.511 MeV)
- Nucleosynthesis
 - Giants, CCSNe (^{26}Al)
 - Supernovae (^{56}Ni , ^{57}Ni , ^{44}Ti)
 - ISM (^{26}Al , ^{60}Fe)
- Cosmic-ray induced lines
 - Sun
 - ISM

^{56}Ni : 158 keV 812 keV (6 d)
 ^{56}Co : 847 keV, 1238 keV (77 d)
 ^{57}Co : 122 keV (270 d)
 ^{44}Ti : 1.157 MeV (78 yr)
 ^{26}Al : 1.809 MeV (0.7 Myr)
 ^{60}Fe : 1.173, 1.332 MeV (2.6 Myr)





AMEGO: All-sky Medium Energy Gamma-ray Observatory

Tracker

Incoming photon undergoes pair production or Compton scattering. Measure energy and track of electrons and positrons

- 60 layer DSSD, spaced 1 cm
- Strip pitch 0.5mm

CZT Calorimeter

Measures location and energy of Compton scattered photons, and head of the shower for pair events

- Array of 0.6x0.6 x 2cm vertical CdZnTe bars

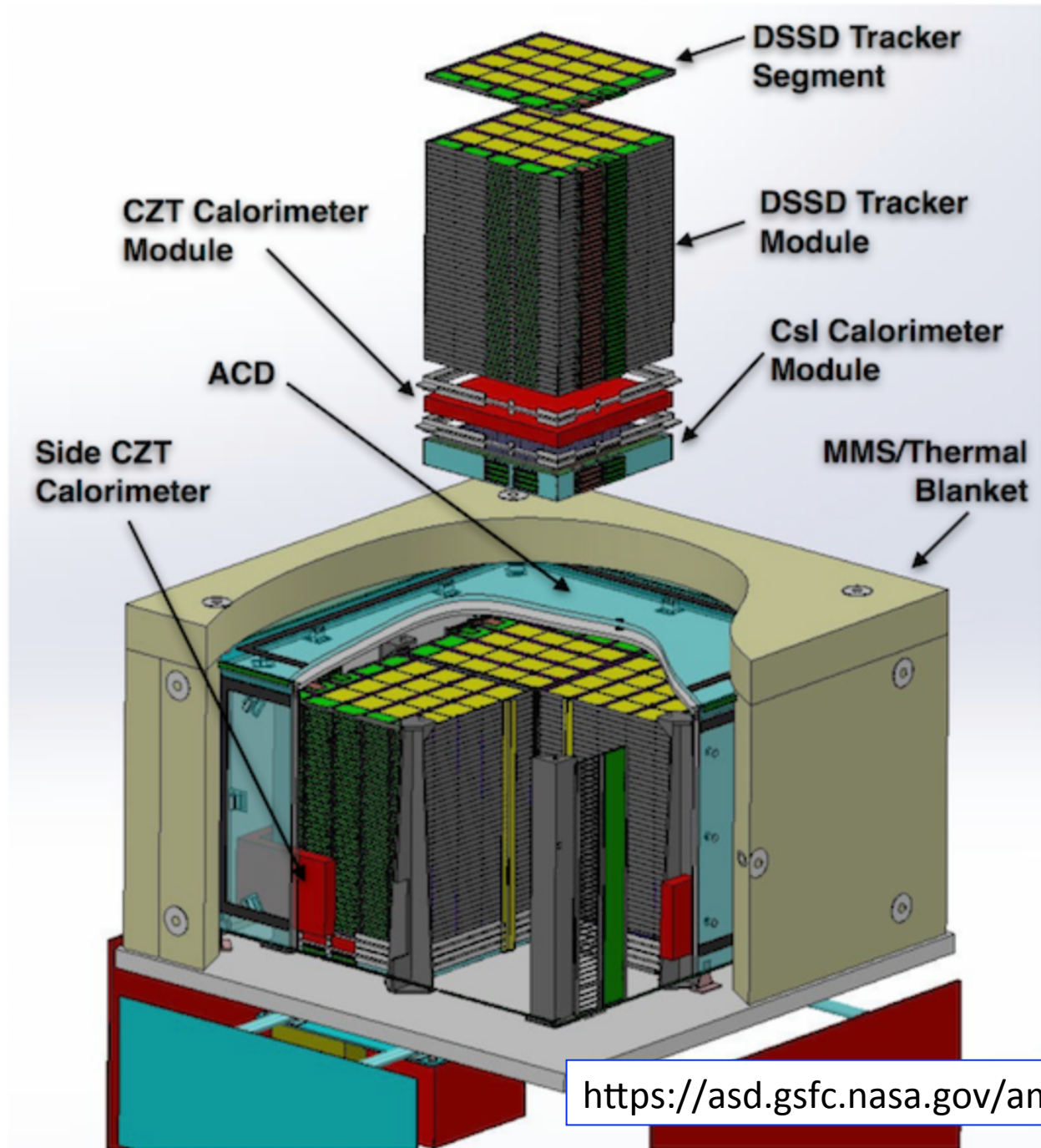
CsI Calorimeter

Extends upper energy range

- 6 planes of 1.5cm x 1.5 cm CsI (TI) bars

Instrument concept:

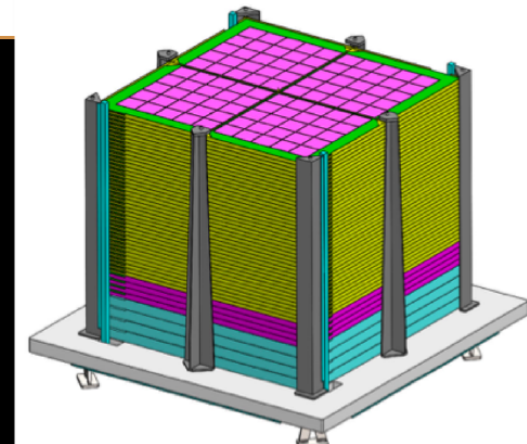
- Maximized performance in 1 MeV – 100 MeV range, with full range 0.2 MeV – 10 GeV
- Simplicity, long-term (~10 years) reliability, max use of already space-qualified technology
- Sensitive to both γ -ray interactions: pair production and Compton scattering
- Minimized amount of passive elements in detecting zone of the instrument (no passive γ -ray converters as in LAT)
- Use fine segmentation of all detecting elements to provide the best particle tracking and event identification



<https://asd.gsfc.nasa.gov/amego/>

AMEGO Instrument Summary

Energy Range	300 keV -> 10 GeV
Angular resolution	3° (3 MeV), 6° (10 MeV), 2° (100 MeV)
Energy resolution	<1% (< 1 MeV), 1-5% (1-100 MeV), ~10% 91 GeV)
Field of View	2.5 sr (20% of the sky)
Line sensitivity	<6x10 ⁻⁶ ph cm ⁻² s ⁻¹ for the 1.8 MeV ²⁶ Al line in a 1-year scanning observation
Polarization sensitivity	<20% MDP for a source 1% the Crab flux, observed for 10 ⁶ s
Continuum sensitivity (MeV cm ⁻² s ⁻¹)	3x10 ⁻⁶ (1 MeV), 2x10 ⁻⁶ (10 MeV), 8x10 ⁻⁷ (100 MeV)

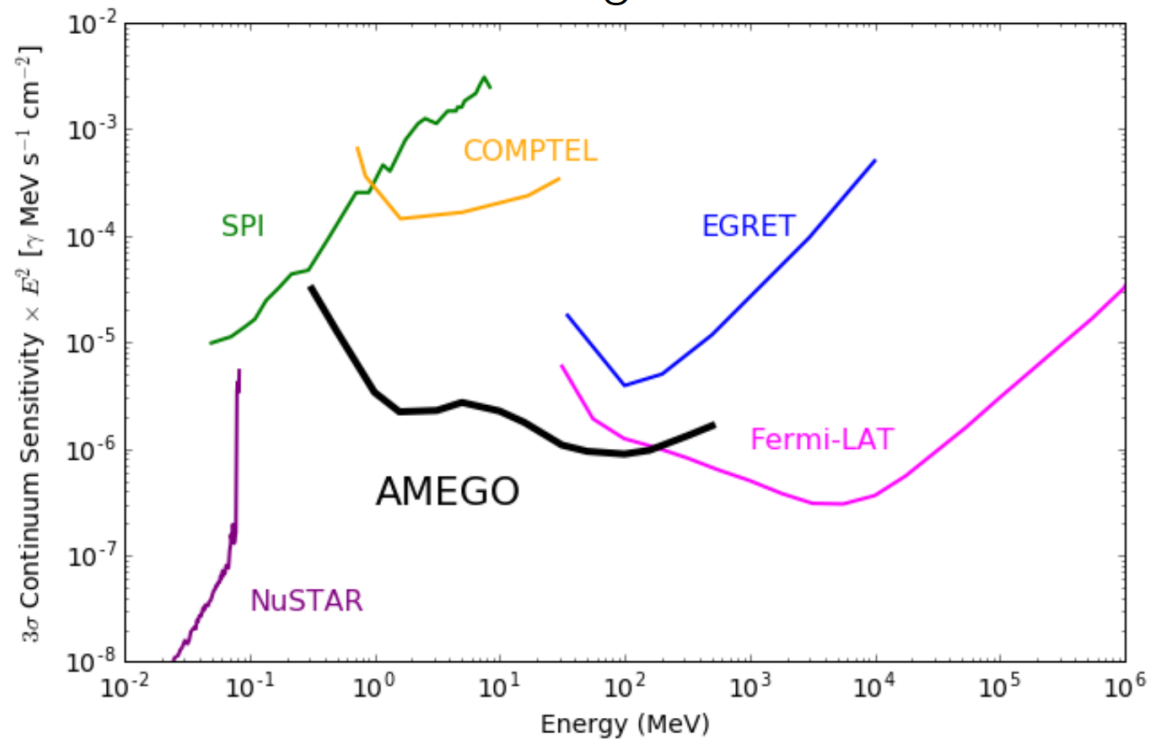


AMEGO



AMEGO Capabilities

Mission Averaged Sensitivities



Summary

12
1

- **The almost unexplored MeV / GeV gamma-ray band is one of the richest energy domains of astrophysics**
- **eASTROGAM/AMEGO will fill the gap and they will be essential observatories to study the extreme transient sky in the era of astronomy's new messengers**
- **ASTROGAM/AMEGO payloads are innovative in many respects, but the technology is ready**

